

# **Design and Demonstration of Smartphone-Based Colorimeter**

By

**Saptami Rani**

A thesis submitted to the Department of Electrical and Electronic Engineering for partial fulfillment of the requirements for the degree of Master of Science in Electrical and Electronic Engineering



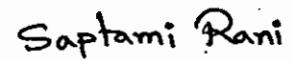
Khulna University of Engineering & Technology  
Khulna-9203, Bangladesh  
**December 2019**

## Declaration

This is to certify that the thesis work entitled "*Design and Demonstration of Smartphone-Based Colorimeter*" has been carried out by *Saptami Rani* in the Department of *Electrical and Electronic Engineering*, Khulna University of Engineering & Technology, Khulna-9203, Bangladesh. The above thesis work or any part of this work has not been submitted anywhere for the award of any degree or diploma.



Signature of Supervisor  
(Prof. Dr. Md. Rafiqul Islam)

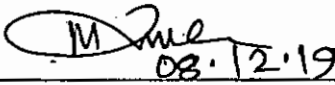
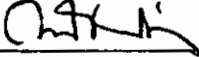
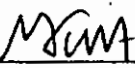
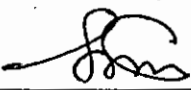



Signature of Candidate  
(Saptami Rani)

## Approval

This is to certify that the thesis work submitted by *Saptami Rani* entitled "*Design and Demonstration of Smartphone-Based Colorimeter*" has been approved by the board of examiners for the partial fulfillment of the requirements for the degree of Master of Science in Electrical and Electronic Engineering in the Department of Electrical and Electronic Engineering, Khulna University of Engineering & Technology, Khulna-9203, Bangladesh in December 2019.

### BOARD OF EXAMINERS

1.   
03.12.19  
Prof. Dr. Md. Rafiqul Islam (I)  
Department of Electrical and Electronic Engineering  
Khulna University of Engineering & Technology, Khulna-9203  
Chairman  
(Supervisor)
2.   
Head  
Department of Electrical and Electronic Engineering  
Khulna University of Engineering & Technology, Khulna-9203  
Member
3.   
Dr. Md. Arafat Hossain  
Assistant Professor  
Department of Electrical and Electronic Engineering  
Khulna University of Engineering & Technology, Khulna-9203  
Member
4.   
Prof. Dr. Md. Mahbub Hasan  
Department of Electrical and Electronic Engineering  
Khulna University of Engineering & Technology, Khulna-9203  
Member
5.   
Prof. Dr. S. M. Abdur Razzak  
Department of Electrical and Electronic Engineering  
Rajshahi University of Engineering & Technology, Rajshahi-6204  
Member  
(External)

**DEDICATED TO MY BELOVED PROTHOMA**

## Acknowledgment

At first, I would like to prostrate in worship to Almighty God for helping me at every stage of my life, especially giving me the mercy, patience, and ability to complete my M.Sc. Engineering program successfully.

I would like to express my gratitude, appreciation, and thanks to my always inspiring, enthusiastic & very supportive supervisor, Prof. Dr. Md. Rafiqul Islam (1) for his constructive suggestion, scholastic guidance, constant inspiration, valuable advice and kind co-operation to carry on the work of “Design and Demonstration of Smartphone-Based Colorimeter”.

My sincere gratitude goes to Protik Chandra Biswas (Assistant Professor, Dept. of EEE, KUET) who provided a significant contribution to this research. He was very generous in helping me working with chemicals and developing smartphone applications for this research work. Especially I would like to mention the contribution of Mr. Protik in writing several papers and the final thesis report.

Special thanks go to Dr. Md. Arafat Hossain (Assistant Professor, Dept. of EEE, KUET) for providing his in-depth knowledge in the 3D printing process. Moreover, his continuous technical supports, valuable suggestions about smart sensing, guidelines for optical instrumentation and advice for scientific report writing are very much helpful to complete this thesis work.

I would also like to thank Prof. Dr. Md. Rafiqul Islam (2), Head of the Department of Electrical and Electronic Engineering for providing me all possible facilities regarding this research work. I wish to thank Md. Joynal Abedin (Senior Instructor, Dept. of Chemistry, KUET) for his cooperation to prepare the chemical test samples.

I am forever indebted to each of my family members for their much-needed support, encouragement, and assistance given throughout my studies. My heartiest thanks to my mother Nishkriti Rani Biswas, for her countless advice and mental support. The thesis would not be possible without their help.

Khulna, December 2019

Thanks to all  
Saptami Rani

## Abstract

In this thesis work, smartphone-based colorimeter is designed and practically implemented utilizing the in-built sensors like CMOS camera, flash LED, and high-power processor of the smartphone. The developed totally self-contained colorimeter is low-cost, light-weight, robust, field-portable and easily accessible. It has smart sensing facilities without the requirement of additional optics and external power supply. The device can be applied for real-time and on-site measurements of different types of analytes in the fields of environmental research, biomedical applications, and agriculture, which are completely absent in the currently used conventional bench-top type colorimetric instruments.

In the real-world, for most of the colorimetric detection, attributes of color such as wavelength, intensity, saturation, etc. vary simultaneously according to the variation of analytes. The conventional smartphone-based colorimeters are mainly designed to measure the analytes considering the change in color information in only one domain which limits the colorimetric measurement in some specific analytes with a narrow band of detection. In this research, the developed smartphone-based colorimeter can quantify any analytes through multiple nonlinear regression based colorimetric assessment in a wide range of detection considering the variation of color attributes in all significant domains.

To demonstrate the smartphone-based colorimeter a 3D optical enclosure is designed and fabricated for ensuring the constant illumination and hence to improve the SNR by isolating the measuring platform from the environmental illumination. Self-referencing is a unique characteristic of the instrument to calculate the color ratio with respect to the colorimetric information of the sample. A customized Android-based smartphone app is developed for the complete functioning of the developed colorimeter. The app is developed with the graphical user interfaces of calibration, assessment of the real-time or previously recorded test samples, save, and share the results of colorimetric measurement for multiple analytes of different colorimetric tests. For the first time, a novel wavelength estimation algorithm is developed to estimate the wavelength information of the reflected light of colorimetric measurement.

To justify the performance of the developed colorimeter, three different colorimetric tests are demonstrated in this research named as Rhodamine B concentration quantifier, digital pH meter, and chlorine concentration quantifier using the Xiaomi Redmi Note 4 smartphone. Three different colorimetric characteristics are found for the three samples: only color tone changes significantly with the variation of Rhodamine concentration, the wavelength of color varies significantly with the variation of pH value in water, and color intensity, wavelength, and saturation all vary simultaneously with the variation of chlorine concentration. For all of the three colorimetric tests, the performance of the designed smartphone-based colorimeter is found excellent compared to the conventional colorimeters. The average error of RhB concentration quantifier within the detection range of (0.2-4.0) PPM is 0.95% whereas the chlorine concentration quantifier shows an average error of 1.16% for the detection range of (0.1-8.0) PPM with sensitivity 0.1 PPM. On the other hand, the digital pH meter detects pH value in the range of (4.0-9.0) with an average of 0.0876% detection error.

It is noted that the present smartphone-based colorimeter is designed and demonstrated using three analytes but the developed device can be applied to measure any colorimetric analytes by proper calibration using the developed smartphone app. So, the developed smartphone-based colorimeter could be a cost effective common platform for the colorimetric measurement of various analytes in different fields of applications.

# CONTENTS

	<b>Page</b>
Title	i
Declaration	ii
Approval	viii
Acknowledgement	v
Abstract	vi
Contents	vii
List of Tables	x
List of Figures	xi
List of Abbreviations	xiv
Nomenclature	xvi
<b>CHAPTER I Introduction</b>	
1.1 Introduction	2
1.2 Literature Review	3
1.3 Scopes of the Present Study	6
1.4 Objectives	9
1.5 Dissertation Organization	10
<b>CHAPTER II Fundamentals of Colorimetric Detection</b>	
2.1 Introduction	12
2.2 Bench-top Colorimeter	12
2.3 Portable Colorimeter	14
2.4 Smartphone-based Colorimeter	16
2.5 Light Source and Detector	20
2.6 Color Models	23
2.7 Conclusion	28
<b>CHAPTER III Design and Fabrication of Smartphone-based Colorimeter</b>	
3.1 Introduction	30
3.2 Optical Layout Design	30
3.3 3D Design and Fabrication	32
3.4 Android-based Smartphone App Development	35
3.5 Wavelength Estimation	38
3.6 Conclusion	41



<b>CHAPTER IV</b>	<b>Results and Discussion</b>	
	4.1 Introduction	43
	4.2 Rhodamine B Concentration Quantifier	43
	4.3 Digital pH Meter	55
	4.4 Chlorine Concentration Quantifier	66
	4.5 Conclusion	78
<b>CHAPTER V</b>	<b>Conclusion</b>	
	5.1 Conclusion	80
	5.2 Future Work	81
	<b>References</b>	82
	<b>Appendix</b>	89

## LIST OF TABLES

<b>Table No.</b>	<b>Description</b>	<b>Page</b>
2.1	Attributes of mostly available commercial bench-top and portable colorimeters	15
3.1	Main features of the designed and fabricated smartphone-based colorimeter	34
4.1	Composition of RhB samples of different concentration	44
4.2	Experimental data table to formulate calibration equations for RhB concentration quantifier	47
4.3	Calibration techniques applied for the calibration of RhB concentration quantifier	50
4.4	Test results of smartphone-based colorimetric RhB concentration quantifier for performance analysis among different calibration techniques	52
4.5	Composition of pH samples of different pH value with universal indicator chemosensor	56
4.6	Experimental data table to formulate calibration equations for pH measurement	58
4.7	Calibration techniques applied for the calibration of digital pH meter	61
4.8	Test results of smartphone-based colorimetric pH measurement for performance analysis among different calibration techniques	63
4.9	Preparation of chlorine samples of different concentrations with KI-starch indicator as chemosensor	67
4.10	Experimental data table to formulate calibration equations for chlorine concentration quantification	70
4.11	Calibration techniques applied for the calibration of chlorine concentration quantifier	73
4.12	Test results of smartphone-based colorimetric measurement of chlorine concentration for performance analysis among different calibration techniques	75
A1	Features and specifications of the Xiaomi Redmi Note 4 smartphone used in designing smartphone-based colorimeter	89

## LIST OF FIGURES

Figure No.	Description	Page
2.1	Pictorial views of commercial bench-top colorimeter, Model: (a) CR-5, Konica Minolta and (b) ColoroMat 100.	13
2.2	Pictorial view of commercial portable colorimeter, Model: (a) DR300 and (b) 3NH NH300.	14
2.3	Illustration of the workflow of mobile phone based first colorimetric prototype system for simultaneous analysis of glucose and protein in urine.	17
2.4	Snapshot images of experimental demonstration of chlorine concentration by using smartphone as an analytical device.	18
2.5	3D schematic illustration of the internal structure of the opto-mechanical closed chamber for colorimetric detection of (a) chlorine and (b) mercury in drinking water on smartphone platform.	19
2.6	Utilization of smartphone flash LED as the optical source in smartphone-based colorimetric detection (A) 3D structure (B) internal components of 3D structure.	20
2.7	Spectral responses of smartphone flash LED covers a wide bandwidth ranging from 400 nm to 700 nm.	21
2.8	Illustration of color image detection and reconstruction procedure by the CMOS image sensor of smartphone.	23
2.9	CIE 1931 color space.	24
2.10	RGB color model illustrating (a) primary and secondary colors (b) RGB color cube with their corresponding red, green and blue color components values in rectangular co-ordinate system.	25
2.11	Representation of HSV color model with their corresponding hue, saturation and value color components.	26
3.1	Schematic optical layout of the designed smartphone-based colorimeter.	31
3.2	3D views of the designed optical enclosure attached with smartphone for colorimetric measurement (a) bottom left side corner view, (b) top right side corner view, (c) right side corner view, (d) top left side corner view, (e) top view and (f) bottom view.	32
3.3	3D fabricated optical enclosure attached with smartphone to measure RhB concentration.	33
3.4	Screenshots images illustrating the workflow of the customized Smartphone Colorimeter app: (a) menu screen, (b) instruction screen, (c) select test type screen, (d) selected or captured image of the test sample uploaded in analyze	36

<b>Figure No.</b>	<b>Description</b>	<b>Page</b>
	screen, (e) colorimetric test results and (f) the calibration screen.	
3.5	(a) Visible light spectrum (Magenta is not part of the visible spectrum of light) (b) HSV color wheel (Visible spectrum wrapped to join blue and red in an additive mixture of magenta. In reality, blue and red are at opposite ends of the spectrum, and have very different wavelengths).	39
3.6	Illustration of wavelength estimation of reflected light for colorimetric smartphone-based measurement with respect to three laser diodes of known wavelength.	40
4.1	Photograph of Rhodamine B samples (0.2-4.0) PPM for calibration and testing of smartphone-based colorimetric measurement.	44
4.2	Screen-shot of the calibration page illustrating the colorimetric analysis of RhB samples: (a) 1.0 PPM and (b) 3.0 PPM.	46
4.3	Polynomial fit curves to calibrate the smartphone-based colorimeter as RhB concentration quantifier by only considering: (a) color ratio, (b) hue, (c) saturation, and (d) value as independent variable.	48
4.4	Percentage of detection error associated with smartphone-based colorimetric measurement of RhB concentration for different calibration techniques.	53
4.5	Screenshot images of RhB concentration quantification using customized smartphone app: (a) 4.00157 PPM (actual concentration 4.0 PPM) and (b) 0.99696 PPM (actual concentration 1.0 PPM).	54
4.6	RhB concentration of seven test samples measured on smartphone-based colorimeter compared with corresponding actual concentration.	54
4.7	Photograph of pH samples (pH value 4.0-9.0) for smartphone-based colorimetric measurement of pH.	56
4.8	Calibration screen of the developed smartphone app illustrating the colorimetric analysis of two samples with different pH value: (a) pH 5.0, and (b) pH 8.0.	57
4.9	Polynomial fit curve to calibrate the smartphone-based colorimeter as digital pH meter by only considering: (a) color ratio, (b) hue, (c) saturation, and (d) value as independent variable.	59
4.10	Percentage error of detection associated with smartphone-based colorimetric measurement of pH value using different calibration techniques.	64
4.11	Screenshots of pH measurement using customized smartphone app: (a) standard buffer solution of actual pH 4.0 (measured pH = 4.00009) and (b) supply water of KUET of actual pH 7.9 (measured pH = 7.92467).	65
4.12	pH value of seven test samples measured on smartphone-based colorimeter and standard pH meter.	65
4.13	Photograph of chlorine samples (0.1-8.0) PPM for proper calibration of	68

<b>Figure No.</b>	<b>Description</b>	<b>Page</b>
	smartphone-based colorimetric measurement of chlorine concentration.	
4.14	Calibration screen of the developed app illustrating the colorimetric analysis of two samples with different chlorine concentration: (a) 0.7 PPM and (b) 7.0 PPM.	69
4.15	Polynomial fit curve to calibrate the smartphone-based colorimeter as chlorine concentration quantifier by only considering: (a) color ratio, (b) hue, (c) saturation, and (d) value.	71
4.16	Percentage error of detection associated with smartphone-based colorimetric measurement of chlorine concentration using different calibration techniques.	76
4.17	Screenshot images of chlorine concentration quantification using customized smartphone app: (a) 0.5156 PPM (actual concentration 0.5 PPM) and (b) 7.9956 PPM (actual concentration 8.0 PPM).	77
4.18	Chlorine concentration of seven test samples measured on smartphone-based colorimeter compared with corresponding actual concentration.	77
A1	Locations of some components and sensors of Xiaomi Redmi Note 4 smartphone (a) front view and (b) back view.	90

## LIST OF ABBREVIATIONS

ABS	Acronytrile Butadiene Styrene
ALS	Ambient Light Sensor
AMOLED	Active Matrix Organic Light Emitting Diode
CAD	Computer Aided Design
CFA	Color Filter Array
CIE	International Commission on Illumination
CMOS	Complementary Metal Oxide Semiconductor
DPD	N,N Diethyl-1,4 Phenylenediamine Sulfate
EMI	Electromagnetic Interference
FDM	Fused Deposition Modeling
FOV	Field of View
GPS	Global Positioning System
HSL	Hue, Saturation, Lightness
HSV	Hue, Saturation, Value
IoT	Internet-of-Things
IR	Infra-red
ISO	International Standardization Organization
jpg	Joint Photographic Experts Group
KI	Potassium Iodide
LCD	Liquid Crystal Display
LED	Light Emitting Diode
LOD	Limit of Detection
LS-SVM	Least Squares-support Vector Machine
NFS	Near-Field Sensors
PLA	Polylactic Acid
POC	Point of Care
PPM	Parts Per Million
RGB	Red, Green and Blue

RhB	Rhodamine B
ROI	Region of Interest
SCApp	Smartphone Colorimeter App
SMS	Short Message Service
SNR	Signal to Noise Ratio
SVM	Support Vector Machine
WHO	World Health Organization
Wi-Fi	Wireless Fidelity
USB	Universal Serial Bus
UV	Ultra-violet
2D	Two Dimensional
3D	Three Dimensional
3G	Third Generation
4G	Fourth Generation

## NOMENCLATURE

$\lambda$	Wavelength
$\lambda_R, \lambda_G, \lambda_B$	Wavelength for red, green and blue laser
$C_R$	Color ratio
$H, S, V$	Hue, Saturation, Value
$H_m$	Modified hue
pH	Acidity/Alkalinity
RGB	Red, Green, Blue
$R_r, G_r, B_r$	Average red, green and blue color values of reference ROI
$R_s, G_s, B_s$	Average red, green and blue color values of sample ROI



# Chapter I

## *Introduction*

---

### **Chapter Outlines:**

**1.1 Introduction**

**1.2 Literature Review**

**1.3 Scopes of the Present Study**

**1.4 Objectives**

**1.5 Dissertation Organization**

---

## 1.1 Introduction

Nowadays, on-site and real-time smart instrumentation for ubiquitous detection of biological, environmental and agricultural items has become a challenging issue due to the limitations of size, cost, and accessibility of the conventional bench-top instruments. These bench-top laboratory instruments based approaches are very expensive and time-consuming where most of the cases real-time monitoring is totally impossible. In recent years, there is a new trend of research to utilize the inherent potentials of smartphone to create smart sensing instruments for onsite and real-time measurements. After the beginning of smartphone era, researchers across the world have been actively engaged to utilize smartphones as a low cost and user-friendly scientific tool for different physical, chemical and biological sensing applications. Attractive embedded features of smartphone, including an array of in-built sensors (high-resolution camera, ambient light sensor, gyroscopes, global position systems, proximity sensor, etc.), increased battery life, fast computational power, easy-to-use apps, and real-time data sharing facilities allow smartphone-based technologies as an alternative of bench-top laboratory instruments. In addition to this, the market of smartphone is drastically growing and the number of smartphone users in the world is expected to reach about 3.5 billion by 2020 which is more than 44% of the world's population [1], [2]. Therefore, smartphone can be the best platform for field portable and real-time smart sensing that can open a new research window of smartphone-based sensing instrumentation [3]. Smartphone-based smart sensing instruments are extensively used as scientific tool due to their advantages as given below

- ❖ fast response
- ❖ cost-effective
- ❖ easily accessible
- ❖ high throughput
- ❖ field portable
- ❖ increased reliability
- ❖ lightweight
- ❖ Internet-of-Things (IoT) facility
- ❖ Wireless connectivity
- ❖ compact form
- ❖ long operating life
- ❖ user-friendly
- ❖ completely self-contained
- ❖ robust for transport
- ❖ real-time detection capability
- ❖ simpler controllability
- ❖ high processing capability and programmability

Due to the innumerable advantages, extensive researches have already been conducted for the development of a number of smartphone-based analytical devices in recent years such as colorimeters, spectrometers, fluorimeters, microscopic imaging and so on [4]-[7]. The development of a smartphone-based sensing instrument was initially led by simple colorimetry. Then this colorimetric based approach has been got popularity due to its technical simplicity and color-dependent information detection capability. Colorimetric detection allows direct imaging of the color change information of any samples or substances onto the CMOS camera sensor of smartphone without any additional optics. On the other hand, spectroscopic and microscopic detection requires additional expensive optics whereas fluorimeters only show the fluorescence at a specific wavelength [7]-[9]. Therefore, a smartphone-based colorimeter is becoming the more attractive and effective solution for point-of-care (POC) medical diagnostic, environmental management, agricultural sector, food quality assessment and so on [4], [10]-[13].

## 1.2 Literature Review

Mobile phone-based first colorimetric detection was achieved by digitizing the color change information of a microfluidic paper where a mobile phone was only used as an imaging device. The captured images were sent to a remote computer for further processing with the help of a trained medical professional located off-site. After analyzing the captured image through a high processing computer, the results were further sent from off-site laboratory to the assay site through established communications infrastructure and thus the whole process consumed huge time [14].

Later on, this work was extended by employing a smartphone as an analytical device. By taking advantage of the fast processing capability of smartphone, a customized smartphone app was developed based on an advanced detection algorithm for image processing to optimize the computational speed [15]. Analyzing the captured images by customized smartphone app, color ratio and color intensity based colorimetric detection provide almost similar results as the bench-top colorimeter. External microcontroller circuit was also used to send the colorimetric readouts to smartphone through Bluetooth module [16] or universal serial bus (USB) connector [17] for analysis using smartphone apps. These smartphone applications have been developed in various platform such as Java [17]-[22], Matlab [16], [23]-[26], Python [27], MIT app inventor [28], ImageJ [29]-[31], OpenCV [32] etc. based on various detection and processing algorithm for exact data acquisition from colorimetric measurement.

The custom-developed smartphone app also provides saving facilities of the measured information in the internal storage of smartphone and provide communication facilities with the end-user to share the colorimetric result through short message service (SMS) [33] or via email [17], [28]. Moreover, the analyzed data and other related information of colorimetric detection were then transmitted to a central server which represents the analyzed results of various locations on a google map through geo-tagging. From central server real time analyzed data can be viewed and shared using internet browsers or through the same smartphone app [28], [34], [35].

However, repeatedly positioning the elements (such as light source, sample holder, etc.) around the measuring platform for accurate colorimetric measurements were not practical. As a result, one of the challenging issues found in direct colorimetric imaging using a smartphone CMOS camera was the variation of ambient light illumination due to the lack of fixed arrangement of colorimetric platform which introduced significant errors in measurements [36]. The variation of illumination under the conditions of outdoor sunlight or indoor fluorescent light or indoor weak light was corrected by compensating differences in ambient lighting condition, imaging distance, imaging angle and cellphone brand utilizing ‘four spots’ device calibration method [37]. The intensity of digitized RGB values of all sensor units of the paper-based colorimetric technique was corrected through utilizing the same black and white backgrounds but this prototype was not suitable for transport due to the requirement of compactness.

To hold all the optics and components used for smartphone-based colorimetric detection at a definite alignment and position, a custom-designed 3D printed closed chamber attached with the in-built camera module of smartphone was reported in these research works [16], [18], [34], [35], [28], [38], [39]. Enclosing all the used components within a closed chamber, the variations of ambient light illumination and the complication of stray light incorporated during measurement have been minimized. Fixed illumination of this compact closed chamber was provided by external light sources such as LED [16], [22], [35] fluorescent lamps [21], [37], [40], laser diode [41] etc. which were powered by a set of external batteries and controlled by ON/OFF switch [16], [22], [35]. The requirement of external power supply to operate the external light sources, however, serves as a hindrance in terms of the portability of smartphone-based colorimetric devices for field tests. Apart from this, one of the important issues for designing high-performance field-portable instrument is the compactness of the device.

In order to avoid the complexity of externally powered light sources, an in-built flash LED was utilized along with the CMOS camera of a smartphone which made the colorimetric detection technique more cost-effective and completely field-portable [18], [23], [28], [34]. To overcome the non-uniform intensity distribution of smartphone flash LED, diffuser optics was used for uniform illumination. In addition to this, white liquid crystal display (LCD) screen, controlled by microcontroller was also used as light source instead of smartphone in-built flash LED in colorimetric detection [42] to ensure uniform illumination. However, LCD screen, microcontroller, and other accessories made the system bulky which is costly, complex and not user-friendly.

Another significant advancement of smartphone colorimetric detection has been made by incorporating a reference into the measurement to overcome the error introduced by background light fluctuation. Some studies utilized the image of white background [36] as a reference or incorporated a reference solution [43] to monitor the sample solution according to reference to extract the color information of colorimetric assessment by comparing with the sample solution. But during measurement with respect to a reference (white background or reference solution) adjacent to the sample solution, per-pixel information of these references were changed according to the illumination of emitted light from source and the reflected light from sample solution. So independently illuminated real-time reference is essential for errorless smartphone-based colorimetric detection.

However, in-built automatic image correction and post-processing mechanism (white balance, filter, ISO select, etc.) on the captured raw image of the smartphone CMOS camera make it difficult to obtain the actual color information from resultant .jpg image. Moreover per pixel color intensity of a raw image is directly proportional to the number of photons received or absorbed by this pixel provides accurate color intensity information which is essential for sophisticated scientific analysis. So .jpg formatted image cannot provide per pixel color information accurately and significant error has been introduced in colorimetric detection using .jpg image format due to information loss. The raw image was introduced for colorimetric analysis to avoid the drawbacks of in-built color correction mechanism and post-processing methods of smartphone CMOS camera for obtaining the real intensity information by using

external high processing device [44]. Because majority of today's smartphone is not capable enough to access and process raw images and require additional high processing units such as computer which limits the field portability of smartphone-based colorimeter. It is expected that the accessibility of raw image extraction and processing feature will incorporate with next generation smartphone. The impact of automatic image correction mechanism of smartphone camera was removed to regain the actual color information at detector output by incorporating more stable color model (such as HSV or HSL) [18]-[20], smart color adaptation algorithm [38], advanced device calibration approach [37], and so on. For quantitative analysis hue parameter of HSV (Hue, Saturation, Value) [18] or HSL (Hue, Saturation, Lightness) [19] color model was used which is more precise and provide more stable color information than RGB values and less sensitive to variations in illumination.

Furthermore, the limited field of view (FOV) of the smartphone camera becomes a challenging issue to achieve high throughput for a smartphone-based colorimeter to analyze multiple parameters of a single analyte simultaneously. It became possible to analyze multiple parameters simultaneously by utilizing the different assay zones of the customized paper-based microfluidic sensor [14], [45]-[47] in colorimetric measurement. However, fabrication and preparation of the paper-based microfluidic sensors are so much complicated and costly. Test strip (dry reagent strip) for colorimetric detection of multiple parameters was introduced to solve the complexity of microfluidic sensor fabrication and limit the need for proper chemosensor preparation [21], [48]. Color change information of the test strip after the reaction was captured by a smartphone camera and custom-developed app quantified optical parameters (such as hue, saturation, lightness, etc.) of the test area to identify and display the value of physical parameter on the smartphone screen [18]-[20].

The images of various colorimetric detection using test strip [24], [44], [49] or sample cell [50], were used as the trained data set to train support vector machine (SVM) as well as the least squares-support vector machine (LS-SVM) to develop the learning algorithm for accurate quantification of unknown analytes and thus artificial intelligence was incorporated with smartphone-based colorimetric detection.

All of the above mentioned smartphone colorimeters have been designed to utilize paper-based microfluidic sensors [14], [45]-[47], [51], test strip [19]-[21], [23], [48], [49] or cuvette [35], [28], [52], [53] as sample holder to analyze the liquid samples only which limits the versatility of the devices. But the investigation of solid and gaseous samples mainly depends on laboratory bench-top instruments. Addressing this issue, smartphone-based colorimeter also developed for the detection of gaseous analytes in the atmosphere around us [54], [55] by processing the reflected light intensity of test zone.

Moreover, smartphone-based colorimetric analysis has been performed through video processing [32] that analyzed many images into a single output metric and particularly effective when a low detection limit is required. Various in-built sensors of smartphone such as ambient light sensor (ALS) [28], [56] compass and gyroscope [25] proximity sensor [57], etc. in addition to flash LED and camera sensor of smartphone have been used to extend the application field of smartphone-based colorimetric detection.

Nowadays vitamin D [58], cholesterol level [59], hemoglobin concentration and HIV antibodies [14] in human blood, glucose and protein concentration in urine [14], [37] DNA detection [41], cancer cell detection [60] have been rapidly and easily done as point of care diagnosis by using smartphone colorimeter. Beyond this sector of biomedical engineering, smartphone colorimeter also plays significant role in environmental impact analysis such as water quality monitoring [33], [50], chemical components detection in polluted soil [61], detection of micro-organism (E-coli, coliform etc) [25], marine toxin detection [62] etc. Apart from these, food toxins quantitation [47]-[39] and food allergens detection [43] are the two examples of food quality monitoring by using a smartphone colorimeter. Smartphone-based colorimeter has also a significant impact on other sectors like the agricultural sector [40], water turbidity detection [57], bloodstain age estimation [63], pattern recognition sensing system [26] and so on. Therefore, smartphone-based colorimetric instrumentation has versatile applications for disease diagnosis, food quality monitoring, environmental and agriculture aspects analysis and so on.

### **1.3 Scopes of the Present Study**

Comprising with the mentioned special features, advantages, and applications of the smartphone-based colorimeter, its wide variety applications are found in different research areas. Self-contained smartphone colorimeters reported up to date use smartphone flash LED with additional optics to uniformly illuminate the enclosed chamber. Mainly diffuser optics, reflectors, white LCD display and so on are used to ensure uniform illumination. These accessories make the smartphone-based colorimetric system bulky, costly, complex and not user-friendly at all. These additional optics reduce the light collection capability of smartphone-based colorimeter considerably. But in colorimetric detection it is more important to ensure constant illumination for every measurement than uniform illumination. Because paper-based specified sample holder is positioned at the definite place with respect to the optical position of smartphone flash LED and CMOS camera detector in the enclosed chamber. Moreover, the position of both sample and reference ROI (Region of Interest) is maintained constant which ensures definite illumination for every measurement. Thus the optics need for uniform illumination can be eliminated from the design consideration without any compromise of device performance and the overall design of smartphone-based colorimeter can be made lighter, robust, simple and inexpensive.

Another significant issue of smartphone colorimetric detection is to choose the appropriate reference to calculate the color ratio of a sample with respect to the reference which is an important attribute for colorimetric detection. In previous studies, white background or reference solution in cuvette was used as reference ROI to determine the color ratio. But reference cuvette in conjunction with sample cuvette makes the optical attachment bulky and cumbersome. Besides, during colorimetric measurement with respect to reference (white background or reference solution) adjacent to the sample solution, per-pixel information of these references is changed according to the illumination of the reflected light from sample solution. So independently illuminated self-reference is essential for error-free detection.

Most of the smartphone-based colorimetric devices reported to date have been designed for sensing the unknown parameter of different analytes according to the information of color ratio and this color ratio is generally calculated based on the RGB color model. Although the primary RGB values of the digitized image are directly used in many smartphone-based colorimetric measurements, from an analytical perspective absolute intensity values are not accurate because the composition of RGB does not change monotonically with spectral wavelength and intensity [64]. The transformation from primary RGB color model to HSV (Hue-Saturation-Value) color map can be one way to improve this accuracy and avoid direct intensity calibration [65]. HSV is a cylindrical coordinate representation of points in RGB color space, where the V axis represents brightness or intensity. Moreover, the impact of the inherent image correction mechanism of a smartphone camera can be reduced to regain the actual color information at detector output by incorporating more stable color model (such as HSV or HSL). So HSV or HSL color map can be more appropriate domain to analyze the color information for colorimetric detection of unknown parameters of different analytes.

Though a few researchers [18]-[20] introduced the HSV color model for smartphone-based colorimetric detection, only single attribute hue or saturation or value from the HSV color model was used as argument to formulate the polynomial to determine the unknown parameters of different analytes. But most of the cases, all of these three attributes are changed simultaneously with the change of physical parameter and so the change of physical parameter cannot be properly quantified by only considering a single attribute.

All of the reported conventional smartphone-based colorimeters can be used for the cases of colorimetric detection when only the wavelength or the intensity is changed separately. In the real-world, for most of the cases, wavelength and intensity both color information is changed simultaneously according to the change of any analytical parameter which has to be quantified through colorimetric measurement. Moreover color information (wavelength or intensity) also changes with the change in detection range i.e. at a specific detection range of an analytical parameter, only wavelength or intensity or both can play significant role for colorimetric detection. For the above-mentioned reasons, the conventional smartphone-based colorimeters have been designed for the measurement of a specific analytical parameter for a limited range of detection. Now, it is high time to design a universal smartphone-based colorimeter that can quantify multiple parameters of different analytes with a wide range of detection. This universal smartphone-based colorimeter can operate for all the conditions where wavelength or intensity of reflected light from sample varies solely or simultaneously. So, it is a great challenge to improve the performance of smartphone colorimeter that will provide actual colorimetric information according to color ratio, color intensity as well as wavelength information such that it can meet the expectation of future market demand.

The existing smartphone-based colorimeters are not able to provide the direct information of wavelength of reflected light from the sample. Nowadays, for obtaining the detail information of wavelength, spectroscopic analysis is preferred. But it can be possible to determine the wavelength information of the reflected light from the sample for smartphone-based colorimetric detection by incorporating appropriate wavelength calibration techniques.

The main purpose of this research is to develop an entirely self-contained universal smartphone-based colorimeter using the in-built optical source (flash LED) and CMOS camera sensor of smartphone where samples are monitored with respect to a self-reference to extract the actual information of color ratio, color intensity, and wavelength simultaneously. A customized smartphone app quantifies these optical parameters to calculate and represent the unknown analytical parameters according to color change information and error of measurement can be reduced significantly. Thus the physical domain information is converted to optical domain to sense and analyze the physical domain parameters.

The accessibility of safe drinking water is a major concern throughout the world and in Bangladesh, the accessible safe drinking water is still low at 34.6% according to the report of UNICEF [66]. So, a real-time water quality monitoring system is a burning issue related to public health of Bangladesh since chemically hazardous materials and micro-organisms cause numerous health diseases such as shigellosis, cholera, hepatitis A, leptospirosis, typhoid fever and so on. Chlorine concentration and pH level are two important indicators of safe drinking water. The presence of permissible amount of chlorine in drinking water is important for disinfection to prevent water-borne diseases caused by pathogenic micro-organisms (Protozoa, Bacteria, Viruses, Algae, etc.) contaminated in drinking water [67], [68]. However the effective disinfection of drinking water using chlorine is controlled by pH [69]. Moreover long time exposure to highly chlorinated water leads to a number of serious health problems including cell damage, increases risk of cancer and asthma [70]. Excluding these health hazards, high chlorination is the primary cause of odor and bad taste in drinking water which discourages people from drinking it. Considering health hazard World Health Organization (WHO) establishes the acceptable limit of 5 mg/l (PPM) of chlorine and 6.5 to 8.5 of pH value for drinking water [71]. In Bangladesh, till now water quality monitoring is generally performed in laboratory by using benchtop instruments. These benchtop laboratory instruments based approaches are very expensive and time consuming where on-site water quality assessment cannot be achieved.

Due to insufficient laboratory facilities in Bangladesh, it is therefore very significant to utilize the designed cost-effective, totally field-portable and easily accessible handheld smartphone-based colorimeter as an effective solution for real-time water quality monitoring. Moreover, it can analyze any liquid sample used for agricultural, environmental, biological as well as medical purposes. As proof of principle, the reported smartphone-based colorimeter has been practically implemented to determine rhodamine B concentration, chlorine concentration and pH level in water.



## 1.4 Objectives

The main objectives of the proposed research work are:

- ❖ To develop a smartphone-based totally self-contained smart sensing instrument: smartphone colorimeter using in-built flash LED and CMOS camera sensor of smartphone.
- ❖ To design and fabricate a very low cost, simple, lighter, field-portable and robust smartphone-based colorimeter by excluding the additional optics used in the conventional smartphone-based colorimeter.
- ❖ To incorporate the self-reference method for colorimetric detection which is totally constant irrespective of the wavelength and intensity of reflected light from sample solution.
- ❖ To design a versatile smartphone-based colorimeter that can be used for any type of colorimetric detection of different analytical parameters for a wide range of detection where wavelength or intensity or both color information are changed solely or simultaneously according to the change of analytical parameters.
- ❖ To estimate the wavelength of reflected light from the sample by incorporating a novel wavelength calibration technique in colorimetric detection.
- ❖ To develop a customized smartphone colorimeter app to capture, analyze, calibrate, save and represent the test results numerically.
- ❖ To evaluate the performance of developed smartphone colorimeter by quantifying RhB concentration, chlorine concentration and pH value of water as proof of principle

## 1.5 Dissertation Organization

The work presented in this research work is organized into five chapters. These five chapters are structured as follows:

**Chapter I** is entitled "**Introduction**". This chapter includes the motivation and objectives of this research work. A brief literature review in the field of smartphone-based colorimeter is also introduced.

**Chapter II** is entitled "**Fundamentals of Colorimetric Detection**". This chapter describes the basic components and operating mechanism of bench-top colorimeter, portable colorimeter and conventional smartphone-based colorimeter. Different types of color models and their applications are also presented in this chapter.

**Chapter III** is entitled "**Design and Fabrication of Smartphone-based Colorimeter**". The design and fabrication procedure of a totally self-contained, very low cost and field-portable smartphone-based colorimeter is reported in this chapter by utilizing the in-built flash LED, CMOS camera sensor, high resolution display and high computational power of smartphone. This chapter also introduces an android-based smartphone app development and wavelength estimation algorithm for colorimetric measurement.

**Chapter IV** is entitled "**Results and Discussion**". In this chapter the performance of the designed smartphone-based colorimeter is evaluated by implementing this instrument as Rhodamine B concentration quantifier, digital pH meter and chlorine concentration quantifier.

**Chapter V** is entitled "**Conclusion**". An appropriate conclusion and recommendations for future work are drawn here.

# Chapter II

## *Fundamentals of Colorimetric Detection*

---

### **Chapter Outlines:**

- 2.1 Introduction**
  - 2.2 Bench-top Colorimeter**
  - 2.3 Portable Colorimeter**
  - 2.4 Smartphone-based Colorimeter**
  - 2.5 Light Source and Detector**
  - 2.6 Color Models**
  - 2.7 Conclusion**
-

## 2.1 Introduction

Colorimeter is a light-sensitive device used to detect color change information such as color ratio, color intensity and wavelength. It is normally used for measuring the transmittance of light passing through a liquid sample or measuring the reflectance of light from a solid or liquid sample. The colorimeters used in industries can be classified as color densitometers and color photometers. The color densitometers measure the color density of primary colors in a color combination of a test sample. The color photometers are used for measuring the reflectance of color as well as the transmission. The working principle of colorimeters is generally based on the Beer-Lambert's Law, according to which the absorption of light transmitted through the medium is directly proportional to the medium concentration. Colorimeters are used for a wide range of applications across the chemical and biological fields including, but not limited to, the analysis of blood, water, nutrients in soil and foodstuffs, determining the concentration of a solution, determining the rates of reaction, determining the growth of bacterial cultures and laboratory quality control. Besides being used for basic research in chemistry laboratories, colorimeters have many practical applications such as testing water quality by screening chemicals such as chlorine, fluoride, cyanide, dissolved oxygen, iron, molybdenum, zinc, and hydrazine. They are also used to determine the concentrations of plant nutrients such as ammonia, nitrate, and phosphorus in soil or hemoglobin in the blood. Colorimetry is also used in color printing, textile manufacturing and paint manufacturing for precise quality inspection.

## 2.2 Bench-top Colorimeters

The colorimeters which are conventionally used in laboratories for colorimetric measurement in the optical domain are generally denoted as bench-top colorimeter and these are bulky, costly, sophisticated and not field-portable at all. The bench-top colorimeters are totally unsuitable for cost-effective on-site and real-time detection and quantification of analytical parameters within a short time without the need for trained personnel.

In order to perform colorimetric measurement by bench-top colorimeter, at first calibrate the device by using blank sample (distilled water) used as standard to set absorbance at 0 and transmittance at 100% and thus remove the effect of dark current. During sample measurement the lid of the sample holder should ideally be kept in the closed position to eliminate the possibility of erroneous results caused by the ingress of stray light. The light emitted from light source is filtered to select the correct wavelength for the specific tests being performed. A beam of light is fed into a liquid sample and the field-portable then flows through a set of lenses. The lenses send this colored light into a photocell for detecting the light passed through the solution and compares the color to a prerecorded standard. A microprocessor then calculates the absorbance or percent transmittance and sends the readings and results to the display screen.

When monochromatic light passes through a colored solution, some specific wavelengths of light are absorbed, which can be identified by measuring the difference between the amount of light at its origin and that after passing the solution. These devices are most commonly used to determine

the unknown analytical parameters based on color information of the transmitted or reflected light from the sample by the application of the Beer-Lambert law which stated that the absorption of light transmitted through the medium is directly proportional to the medium concentration. So bench-top colorimeter mainly consists of light sources for sample illumination, detectors to sense the desired color information, optics (lenses, diffusers, reflectors, etc.) for appropriate and proper light collection, processing unit to analyze, calculate, estimate, save and display the desired readings and results on an LCD or LED screen, sample holder in an enclosed chamber to isolate the effect of stray light from environment. In addition, a bench-top colorimeter contains a power supply module with voltage regulator and protection circuitry. Routine maintenance is required for bench-top colorimeter to monitor its functionality and ensure optimum performance. The pictorial view of two commercial bench-top colorimeters is shown in Fig. 2.1.



Fig. 2.1: Pictorial view of commercial bench-top colorimeter, Model: (a) CR-5, Konica Minolta and (b) ColoroMat 100.



Fig. 2.2: Pictorial view of commercial portable colorimeter, Model: (a) DR300 and (b) 3NH NH300.

### 2.3 Portable Colorimeters

Bench-top colorimeters are very bulky and thus only useful for laboratory-based testing rather than real-time on-site detection. In some cases, samples in the fields of environmental and clinical items analysis are likely to change their properties with passes of time and so their analytical results should be obtained as soon as possible. This leads to the development of a field-portable colorimeter for real-time on-site colorimetric measurement. A portable colorimeter does not involve complicated components and thus it becomes light in weight, compact and cheaper than bench-top colorimeters. It is capable of being operated by small dry batteries and so it is suitable for real-time on-site colorimetric applications. Apart from this, the portable colorimeter must be calibrated every time as it is used for colorimetric measurement. Recently commercial portable colorimeters are marketed for on-site applications as pictured in Fig. 2.2 which are very expensive. The commercial bench-top and portable colorimeters that are mostly available in market are tabulated in Table 2.1 with their fundamental features and market price for proper comparison.

**Table 2.1: Attributes of mostly available commercial bench-top and portable colorimeters**

Type (Model)	Detector	Light source	Display	Dimension	Weight	Wavelength range	Power supply	Price
<b>Bench-top Colorimeter</b> (Model 605, JENWAY)	Silicon photocell	Tungsten filament	2½ digit, 17mm LCD display	300 × 355 × 120 mm	3kg	400-710 nm	115V or 230V, 50/60Hz, 20W, AC	\$350
<b>Bench-top Colorimeter</b> (LCOM-A10, LABTRON)	Silicon Photo-cell	6V, 0.5 A tungsten lamp	LED three-digit display	280 × 220 × 122 mm	3 kg	420-660 nm	110V or 220V, 10W, AC	\$290
<b>Bench-top Colorimeter</b> (CR-5, Konica Minolta)	Dual 40-element silicon photodiode arrays	Pulsed xenon lamp (with UV cut filter)	5.7 inch TFT color LCD	475 × 192 × 261 mm	5.8 kg		100-240V, 50/60 Hz, AC	\$1400
<b>Bench-top Colorimeter</b> (ColoroMat 100)	Silicon photo diode	Halogen lamp, 12 v, 20 W	Graphic Display	140 × 380 × 135 mm	4.8 kg	340-900 nm	85-265V, 47-63 Hz, 42.5 W, AC	\$734
<b>Bench-top Colorimeter</b> (Saccharoflex 2020)		Tungsten halogen lamp, 12 V, 20 W	LCD, one line, 16 characters	220 × 260 × 480 mm	8.3 kg	495-620 nm	100-240V, 50-60Hz, AC	\$1500
<b>Bench-top Colorimeter</b> (SMART 2, LAMOTTE)	4 silicon photodiodes with integrated interference filters	4 LEDs	Graphical 4 line, 16 character per line LCD display	8.5 × 16.2 × 16.7 cm	312 gm		Battery Operation: 9 volt alkaline Line Operation: 120/220V, 50/60 Hz with adapter	\$530
<b>Portable Colorimeter</b> (3NH NH300)	Silicon photoelectric diode	D65 D50 A		205 × 70 × 100 mm	500gm		Rechargeable lithium-ion battery 3.7V, 3200mAh	\$953
<b>Pocket Colorimeter</b> (DR300)	Silicon photodiode	LED	LCD with backlight	34 × 69 × 157 mm	0.25 kg	500-655 nm	Four AAA alkaline batteries	\$440

## 2.4 Smartphone-based Colorimeter

Both of the bench-top and portable colorimeters require some essential components such as light source, processing unit, detector, display, and power supply. If a smart sensing instrument can be incorporated that equipped with all of the above components inherently then colorimetric measurement will be most simple and cost-effective. To meet this, researchers across the world have been restlessly working to implement smartphones as a low cost and user-friendly colorimetric tool for the quantification of analytical parameters since all of the required components of conventional colorimeters are available in smartphones. At beginning, smartphones were used mainly for communication purposes but with the enormous advancement of smartphone technologies over time such as in-built flash LED, high-resolution CMOS detector, fast computational power, high-resolution display, and long-lasting battery together have paved the way to develop cost-effective and easily accessible modern smartphone-based colorimeter as an effective alternative of highly expensive bench-top and portable colorimeters. Moreover, nowadays smartphones can transmit real-time data to anywhere in the world because of Internet-of-Things (IoT) connectivity such as 3G/4G, Wi-Fi, Bluetooth, GPS, and near-field sensors (NFS) which have enabled smartphone colorimeter to operate in a vast range of environments across the globe where bulky bench-top colorimeters cannot be deployed.

The pioneering work of mobile phone-based colorimetric detection was achieved in 2008 by developing a prototype system for quantifying bioassays and for exchanging the results of the assays digitally with trained personnel located off-site. Here mobile phone was used as an imaging device to capture images of colorimetric assay of paper-based microfluidic devices i. e. CMOS image sensor of the mobile phone was only used. Digitizing the color change information of the microfluidic paper by mobile phone camera, the captured images were sent to an off-site laboratory for further analysis with the help of high processing computer by a trained medical professional. The results of colorimetric assay provided by an expert were then exchanged to the assay site through established communications infrastructure [14]. The workflow of this colorimetric prototype was illustrated in Fig. 2.3. The whole procedure consists of a series of works starting from preparation of paper-based microfluidic device to perform colorimetric assay and finally received the results of colorimetric measurement from a medical professional. The smartphone at that early age was not capable of image processing, so an external high processing computer was required for image processing to analyze the color change information and quantify the unknown parameter. As a result, this prototype system is very time consuming which is not applicable for emergency disease diagnosis and real-time monitoring purposes.



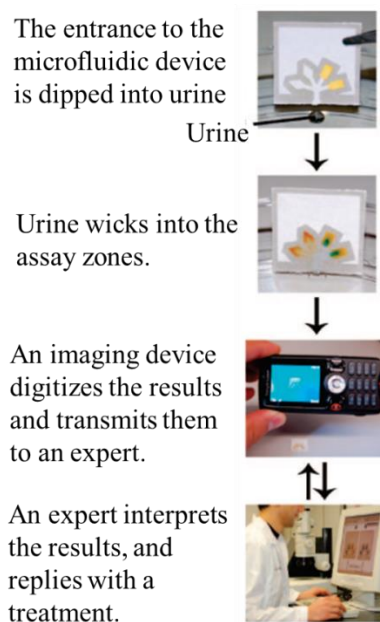


Fig. 2.3: Illustration of the workflow of a mobile phone-based first colorimetric prototype system for the simultaneous analysis of glucose and protein in urine [14].

With the advancement of smartphone sensing capabilities and processing power, the smartphone becomes an analytical tool as powerful as low-cost personal computers thus overcome the requirement of external computer for colorimetric measurement. In paper [36], smartphone was used not only for imaging purposes but also for processing, extracting the color change information, calculating the analyte concentration and presenting the results of colorimetric measurement to the user. It had been made possible through the development of a customized smartphone app based on advanced detection algorithm for image processing in order to optimize the computational speed and provide accurate analytical measurements. Analyzing the captured images by customized smartphone app, the intensity of color associated with each colorimetric assay was detected to find color ratio and based on this color ratio chlorine concentration in drinking water was measured by using a smartphone-based colorimeter shown in Fig. 2.4. In this case both CMOS image sensor and processing unit of smartphone was utilized for direct colorimetric measurement which provided almost similar results as the laboratory bench-top colorimeters.

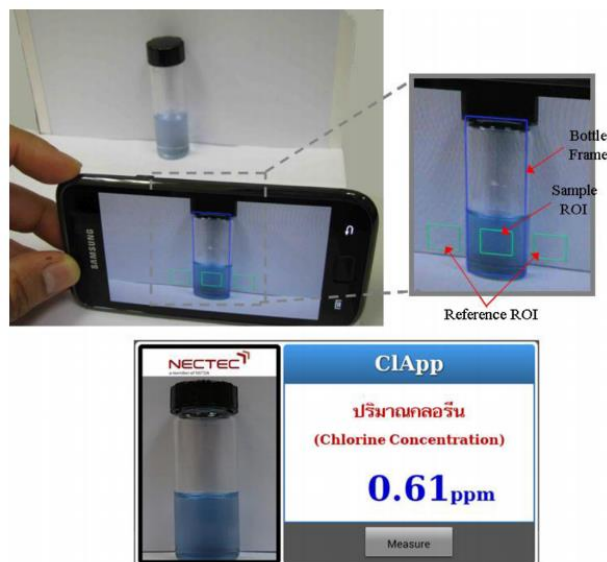


Fig. 2.4: Detection of chlorine concentration by using smartphone as an analytical device [36].

One of the major drawbacks of direct colorimetric measurement was to manually position the components (such as light source, sample holder, etc.) within the measuring platform at the same distance from camera lens of the smartphone for precise colorimetric measurements. The reason behind this is that with change in the distance between the camera lenses to the sample holder, the amount of light collection by the smartphone camera was also changed which introduced different analytical results of a single analyte. As a result, the lack of fixed and compact arrangement of colorimetric platform introduced significant errors in smartphone-based colorimetric measurements.

To meet the importance of compact colorimetric platform, a custom-designed 3D printed lightweight opto-mechanical attachment was introduced [16], [18], [28], [34], [35], [38], [39] which made of plastic materials (such as PLA, ABS, etc.) and attached with the CMOS camera unit of smartphone. This 3D attachment was designed in such a way to integrate all the optics (reflector, diffuser, etc.) and components used for smartphone-based colorimetric detection at definite position with definite alignment specified by the designer. Positioning all the used optics and components to their corresponding slot within the fabricated closed chamber, the variations of light illumination due to the distance variation between the camera lenses and the sample holder was removed. Moreover, the complication of stray light incorporated during colorimetric measurement had been terminated by using this closed enclosure that ensured constant analytical results of a single analyte with highest accuracy.

As the resultant smartphone-based colorimetric platform became totally enclosed, external light sources were used to provide fixed illumination to the enclosed chamber. These external light sources were powered by external batteries and controlled by ON/OFF switch [16], [22] [35]. The 3D structure of the fabricated optomechanical attachments is shown in Fig. 2.5.

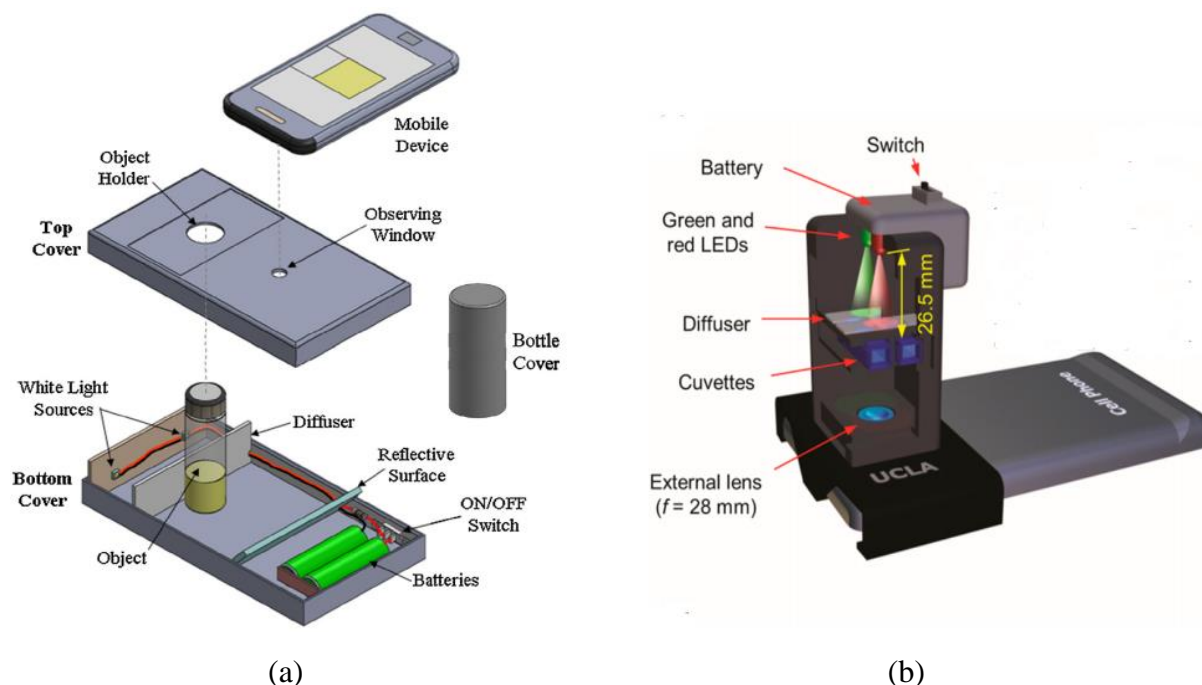


Fig. 2.5: 3D schematic illustration of the internal structure of the opto-mechanical closed chamber for colorimetric detection of (a) chlorine [18] and (b) mercury [35] in drinking water on smartphone platform.

Here, diffuser optics was used to ensure uniform illumination but at the same time it also reduced the intensity of light emitted from light source. Again the requirement of external batteries to operate the external light sources increased the overall weight of the opto-mechanical attachment and serves as a hindrance in terms of the portability of smartphone-based colorimetric devices for field tests. In addition to this, the lifetime of the external LEDs, as well as external batteries, is not long enough and as a result replacement of these light sources and batteries is required at a regular interval in case of failure. However, the important considerations for designing a high-performance field-portable instrument are the compactness, lightweight and sustainability of the device for long duration.

In order to avoid the complexity of externally powered light sources, in-built flash LED has been utilized along with the CMOS camera sensor of a smartphone which made the colorimetric detection technique more cost-effective and completely field-portable [23], [28], [34]. The lifetime of smartphone flash LED is so long compared to other external light sources used in smartphone-based colorimetric measurement and it does not require additional batteries to operate as it gets power from long-lasting lithium-ion battery of smartphone. Moreover flash LED of smartphone ensures high-intensity constant illumination to the enclosed chamber of smartphone attachment without any types of maintenance. The 3D structure of smartphone-based colorimeter where illumination is derived from the in-built flash LED of the smartphone itself is shown in Fig. 2.6.

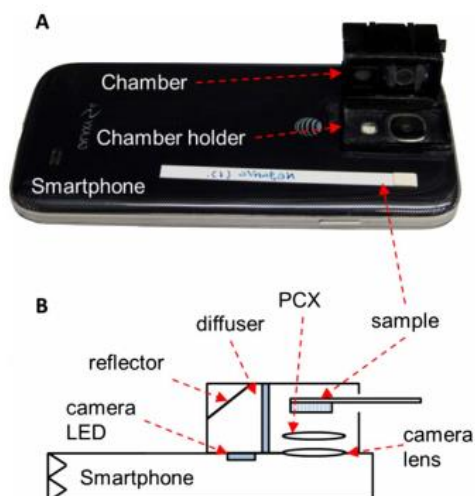


Fig. 2.6: Utilization of smartphone flash LED as the optical source in smartphone-based colorimetric detection (A) 3D structure (B) internal components of a 3D structure [23].

Besides reflector and diffuser, the additional plano-convex lens is positioned in front of camera lens to maximize the light collection as diffuser optics reduces the intensity of light. In the present case, light source, processing unit, and detector, three essential parts of colorimetric measurement are provided by smartphone but additional optics incorporated here which increases the fabrication cost of this type of smartphone-based colorimeter [23].

## 2.5 Light Source and Detector

In this research, we proposed a very low cost, field portable and entirely self-contained universal smartphone colorimeter that does not require any optics and can perform any types of colorimetric measurement with the highest accuracy by utilizing the in-built white flash LED (light source) and CMOS camera sensor (detector) of smartphone.

### 2.5.1 Light Source

One of the essential parts of smartphone-based colorimetric detection is an optical source to illuminate the measuring platform. Earlier smartphone-based direct colorimetric measurement was performed by using the ambient light of outdoor sunlight. But direct colorimetric imaging using smartphone CMOS camera introduced significant errors due to the variation of ambient light illumination [36]. The problem of direct colorimetric imaging was removed by incorporating one or more externally powered light sources of different types such as LEDs [16], [22], [35], fluorescent lamps [21], [40], outdoor sunlight [37], white LCD screen [42] etc. to provide fixed illumination for the closed colorimetric platform. In advanced smartphone colorimeters, in-built flash LED of smartphone was utilized as light source to remove the complexity of externally powered light sources. White illumination of smartphone flash LED,

with its long lifetimes and energy efficiencies made the smartphone-based colorimetric detection more cost-effective and completely field-portable [18], [23], [28], [34]. Moreover, as the resolution of the camera sensors is increasing, the size of each pixel is decreasing and consequently the light sensitivity is dropping. Thus, white LED of smartphone can be an efficient alternative to capture quality images that require very small amount of energy from the lithium-ion battery of smartphones (usually between 2.8 V and 4.2 V) and provide continuous constant illumination. This bright white flash LED of smartphone is a current-driven device in which the light output depends directly on the forward current passing through it and has very short rise times, in the range of 10 to 100 ns. The white light is produced by the combination of the blue photons emitted from forward biasing InGaN chip and yellow light, a result of phosphor excitation by blue photons. The resultant lighting quality is comparable to that of cool white fluorescent lamps, with a color rendering index near 85. In addition to lower power consumption with drive circuitry, no significant electromagnetic interference (EMI) generated from driving an LED flash. On the other hand, most of the digital camera modules currently being used in camera phones have a 50 to 60-degree field of view and need a minimum of 3 to 5 lux to capture a good picture. Considering this, camera flash has been designed by the manufacturers with 50 to 80-degree illumination angle. Because an illumination angle wider than 80 degrees will cause a portion of light to fall outside the camera's coverage, under-utilizing the light output from the LED, on contrary a flash with a smaller illumination angle might cause dark areas on the corners of the captured image. The spectral response of this broadband light source is shown in Fig. 2.7 which covers the whole visible range from 400 nm to 700 nm but lacks cyan (around 475 nm) spectral parts [72].

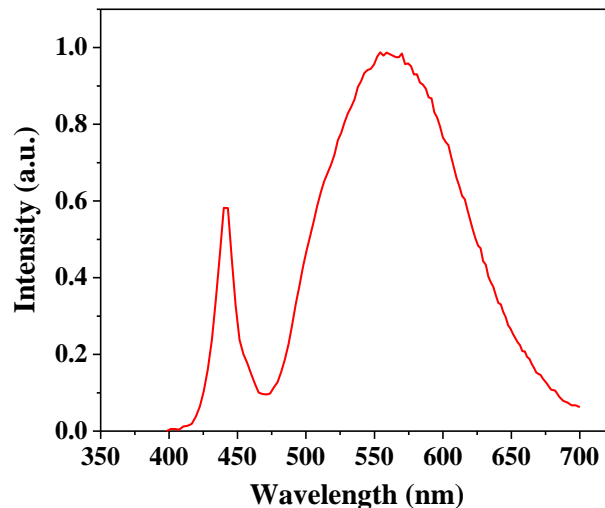


Fig.2.7: Spectral responses of smartphone flash LED covers a wide bandwidth ranging from 400 nm to 700 nm.

### 2.5.2 Detector

In the developed universal smartphone colorimeter, a high-resolution CMOS camera of smartphone is used to detect the color change information of colorimetric measurement. The detail working procedure of CMOS detector is illustrated in Fig.2.8. Digital image sensors are a vital part of the smartphone camera. They are the light-sensitive 'film' that records the image and allows taking a picture. A CMOS camera sensor is mainly made up of three different layers of micro-lens, Bayer filter, and sensor substrate.

When the smartphone camera is turned on, the incoming light containing both infra-red (IR) and visible light components pass through the IR blocking filter. IR filter blocks light outside the visible spectrum to improve color fidelity and image quality. Then the resultant visible light is passed through a low pass filter to block the high spatial frequencies and reduce moiré effect. The output light of the low pass filter is passed through a layer of micro-lens that sits above the Bayer filter and helps each pixel to collect as much light as possible. The pixels of the CMOS sensor do not sit precisely next to each other and there is a tiny gap between them. Any light that falls into this gap is wasted light, and will not be used for the exposure. The micro-lens aims to eliminate this light waste by directing the light that falls between two pixels into one or other of the adjacent pixels. The collected light is then focused on the CFA (color filter array) also known as Bayer sensor which is an array of RGB color filters arranged in Bayer pattern and placed in front of the image sensor array of a camera to capture definite color information. Because of the alternating Red/Green and Blue/Green arrangement, it is sometimes called an RGBG filter. Each color filter of CFA corresponds to a pixel in the sensor array allows a specific wavelength of light in red, green or blue band only to pass, which is predetermined during the camera design. This is achieved by filtering out the other wavelengths of unwanted color except red, green and blue. For example, the red filters will only allow red light photons to pass into the pixel below it. Similarly, the green and blue filters will only allow green and blue light, respectively, to pass into the pixels below [37].

The Bayer filter uses twice as many green filters as compared to red or blue filters because both the M and L cone cells of the retina of human eyes are highly sensitive to green light rather than red or blue light and has a much greater resolving power in that range. The purpose of color filters is to control the color light reaching the sensor array because the image sensors can only detect light intensity, and not wavelength, which indicates the color of light. The image sensor array is made of silicon material and composed of millions of light-sensitive areas or pixels which are responsible for capturing the intensity of the pre-filtered light passing through CFA. The sensor array is not actually flat and can be thought of as a group of buckets that trap the incoming light and allow it to measure. The number of photons falling into each bucket determines the brightness level at each pixel.

The raw output from an image sensor overlaid with CFA is called as or the mosaiced image which contains only red, green, blue color information. The mosaiced image needs to be converted to a full-color image by a process called color image demosaicing, which is a digital image processing used to reconstruct a full-color image from the incomplete color samples output from an image sensor. To reconstruct a full-color image, various demosaicing algorithms

are used that involve interpolation of missing color values from nearby pixels. Through interpolation, the color of a blank pixel is computed as the average of the two or four adjacent pixels color. The estimated color value of all pixels is recorded as 8-bit number (0 to 255) and manipulated to reconstruct the full-color image on the smartphone screen, arranged in a 2D matrix of red, green and blue AMOLEDs (Active Matrix Organic Light Emitting Diode). Therefore the color intensity of smartphone-based colorimetric detection is the per-pixel RGB value of the image directly read from smartphone screen by using a smartphone app.

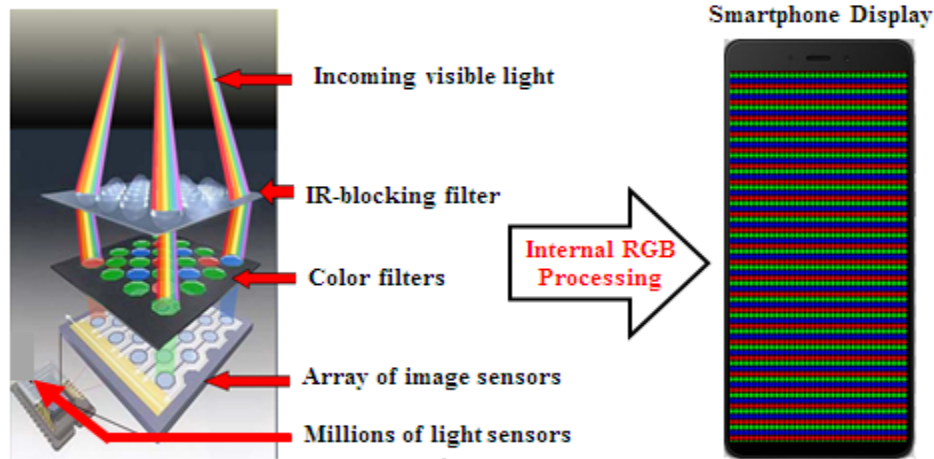


Fig. 2.8: Illustration of color image detection and reconstruction procedure by the CMOS image sensor of a smartphone [73].

## 2.6 Color Models

A color model is a digital representation of possibly contained colors formally and numerically within a mathematical formula. It is a system for measuring colors that can perceive by humans and a process of combining different values as a set of primary colors (red, green, and blue) [74]. Color models are divided into two categories; additive and subtractive. Colors perceived in additive models are the results of transmitted light but color perceived in subtractive models are the results of reflected light. Additionally each color model has its own representation space and components, with the ability to transform from one color model to another through standard formula. Different color models are suitable for different applications and thus the selection of proper color models for a specific application depends on the properties of the model.



### 2.6.1 CIE color spaces

The most popular system of color representation is the International Commission on Illumination (CIE) system, first published in 1931, which has become the international platform to standardize and reproduce colors across many different professions and industries and is considered to be the basis of modern colorimetry. For the first time, CIE 1931 color space defined quantitative links between distributions of wavelengths in the electromagnetic visible spectrum and physiologically perceived colors in human color vision. It is a mapping system that uses tristimulus (a combination of 3 color values that are close to red, green or blue) values, which are plotted on a 3D space and their combination can reproduce any color that a human eye can perceive. This color space illustrates the proportions of each primary color rather than the actual amount used and able to accurately represent every single color according to the chromatic response of human eye [75]. The chromaticity diagram of CIE color space is shown in Fig. 2.9.

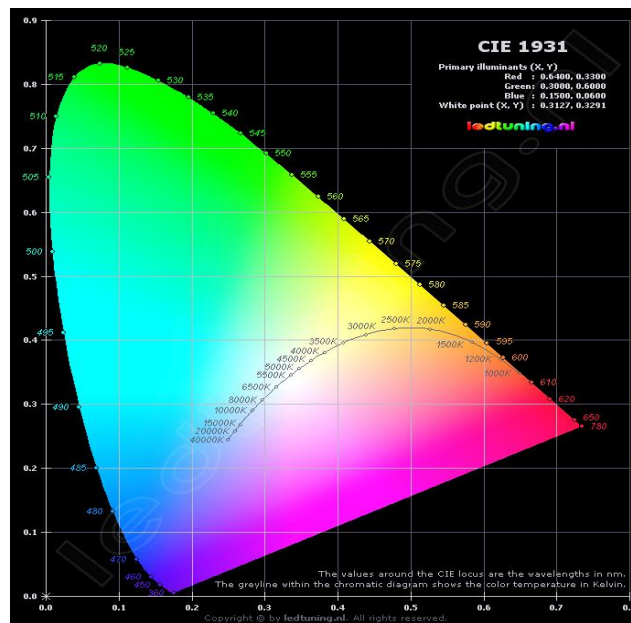


Fig. 2.9: CIE 1931 color space.

### 2.6.2 RGB color model

The RGB (red, green and blue) color model is an additive color model in which red, green and blue light are added together in various ways to reproduce a vast array of colors. The main purposes of the RGB color model are to sense, represent and display the images in electronic systems, such as television screens, computer monitors, and smartphones. RGB color model represents the color information of the input digital image acquired by a camera or scanner in terms of three primary color components from the light beam collected by camera lens [76].



To form a color with RGB, three light beams (one red, one green, and one blue) must be superimposed and each of these color components has an arbitrary intensity value ranges from 0 (least saturated) to 255 (most saturated). This means that 16,777,216 different colors can be reproduced in the RGB color space where zero intensity for each component represents the darkest color (no light, considered as black), and full intensity of each represents a white. If all the components have same intensity then the resultant color will be a shade of gray, darker or lighter depending on the intensity. However, in case of different intensity, the result is a colorized hue, more or less saturated depending on the difference of the highest and lowest intensities of the primary colors employed. When one of the components has the highest intensity, the color is a hue near this primary color. On the other hand, if two components have the same highest intensity the induced color is a hue of a secondary color (yellow, cyan and magenta). It means secondary color is the sum of two primary colors of equal intensity. For example cyan is the composition of equal intensity green and blue colors, similarly magenta is the composition of equal intensity red and blue colors, and yellow is the composition of equal intensity red and green colors. Every secondary color is the complement of one primary color and when a primary and its complementary secondary color are combined together then white color is formed. The formation of secondary colors and the corresponding RGB values are shown in Fig. 2.10.

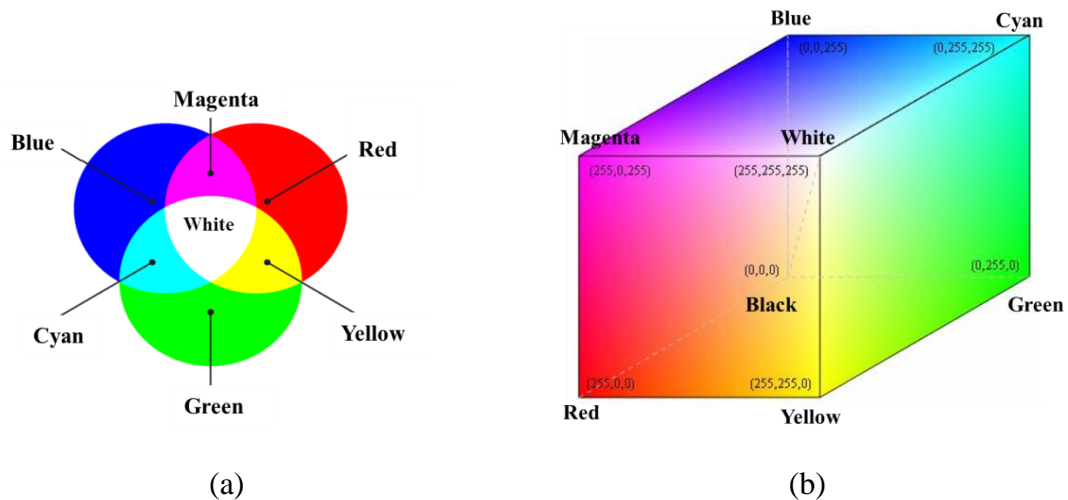


Fig. 2.10: RGB color model illustrating (a) primary and secondary colors (b) RGB color cube with their corresponding red, green and blue color components values in rectangular co-ordinate system.

In general, the color image reconstructed on a smartphone screen is a combination of RGB color components, as a result, RGB values can obtain directly from any color image by splitting the color of each pixel. Therefore, RGB color model is best suited for on-screen applications such as image processing where per-pixel information of a color image represents the value of RGB color components. However, RGB is a device-dependent color model that means different devices detect or reproduce a given RGB value differently since the color elements (such as

phosphors or dyes) and their response to the individual R, G, and B levels vary from manufacturer to manufacturer, or even in the same device over time. Thus an RGB value does not define the same color across devices without some kind of color management. Apart from this, RGB color model is highly sensitive to light and with change in light illumination the analytical results based on this model also changes.

### 2.6.3 HSV Color Model

HSV (hue, saturation, value) is a well-known hue-based representation of the RGB color model which describes colors (hue) in terms of their shades (saturation) and brightness (value). HSV is a cylindrical coordinate system equivalent to the RGB rectangular coordinate system but in HSV color model, a color is defined by its wavelength, tone and brightness or blackness value and thus it resembles the human color perception more than the RGB additive color model. The hue is angularly distributed; therefore its values vary between  $0^\circ$  and  $360^\circ$ . Hue represents the type of color (such as red, green) according to its angular dimension, starting at the red primary at  $0^\circ$ , passing through the green primary at  $120^\circ$  and the blue primary at  $240^\circ$ , and then wrapping back to red at  $360^\circ$  (Fig. 2.11). The saturation of a color is described in percentages and varies between 0% and 100% (or 0 to 1). 100% saturation means a completely saturated and pure color, the smaller the saturation, the more the color turns to a neutral gray and the more faded the color will appear. The brightness of any color is represented by value, changes along the central vertical axis of HSV geometry, ranges from black at brightness 0 or value 0 at the bottom, to white at brightness 1 or value 100% at the top. If both, the saturation as well as the brightness is 100%, a pure color result. 0% saturation and 100% brightness represents white color and for all cases in which the brightness is 0%, it represents black.

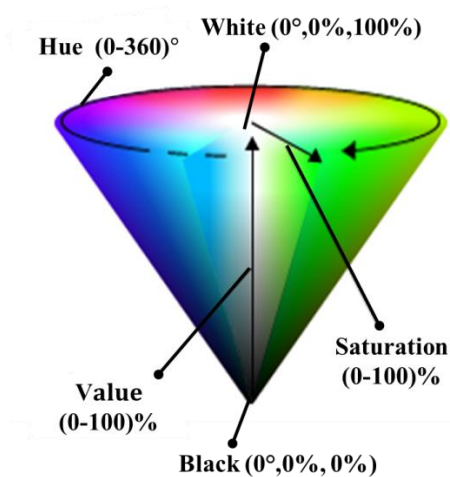


Fig. 2.11: Representation of HSV color model with their corresponding hue, saturation and value color components.

HSV color model has important applications in computer vision and image analysis for feature detection or image segmentation. In case of illumination fluctuation or in high illumination conditions simple RGB color model is not suitable. In these conditions, more stable HSV color models are mostly preferable to extract the actual information of the image since it is invariant to illumination changes and robust to any illumination conditions.

#### 2.6.4 Conversion from RGB to HSV color model

Colors of any substances or liquids can be processed using the RGB color model or HSV color model. As RGB color model is more sensitive to light illumination, the RGB color components of an object in a digital image are correlated with the amount of light hitting the object. As a result, with variation of light illumination, per pixel color information of an image described in terms of RGB will be changed. Moreover, the color of light is a function of its wavelength (depends on hue) and with the change of wavelength alternative color is formed. For quantitative analysis where color stability plays an integral role, HSV color model is most suitable to obtain more precise and more stable color information over RGB model. Additionally, HSV color model is less sensitive to illumination variations and represents color according to their wavelength or hue parameter. The directly obtained RGB values of any color image can be easily converted to HSV parameters through standard formula [49].

To convert RGB color components into HSV color components, at first the achieved per pixel RGB values of a color image is divided by 255 to change the range from (0~255) to (0~1).

$$R' = \frac{R}{255} \quad (2.1)$$

$$G' = \frac{G}{255} \quad (2.2)$$

$$B' = \frac{B}{255} \quad (2.3)$$

Then the maximum and minimum values from these  $R'$ ,  $G'$  and  $B'$  values are calculated as

$$C_{max} = \max(R', G', B') \quad (2.4)$$

$$C_{min} = \min(R', G', B') \quad (2.5)$$

$$\Delta = C_{max} - C_{min} \quad (2.6)$$

Where  $\Delta$  is the deviation between the smallest and largest value of  $R', G', B'$ . Now based on the values of  $C_{max}$  and  $\Delta$ , HSV color components are calculated as follows

$$H = \left\{ \begin{array}{l} 0^\circ \\ \frac{(R' - B')}{\Delta} \times 60^\circ \\ \left\{ \frac{(B' - R')}{\Delta} + 2 \right\} \times 60^\circ \\ \left\{ \frac{(R' - G')}{\Delta} + 4 \right\} \times 60^\circ \end{array} \quad \begin{array}{l} \Delta = 0 \\ C_{max} = R' \\ C_{max} = G' \\ C_{max} = B' \end{array} \right\} \quad (2.7)$$

$$S = \left\{ \begin{array}{l} 0 \\ \frac{\Delta}{C_{max}} \times 100\% \end{array} \quad \begin{array}{l} C_{max} = 0 \\ C_{max} \neq 0 \end{array} \right\} \quad (2.8)$$

$$V = \{C_{max} \times 100\% \} \quad (2.9)$$

## 2.7 Conclusion

In this chapter, the fundamentals of various colorimetric detection (including bench-top, portable and smartphone-based colorimeter) with their advantages and disadvantage are represented elaborately. From all of the above discussion it can be concluded that the low cost, field portable smartphone-based universal colorimeter can open a new window in the field of colorimetric detection. A colorimeter is the most inexpensive and simplest analytical instrument that has versatile applications for the detection of biological, environmental and agricultural items as well as in color printing, textile manufacturing, and paint manufacturing purposes. However, it does not work in ultra-violet (UV) and infra-red (IR) regions and cannot be used for colorless compounds. In addition to these similar colors from interfering substances can produce errors in colorimetric measurement.

# Chapter III

## *Design and Fabrication of Smartphone-based Colorimeter*

---

### Chapter Outlines:

**3.1 Introduction**

**3.2 Optical Layout Design**

**3.3 3D Design and Fabrication**

**3.4 Android-based Smartphone App Development**

**3.5 Wavelength Estimation**

**3.6 Conclusion**

---

### 3.1 Introduction

In this chapter, a totally self-contained, low cost and field-portable smartphone-based colorimeter is designed and fabricated utilizing the in-built flash LED, CMOS camera sensor, high resolution display and high-computational-power smartphone by excluding the additional expensive optics, external light sources and external power supply used in the conventional smartphone-based colorimeters. 3D printing technology is incorporated to fabricate the designed smartphone-based colorimeter. For the proper functioning of the fabricated smartphone-based colorimeter, a customized smartphone app is developed to capture the digital image and then process it to investigate the color change information of any colored analyte. The developed app can also be used to calibrate the designed smartphone-based colorimeter and saved the results of colorimetric detection. A novel interpolation and extrapolation algorithm is proposed and incorporated with the developed app to estimate the wavelength of the reflected light from the test specimen.

### 3.2 Optical Layout Design

Optical layout of the proposed smartphone-based colorimeter is shown in Fig. 3.1 which consists of two parts; a smartphone and an optical enclosure in which sample holder has to be placed. Self-contained feature is achieved by utilizing internal power supply, in-built flash LED, CMOS camera detector and high-speed processor embedded with the smartphone. The goal of self-illumination of this sensing instrument is achieved by utilizing smartphone flash LED as light source which ensures constant and sufficient illumination for the smartphone-based colorimetric measurement. The constant illumination irrespective of testing environment is maintained by the perfectly designed optical enclosure which prevents variation of illumination by blocking unwanted optical signals from environment. The flash LED also facilitates to measure without using powerful external light sources and provides a low cost, field-portable and compact smartphone-based colorimeter. Its wide spectral ( $\lambda= 400\sim 700$  nm) emission propagates in all directions and provides continuous and constant illumination to the measuring platform and the sample holder placed in front of the in-built flash LED. The sample holder can hold the test sample (liquid or solid substance) that form color in presence of a specific chemosensor.

The light from flash LED strikes on the plane surfaces of the 3D enclosure surrounding the measuring platform and changes the direction of propagation due to the reflection from smooth white surfaces. So the cuvette (12.5×12.5×45) mm containing sample is illuminated by the directly emitted light as well as the reflected light from the surfaces of the enclosure. The incoming light denoted by the white arrow in Fig. 3.1 contains all wavelength components of the visible spectrum and when it passes through the sample solution (10 mm optical path length), a specific wavelength band is absorbed by the colored sample solution in the glass cuvette. Apart from the absorbed wavelength, the reflected signals propagate toward the CMOS camera of the smartphone from the smooth white surface of the optical enclosure just behind the cuvette denoted by the magenta arrow in Fig. 3.1. The cuvette has been positioned within the FOV of the

camera to collect the maximum amount of reflected light from the test sample by the in-built focusing lens of the smartphone camera and imaged by CMOS camera sensor. So the light collected to the CMOS detector of smartphone is mainly the reflected light from the test sample. The captured image is processed by the customized app with the help of in-built processor of smartphone and displays the analyzed results on the high resolution smartphone screen. In this optical layout design, axis of the smartphone flash LED is used as the reference axis to assemble all other components of the smartphone-based colorimeter. Additional expensive optics (such as diffuser, reflectors and external lens) used in conventional smartphone-based colorimeters for sufficient light collection and uniform illumination are not used in the designed smartphone-based colorimeter to ensure the most cost effective optical design. There is no significant degradation in performance because of the exclusion of the expensive optics used in conventional smartphone-based colorimeter. It is important to ensure constant illumination rather than uniform illumination for the colorimetric detection.

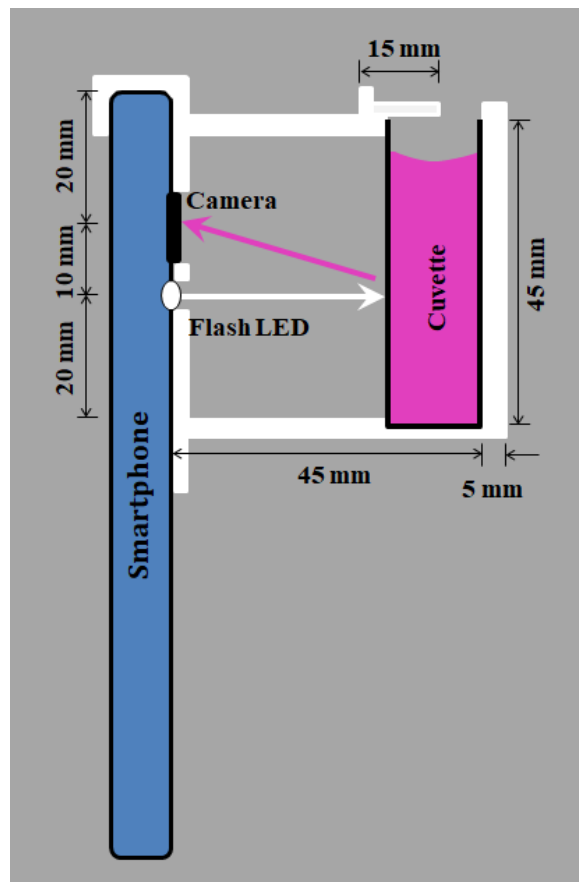


Fig. 3.1: Schematic optical layout of the designed smartphone-based colorimeter.

### 3.3 3D Design and Fabrication

To assemble the components of smartphone-based colorimeter at the appropriate position and alignment with smartphone, a 3D optical enclosure is designed in AutoCAD Mechanical 2018 which is compatible to Xiaomi Redmi Note 4 smartphone (13 MP rear facing camera, 1080×1920 pixels display resolution) as depicted in Fig. 3.2. The optical enclosure is designed in such a way to fit perfectly with the CMOS camera and flash LED unit of the specified smartphone. In order to do so, two windows one for CMOS camera and other for flash LED of smartphone are designed at a vertical distance of 20 mm and 30 mm far from the top of the smartphone having diameter 10 mm and 4 mm respectively for illumination through the inherent flash LED and capture the images of colorimetric measurement using CMOS camera.

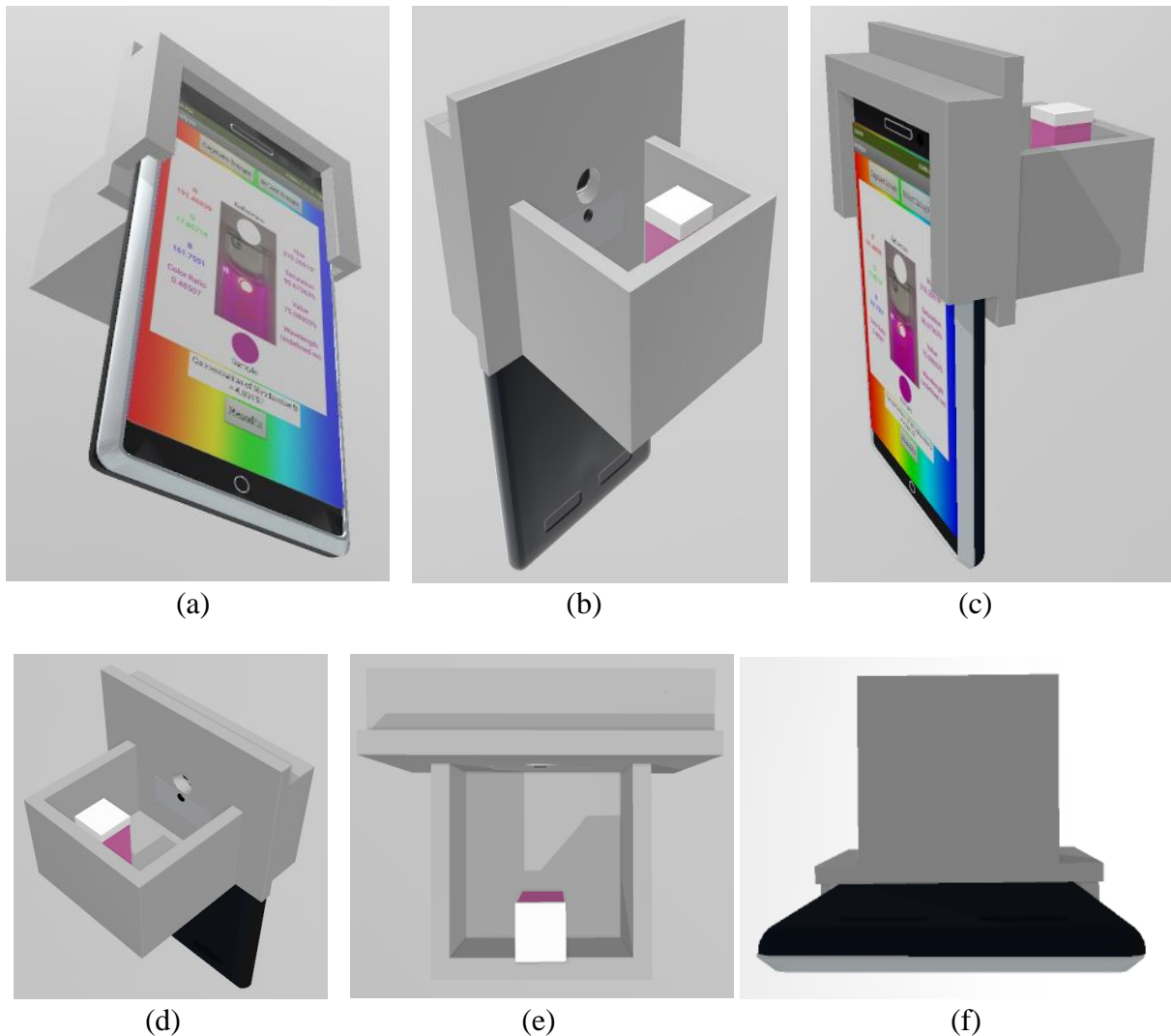


Fig. 3.2: 3D views of the designed optical enclosure attached with smartphone for colorimetric measurement (a) bottom left side corner view, (b) top right side corner view, (c) right side corner view, (d) top left side corner view, (e) top view and (f) bottom view.



A slot of  $13 \times 13 \times 2$  mm is designed at the bottom surface of the enclosure at a distance of 38.5 mm far from the horizontal axis of the flash LED to hold the sample holder (cuvette). A sliding shutter on the top of the sample holder is also designed to make the attachment optically enclosed and excludes the stray light entering into the 3D optical enclosure. Thus blocks ambient light and ensures constant illumination. All of the walls of the 3D attachment are designed considering a thickness of 5 mm which serves the purpose of optical isolation and the smooth white inner surfaces of the optical enclosure also work as reflector.

The designed optical enclosure is then saved in .stl file format. Before uploading the model in 3D printer, the model is needed to be sliced using slicing software that converts the .stl file into the machine readable .gcode file and defines the X, Y, Z coordinates of the model. Ultimaker Cura 4.0.0 is used as the slicing software to set all printing parameters and slice the 3D model according to the defined printing parameters. After slicing, the resultant .gcode file is saved and uploaded the file to the 3D printer through SD card. The designed smartphone attachments are fabricated using FDM (Fused Deposition Modeling) technology based Creality 3D printer of model 'Ender-3 pro'. For fabricating white colored PLA (Polylactic Acid) filament of diameter 1.75 mm is used. Here white PLA is chosen for printing purpose to avoid light absorbance by the inner surfaces of the fabricated optical enclosure.

For printing the 3D attachment of optical enclosure, white PLA filament is loaded to the printer extruder through a nozzle which heats the plastic filament to the melting point of the polymer. To do this, nozzle temperature of the extruder is fixed according to the type of filament. The nozzle head able to move in two coordinates (X and Z) above a printing bed moving in Y coordinate and deposits the melted filament layer by layer on the printing bed according to the structure of the designed object to fabricate the model.

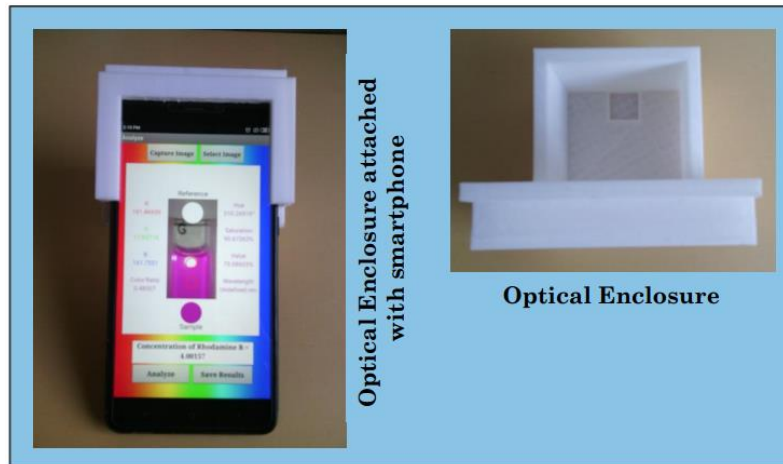


Fig. 3.3: 3D fabricated optical enclosure attached with smartphone to measure RhB concentration.

After completing the printing, the printed attachment is taken off from the printing bed by using a spatula and cleaned the supporting materials before attaching the model to the smartphone. To perform the experiment under totally enclosed colorimetric platform, a top cover is also designed and fabricated by the 3D printer which acts as a shield of stray light and thereby limits the variation of illumination and improves the system SNR.

This attachment keeps the sample holder at a specified lateral and vertical position from the camera lens for every colorimetric measurement and acts as a shield for stray light. The smartphone can be inserted from the bottom side of the fabricated 3D attachment and perfectly fitted with the specified camera and flash LED slots of the 3D attachment. For on-site measurements, the fabricated optical enclosure (weight 70 gm) temporarily has to be attached with smartphone to perform colorimetric measurement using the customized smartphone app. The features of the designed and fabricated smartphone-based colorimeter are summarized in Table 3.1.

**Table 3.1: Main features of the designed and fabricated smartphone-based colorimeter**

<b>Type (Model)</b>	<b>Smartphone-based Colorimeter (Model 001, EEE, KUET)</b>
<b>Detector</b>	<b>CMOS Camera Detector of Smartphone (13 MP, f/2.0, 1.12<math>\mu</math>m, PDAF)</b>
<b>Light Source</b>	<b>In-built White Flash LED of Smartphone (<math>\lambda=400\sim 700</math> nm, 2.8 V, 100 mA)</b>
<b>Display</b>	<b>Type:</b> IPS LCD capacitive touchscreen of Smartphone, 16M colors <b>Size :</b> 5.5 inches, 83.4 cm <sup>2</sup> <b>Resolution:</b> 1080 $\times$ 1920 pixels, 16:9 ratio
<b>Dimension</b>	<b>86<math>\times</math>70<math>\times</math>75 mm</b> (Without considering the size of smartphone) <b>86<math>\times</math>70<math>\times</math>165 mm</b> (With considering the size of smartphone)
<b>Weight</b>	<b>70 gm</b> (Without considering the weight of smartphone)
<b>Wavelength Range</b>	<b>410-680 nm</b>
<b>Power Supply</b>	<b>No external power supply is needed</b>
<b>Price</b>	<b>3.0 USD</b> (Excluding smartphone)

### 3.4 Android-based Smartphone App Development

For the colorimetric detection of unknown parameters of an analyte, android app ‘Smartphone Colorimeter’ is developed on cloud based ‘MIT App Inventor 2’ platform to digitally process the single image containing both sample and reference. Easily accessible ‘Smartphone Colorimeter’ app can be installed and operated with any android smartphone platform. The app consists of three operating buttons named as ‘Instructions’, ‘Select Test Type’ and ‘Calibration’ [Fig. 3.4(a)]. Each operating button linked with a separate window to perform a specific operation and enable to back main screen or forward the next step. By pressing the ‘Instruction’ button, a new screen named ‘Instruction’ is opened which describes the measurement guidelines and operation of the app [Fig. 3.4(b)].

In this research work, three different colorimetric measurements named as: Rhodamine B concentration quantifier, chlorine concentration quantifier and digital pH meter are incorporated within the customized app as shown in the ‘Select Test Type’ screen [Fig. 3.4(c)]. For RhB concentration quantifier, the device is calibrated by using known concentration RhB samples in the range of (0.2-4.0) PPM. Similarly, the chlorine concentration quantifier is calibrated against known concentration chlorine samples in the range of (0.1-8.0) PPM and the digital pH meter is calibrated against standard buffer samples with known pH in the range of (4.0-9.0). By selecting the desired colorimetric test from the list in the ‘Select Test Type’ screen, the specific measurement can be done. When a specific test type is selected, the ‘Analyze’ screen corresponds to the selected test type is opened to perform the colorimetric measurement [Fig. 3.4(d)]. In this app, there are options to analyze real time sample as well as analyze the image of previously recorded sample.

To analyze real time samples, the fabricated attachment is attached with the camera unit of the smartphone and inserted the sample holder at the definite cuvette slot inside the attachment. After placing the top cover of the attachment, the white flash LED of the smartphone is turned on to illuminate the sample in the enclosed chamber. The colorimetric information of the test sample is captured through tapping the ‘Capture Image’ button using the smartphone CMOS camera sensor. Then the captured image is processed by utilizing the fast processing capability of the smartphone to measure the desired analytes. To do so, two regions of interest (ROIs), one for sample and another for reference are selected on the image canvas which are aligned vertically in the same line [Fig. 3.4(d)]. The sample and reference ROIs are denoted by two red circles and zoomed in for exact identification and clarification of the ROIs. The purpose of the sample ROI is to collect the data in red, green, and blue color planes from the image of the test sample under investigation. A  $7 \times 7$  pixel array from this ROI is selected as the dimension of sample ROI. Per pixel RGB value of the selected ROI is extracted and the average RGB values are calculated by considering the total 49 pixels. Pixel array is selected instead of single pixel to achieve actual color information of the test sample under investigation by reducing detection error level.



Fig. 3.4: Screenshots images illustrating the workflow of the customized Smartphone Colorimeter app: (a) menu screen, (b) instruction screen, (c) select test type screen, (d) selected or captured image of the test sample uploaded in analyze screen, (e) colorimetric test results and (f) the calibration screen.

The white beam spot of the flash LED is chosen as the analyte independent reference ROI because the light energy at the beam spot of flash LED is very high. Thus the beam spot reflects white light rather than the original color of the test sample. Moreover, the intensity of the flash LED is maintained at a constant level below the saturation by properly designing the optical enclosure. In paper [36], a white background adjacent to the sample holder was considered as reference where the reflected light from the test sample affect the reference. As a result, the reference showed a color which is a shade of the test sample color rather than white. It clarify that, the color information of the reference is depended on test sample and introduces significant deviation in smartphone-based colorimetric measurement. Here, the selected reference ROI is also a 7x7 pixel array. The averaged RGB value of this reference ROI is used in conjunction with the averaged RGB value of sample ROI to calculate the color ratio according to the Eq. (3.1).

$$C_R = \frac{R_s/R_r + G_s/G_r + B_s/B_r}{3} \quad (3.1)$$

Here,  $R_s$ ,  $G_s$ , and  $B_s$  are the average color values corresponding to the red, green, and blue color components inside the sample ROI respectively. Similarly, the average RGB color values from the reference ROI are denoted as  $R_r$ ,  $G_r$ , and  $B_r$  respectively. Then the  $R_s$ ,  $G_s$  and  $B_s$  are converted to corresponding HSV color components by implementing RGB to HSV color conversion algorithm discussed in the previous chapter (section 2.6.4). A unique interpolation algorithm (section 3.5) is introduced to estimate the wavelength of the reflected light from the test sample. So, in this app the main attributes to quantify the parameters responsible for color change are average RGB value in the sample ROI, color ratio with respect to a specified reference ROI, HSV color information of the sample and estimated wavelength.

These attributes are used to generate calibration data table which is saved to the internal storage of smartphone. Further this calibration data table is used in origin software platform to formulate a calibration equation by using single or multiple nonlinear regression analysis. According to the value of determination coefficient found from nonlinear regression analysis, the best combination of the attributes is determined to formulate the desired polynomial. Finally the best fitted polynomial is utilized as the calibration equation and incorporated with the detection algorithm of the customized app to quantify the particular parameter of any colorimetric test within the calibrated detection range. Upon clicking the ‘Analyze’ button on the ‘Analyze’ screen, the fabricated smartphone-based colorimeter measures all of the above attributes corresponds to the test sample. With the help of the calibration equation, the customized app can be used to calculate the concentration of RhB or chlorine or pH value of an unknown test sample as shown in Fig. 3.4(e). The final results of a colorimetric test can be saved to the internal storage of the smartphone through ‘Save Results’ button in the same window for further analysis and sharing.

In this app, there is an option to recalibrate the existing colorimetric tests. There is also an opportunity to incorporate new colorimetric test rather than the existing tests with the help of ‘Calibration’ option. To add a new colorimetric test, at first the designed smartphone-based colorimeter has to calibrate by using the known analytes for a definite detection range by

pressing the 'Calibration' button from the menu screen of the app. By tapping the 'Calibration' button a new window named 'Calibration' will top-up. 'Calibration' window of the customized app first prompts the user to enter information about the desired colorimetric test, such as the name of the test and sample quantity of the test solution which is used to calibrate the smartphone-based colorimeter for the desired colorimetric measurement [Fig. 3.4(f)]. Then the image of that specified test sample has to capture or select from internal storage of the smartphone. The RGB and HSV color components with corresponding color ratio and wavelength information can be obtained by pressing the 'Analyze' button in the 'Calibration' screen. The obtained results then saved in the internal storage of the smartphone through 'Save' button on the same screen and all other samples of the specified test within the desired detection range have to analyze in the similar procedure to complete device calibration. Then the best fitted calibration equation has to formulate by utilizing the calibrated data to determine the desired parameters of an unknown sample within the calibrated detection range.

After calibration, the designed app can be used to quantify sample parameters associated with colorimetric change and so the developed smart sensing instrument can be called as universal smartphone colorimeter. Therefore, this universal smartphone colorimeter can be adapted for any colorimetric measurement within the desired range of detection. The proposed meter is also able to measure solid sample.

### 3.5 Wavelength Estimation

Color of any substance or liquid is defined by the wavelength of the reflected light. So with change in wavelength alternative color is formed. RGB color model cannot represent any information about the wavelength of the reflected light. Thus, in order to obtain the wavelength information of reflected light RGB color components are converted into corresponding HSV color components. In HSV color model, hue denotes the numerical representation of color, saturation represents how white the color is and value represents the brightness of the color. Thus among the HSV color components, hue is correlated with wavelength and also known as the color appearance parameter. In this research, wavelength information of a smartphone-based colorimetric measurement is estimated by correlating with hue parameter of HSV color model.

For wavelength estimation, three laser diodes ( $\lambda_R = 647$  nm  $\lambda_G = 540$  nm and  $\lambda_B = 414$  nm) are utilized which are already calibrated using bench-top laboratory spectrometer (Vernier type advance 4 spectrometer, model no: 1603, RAC Exports). These laser diodes act as the light source instead of flash LED and focus their light beam toward the focusing lens of the CMOS camera of the smartphone sequentially to capture the image of these beam spots. The average RGB values of the beam spots of these laser diodes are measured directly from the captured image of those beam spots. The HSV values of the beam spots are calculated from their corresponding measured RGB values using the customized smartphone app. For red, green and blue lasers, the obtained hue values are  $349^\circ$ ,  $124^\circ$  and  $252^\circ$  respectively.

It is well known that the hue component in HSV color model is distributed angularly but the wavelength of light is not distributed angularly in the visible band of electromagnetic spectrum [Fig. 3.5]. It is seen that, magenta is an extra-spectral color which is not found in the visible spectrum of light [Fig. 3.5(a)] and does not have its own wavelength unlike all the other spectrum colors. But in HSV color model, magenta is defined by hue in the range of ( $H \approx 270^\circ - 330^\circ$ ) with a central hue component at  $300^\circ$  as shown in Fig 3.5(b). Magenta color is physiologically and psychologically perceived by human brain as the mixture of red and blue light, with the absence of green.

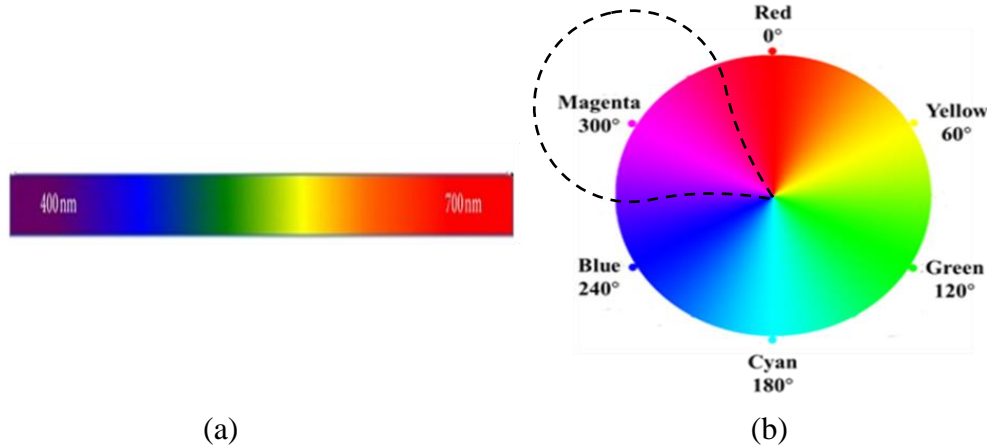


Fig. 3.5: (a) Visible light spectrum (Magenta is not part of the visible spectrum of light) (b) HSV color wheel (Visible spectrum wrapped to join blue and red in an additive mixture of magenta. In reality, blue and red are at opposite ends of the spectrum and have different wavelengths).

In this thesis, the wavelength is estimated from the hue component of HSV color model. In order to do so, the angular distribution of hue is unwrapped by considering the spectral void in the magenta region and thus the value of hue is modified by using the following Eq. 3.2. Where,  $H_m$  is the modified value of hue calculated from actual hue ( $H$ ).

$$H_m = \begin{cases} H & \text{if } 0^\circ \leq H < 330^\circ \\ (H - 360^\circ) & \text{if } 330^\circ \leq H \leq 360^\circ \end{cases} \quad (3.2)$$

For wavelength estimation, the visible band of wavelength is segmented into two parts; red to green and green to blue. The wavelength and hue corresponds to red laser are 647 nm and  $349^\circ$  respectively whereas the wavelength and hue corresponds to green laser are 540 nm and  $124^\circ$ . Since hue is angularly distributed so hue ( $-11^\circ$ ) contains the same color information as hue  $349^\circ$ . Using the hue components and corresponding wavelength of red and green lasers, a wavelength estimation equation in the region between red to green specified by ( $0^\circ < H \leq 124^\circ$  and  $330^\circ \leq H \leq 360^\circ$ ) i.e. ( $-30^\circ < H_m \leq 124^\circ$ ) is formed that passes through these two points expressed by Eq. 3.3 and shown in Fig. 3.6.

The wavelength of any reflected light having modified hue component in the range of  $(-11^\circ < H_m \leq 124^\circ)$ , can be easily calculated through interpolation using this equation and the modified hue component in the range of  $(-30^\circ \leq H_m \leq -11^\circ)$ , can be easily calculated through this equation by extrapolation.

$$\lambda = \{(-0.792593 \pm 0.02) \times H_m + 638.281482 \quad \text{if } -30^\circ < H_m \leq 124^\circ\} \quad (3.3)$$

On the other hand, the wavelength and hue corresponds to blue laser are 414 nm and  $252^\circ$  respectively. Similarly, using the wavelength and hue values of green and blue laser, a wavelength estimation equation is also formed in the region between green to blue specified by  $(124^\circ < H \leq 270^\circ)$  i.e.  $(124^\circ < H_m \leq 270^\circ)$ . The wavelength of any reflected light having modified hue component in the range of  $(124^\circ < H_m \leq 252^\circ)$ , can be easily estimated through interpolation using the equation given by Eq. 3.4 and modified hue component in the range of  $(252^\circ < H_m \leq 270^\circ)$ , can be easily estimated through the Eq. 3.4 by extrapolation.

$$\lambda = \{(-0.984375 \pm 0.02) \times H_m + 662.0625 \quad \text{if } 124^\circ < H_m \leq 270^\circ\} \quad (3.4)$$

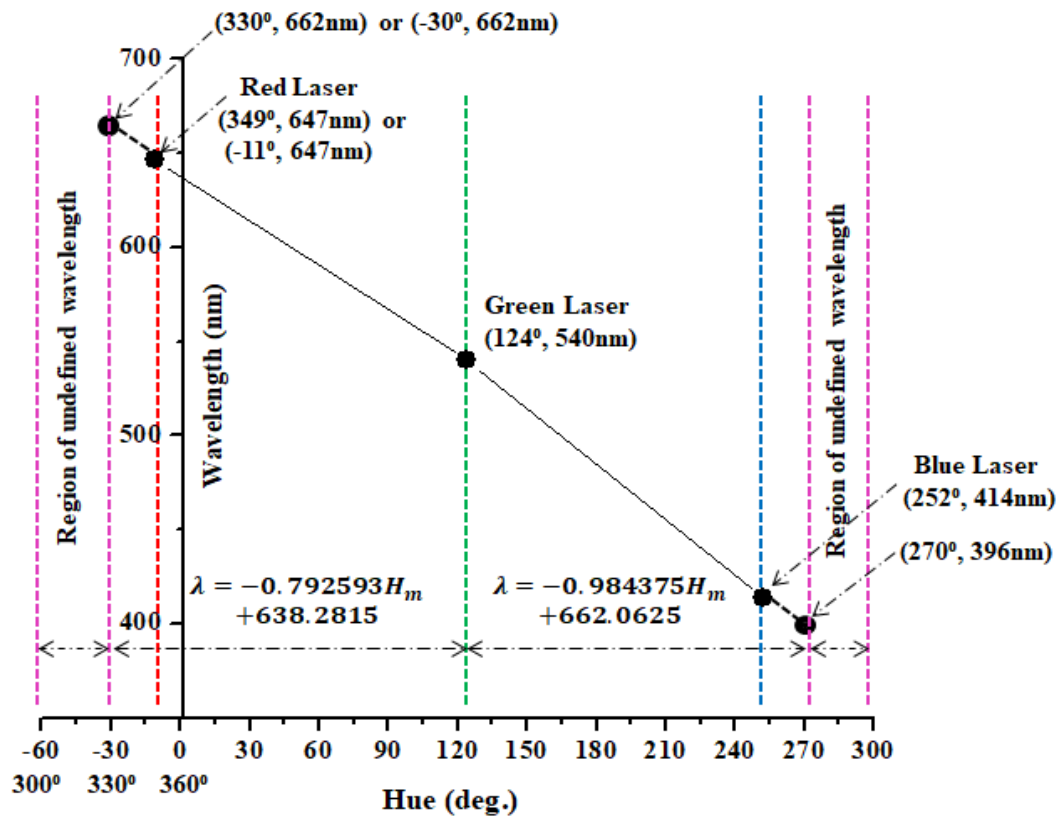


Fig. 3.6: Illustration of wavelength estimation of reflected light for colorimetric smartphone-based measurement with respect to three laser diodes of known wavelength.



But within the hue range of ( $270^\circ < H < 330^\circ$ ) i.e. ( $270^\circ < H_m < 330^\circ$ ), magenta color is formed which has no existence in the visible light spectrum and does not have its own wavelength unlike the other spectrum colors as discussed above. Thus, within this range of hue, wavelength is denoted as undefined as expressed by Eq. 3.5.

$$\lambda = \{Undefined \quad if \quad 270^\circ < H_m < 330^\circ\} \quad (3.5)$$

Therefore, the wavelength of light reflected from various color during colorimetric measurement can be calculated using the hue parameter.

### 3.6 Conclusion

In this research, a versatile smartphone-based smart sensing instrument for colorimetric quantification of different analytes in a single platform is designed and fabricated using flash LED, CMOS camera detector, LCD display and high processing power of smartphone. The developed smartphone-based colorimeter is very low cost, field portable, robust and can promote diverse fields of bio-analytical investigations with the help of customized 'Smartphone Colorimeter' app. 3D printing technology is incorporated to fabricate the designed smartphone-based colorimeter. Moreover, the wavelength information of the reflected light during colorimetric measurement is estimated by developing a novel wavelength estimation algorithm.

# Chapter IV

## *Results and Discussion*

---

### **Chapter Outlines:**

**4.1 Introduction**

**4.2 Rhodamine B Concentration Quantifier**

**4.3 Digital pH Meter**

**4.4 Chlorine Concentration Quantifier**

**4.5 Conclusion**

---

## 4.1 Introduction

The designed smartphone-based colorimeter has the ability to examine a wide range of analytes through the application of specific chemosensor dye. Because it is designed to handle all the cases of colorimetric measurement where wavelength or intensity or both are changed separately or simultaneously according to the quantity of the desired analytical parameters. As a part of the proof of principles, in this chapter, Rhodamine B concentration, pH value and chlorine concentration are measured through different approaches and then compared the results with those obtained from conventional instruments to confirm the accuracy of the designed colorimeter.

## 4.2 Rhodamine B Concentration Quantifier

Rhodamine B concentration is demonstrated in this research to study the performance of the designed colorimeter in the case of colorimetric measurement where the wavelength of the test specimen is unchanged with the change of analytes properties which has to be determined. In the present case, color intensity or tone of the test samples is changed with the variation of the concentration but the wavelength is independent of the concentration. Rhodamine B (RhB,  $C_{28}H_{31}ClN_2O_3$ ) is a chemical compound and dye that has a constant hue parameter which means it has constant wavelength but only saturation parameter in the HSV color model is changing with the change of its concentration in distilled water.

### 4.2.1 Sample Preparation

Different concentration RhB solutions ranging from 0.2 to 4.0 PPM (parts per million) are prepared by dissolving RhB into distilled water. At first 10 mg RhB dye is dissolved in 100 ml of distilled water. This gives 10 mg/100 ml which is equal to 100 PPM RhB stock solution (mother solution). This stock solution is further diluted in different amounts of distilled water sequentially to get the desired RhB samples of concentration (0.2-4.0) PPM. For example, to obtain a 0.5 PPM RhB solution, 50  $\mu$ l of previously prepared stock solution of 100 PPM is added with 10 ml of distilled water by using a high precision micropipette (Microlit, VVCS-10). This stock solution is easily mixed with distilled water and finally, we get RhB solution of concentration 0.5 PPM. Since the liquid sample holding capacity of the glass cuvette (sample holder) used here is  $\sim$ 3.5 ml, so  $\sim$ 10 ml RhB solutions of various concentrations are enough for demonstration. The required amount of stock solution and distilled water used to prepare all RhB samples covering the range of (0.2-4.0) PPM for device calibration and testing are summarized in Table 4.1 and their photographs are shown in Fig. 4.1.

**Table 4.1: Composition of RhB samples with different concentration**

Sl. No.	Desired RhB Concentration (PPM)	Required Stock Solution of 100 PPM ( $\mu$ l)	Required Distilled Water (ml)
01	0.2	20	10
02	0.3	30	10
03	0.4	40	10
04	0.5	50	10
05	0.6	60	10
06	0.7	70	10
07	0.8	80	10
08	0.9	90	10
09	1.0	100	10
10	1.5	150	10
11	2.0	200	10
12	2.5	250	10
13	3.0	300	10
14	3.5	350	10
15	4.0	400	10

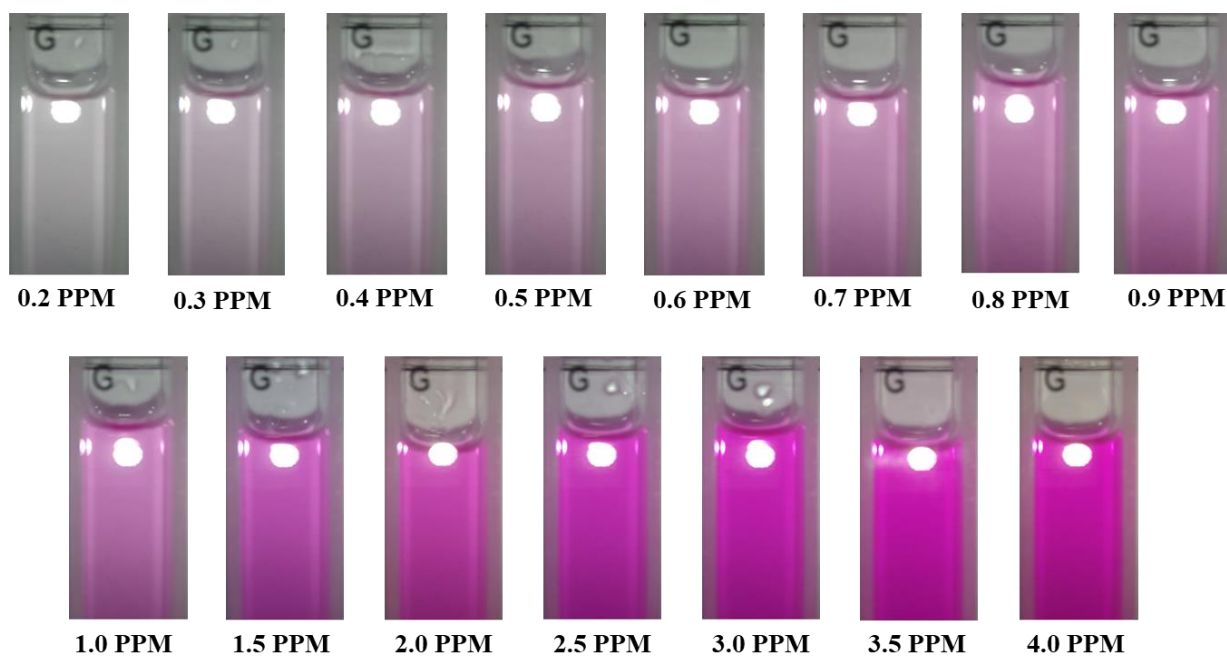


Fig. 4.1: Photograph of Rhodamine B samples (0.2-4.0) PPM for calibration and testing of smartphone-based colorimetric measurement.

### 4.2.2 Calibration of RhB Concentration Quantifier

Before implementing a smartphone-based colorimeter as RhB concentration quantifier, the first step is to calibrate the designed smartphone-based colorimeter properly using the samples of RhB having known concentration. There is an option in the menu screen of the developed smartphone app to calibrate the colorimeter for a new analyte or recalibrate the existing tests. Using the calibration option in the designed app, the smartphone-based colorimeter is calibrated according to total 15 RhB samples of known concentration. For the first sample, the test name and the concentration of RhB of that sample are written down at the specified boxes. Then, the sample of known RhB concentration is taken in a 3.5 ml glass cuvette (1 mm thick, outer dimension 12.5×12.5×48.0 mm and path length 10 mm) and sealed perfectly. The sealed cuvette is then inserted vertically to the assigned cuvette slot in the 3D fabricated chamber and enclosed the chamber using top cover to avoid the leakage of stray light entering into the measuring platform. After that, the smartphone flash LED is turned on which is used as the light source that provides constant illumination in the enclosed sample. The digital image of the RhB sample is picked by clicking on the button named as ‘Capture Image’. The color information of the RhB sample such as RGB value, color ratio, and HSV attributes is determined by analyzing the digital image and saved to the internal storage of the smartphone for developing the calibration formula using nonlinear regression modeling. The similar procedure is repeated sequentially for the other RhB samples of known concentration by pressing the button “Next Sample”. For proper illustration, screenshots of the calibration screen for the RhB samples having concentrations 1.0 and 3.0 PPM are shown in Fig. 4.2. There are two regions of interest (ROI), aligned vertically on the display of the smartphone, one for the sample and another for reference. The white (255, 255, 255) beam spot of the flash LED is utilized as the reference ROI and a matrix of  $7 \times 7$  pixels from this reference ROI is used to calculate the average RGB values of reference. On the other hand, from the sample ROI the data correspond to red, green, and blue color planes are needed from the image of a sample under investigation. To do so, another matrix of  $7 \times 7$  pixels is selected as the sample ROI to determine the average RGB values from the RhB sample. From these two ROIs, the RGB as well as HSV color components, color ratio, and wavelength information are calculated by the app developed under the smartphone environment. Although the customized app displays the value of color components, color ratio, and wavelength information directly as shown in Fig. 4.2, determination of the RhB concentration of an unknown sample requires additional manipulation of these data to form a calibration equation. So the smartphone-based colorimeter must be calibrated against the RhB samples of known concentration in order to measure an unknown RhB sample. The calibrated data of 15 RhB samples within the concentration range of (0.2-4.0) PPM are summarized in Table 4.2 to formulate calibration equations.

Table 4.2 depicts that the value of RGB color components are almost same at low RhB concentration (0.2 PPM). However, with increase in RhB concentration from 0.2 to 4.0 PPM, the values of the red components increases slowly (165.53-191.47) with a drastically decrease in green components (163.53-17.86) and negligible variation in blue components. At the high RhB concentration (4.0 PPM), the highly intense red and blue light along with a very low intense green light form pure magenta color. But the reference ROI is highly intense and shows a

constant RGB color component valued as (255, 255, 255) throughout the measurement range. The intensity and wavelength of the reflected light from the sample solution have no impact to change the color information of the beam spot of the flash LED because of its high intensity compared to the intensity of reflected light from the sample solution. So the beam spot of the flash LED is used as a sample independent reference ROI to calculate the color ratio. It is well known that color ratio is directly proportional to the value of RGB color components of the sample ROI (Eq. 3.1) and as a result color ratio is high at low RhB concentration but with increase in RhB concentration from 0.2 to 4.0 PPM, the value of color ratio follows a decreasing nature from 0.6475 to 0.4851. In addition to this, the variation of hue attributes is negligible ( $309.92\sim 312.58$ )° over the detection range because there is no change in color (Fig. 4.1) as RhB concentration increased from 0.2 to 4.0 PPM and consequently hue shows almost constant value. However, there is a trend of increasing saturation from 1.66% to 90.67% as the sample color changes in only one tone with increase in RhB concentration from 0.2 PPM to 4.0 PPM. At low concentration (0.2 PPM), the saturation parameter is low (1.66%) resulting a highly faded color of magenta but with increase in RhB concentration, the saturation parameter gets increased to 90.67% which gives pure magenta color. Magenta color of RhB solution is a secondary color, made by combining equal amounts of red and blue light at a high intensity and is the complementary color of green. Most of the time, our brain averages the wavelengths of light in order to come up with a color. However, if equal amounts of blue light and red light are mixed, magenta color is formed rather than green color obtained from their average wavelength. The reason behind that human brains have constructed a color to bridge the gap between red and blue because it does not exist in the visible light spectrum as discussed in chapter III (section 3.5) [77]. Therefore, in case of RhB dye, wavelength is undefined as mentioned in Table 4.2.

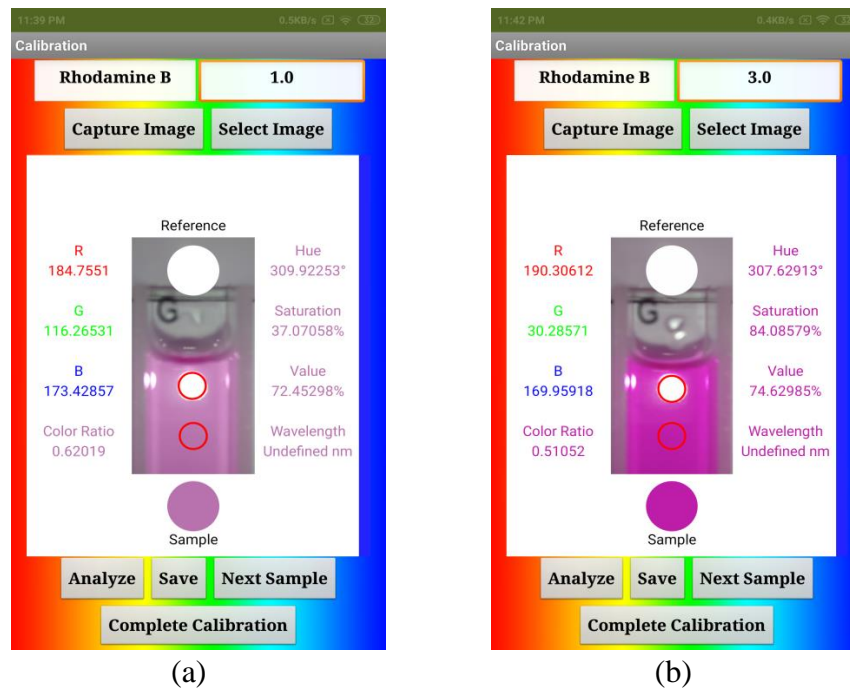


Fig. 4.2: Screen-shot of the calibration page illustrating the colorimetric analysis of RhB samples: (a) 1.0 PPM and (b) 3.0 PPM.

**Table 4.2: Experimental data table to formulate calibration equations for RhB concentration quantifier**

[RhB] (PPM)	RGB (Sample)			RGB (Reference)			Color Ratio (C <sub>R</sub> )	HSV (Sample)			Wavelength (nm)
	R	G	B	R	G	B		H°	S%	V%	
0.2	165.53	163.53	166.29	255	255	255	0.6475	310.56	1.66	65.21	Undefined
0.3	167.55	155.55	165.55	255	255	255	0.6388	310.00	7.16	65.71	Undefined
0.4	172.27	149.51	167.14	255	255	255	0.6391	312.51	13.21	67.56	Undefined
0.5	173.49	143.24	166.80	255	255	255	0.6321	312.28	17.43	68.04	Undefined
0.6	178.41	139.41	170.41	255	255	255	0.6382	312.31	21.86	69.96	Undefined
0.7	182.0	132.33	170.33	255	255	255	0.6335	312.10	27.29	71.37	Undefined
0.8	181.29	125.29	170.29	255	255	255	0.6233	311.79	30.89	71.09	Undefined
0.9	181.65	119.65	168.65	255	255	255	0.6143	312.58	34.13	71.24	Undefined
1.0	184.76	116.27	173.43	255	255	255	0.6202	309.92	37.07	72.45	Undefined
1.5	182.61	79.73	171.86	255	255	255	0.5676	310.27	56.34	71.61	Undefined
2.0	190.80	65.45	167.63	255	255	255	0.5541	311.09	65.69	74.82	Undefined
2.5	187.39	43.90	171.82	255	255	255	0.5269	311.51	76.57	73.49	Undefined
3.0	190.31	30.29	169.96	255	255	255	0.5105	310.63	84.09	74.63	Undefined
3.5	196.82	21.72	171.37	255	255	255	0.5097	311.72	88.97	76.18	Undefined
4.0	191.47	17.86	161.56	255	255	255	0.4851	310.27	90.67	75.09	Undefined

Among the attributes of colorimetric measurement, saturation changes significantly with RhB concentration compared to the change of color ratio, hue and value attributes. Now the attributes of colorimetric detection are individually considered as the independent variable to develop polynomials (Eq. 4.1- 4.4) for device calibration and the corresponding fit curves obtained from single nonlinear regression analysis are shown in Fig. 4.3 to illustrate the individual impacts of the above mentioned attributes on RhB concentration in the range of (0.2-4.0) PPM using the designed smartphone-based colorimeter.

$$[RhB] = -9323.57486 + 80993.38292C_R - 279449.91095C_R^2 + 479065.56519C_R^3 - 408204.08311C_R^4 + 138320.22865C_R^5 \quad (4.1)$$

$$[RhB] = -0.01126 - 1.40227H - 109.10305H^2 + 1.04859H^3 - 0.00336H^4 + 3.58673 * 10^{-6}H^5 \quad (4.2)$$

$$[RhB] = 0.13811 + 0.0319S - 0.00139S^2 + 5.47643 * 10^{-5}S^3 - 8.08174 * 10^{-7}S^4 + 4.2498 * 10^{-9}S^5 \quad (4.3)$$

$$[RhB] = 352649.11896 - 25517.71805V + 737.80561V^2 - 10.65462V^3 + 0.07684V^4 - 2.2143 * 10^{-4}V^5 \quad (4.4)$$

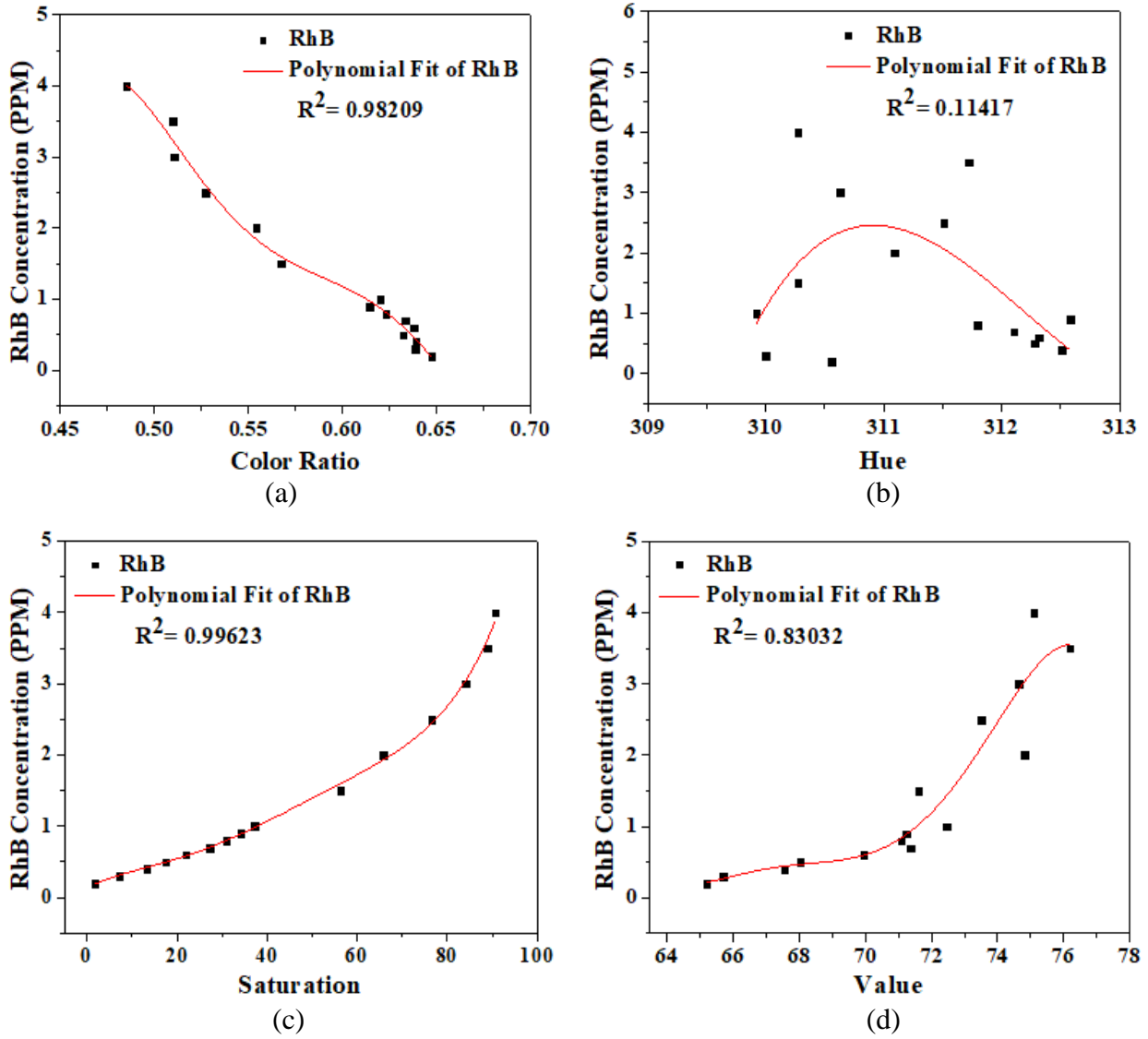


Fig. 4.3: Polynomial fit curves to calibrate the smartphone-based colorimeter as RhB concentration quantifier by only considering: (a) color ratio, (b) hue, (c) saturation, and (d) value as independent variable.

All of the above-mentioned polynomials are formulated using single independent variables such as color ratio, hue, saturation or value. From Fig. 4.3, it is found that saturation varies most significantly with the variation of RhB concentration though color ratio and value has small influence on RhB concentration. To verify the impact of multiple attributes (color ratio, hue, saturation or value), calibration of RhB concentration quantifier is carried out in the next section through multiple nonlinear regression analysis. Consequently, the developed polynomial considering hue and saturation is expressed by Eq. 4.5.



$$[RhB] = 9.95118 * 10^{-4}H^3 + 3.28101 * 10^{-3}H^2S - 3.68474 * 10^{-5}HS^2 + 5.82579 * 10^{-6}S^3 - 1.01113H^2 - 2.03912HS + 1.10576 * 10^{-2}S^2 + 340.14551H + 316.85105S - 37921.3125 \quad (4.5)$$

The combined effects of both hue and value attributes are taken as the independent variables of multiple nonlinear regression analysis and the corresponding polynomial is represented by Eq. 4.6.

$$[RhB] = -7.72421 * 10^{-3}H^3 + 7.35592 * 10^{-3}H^2V - 2.48402 * 10^{-2}HV^2 + 4.88551 * 10^{-3}V^3 + 6.58187H^2 - 1.14497HV + 6.73367162V^2 - 1970.91309H - 288.20555V + 207176.5625 \quad (4.6)$$

The relationship of saturation and value with RhB concentration is mathematically expressed by a third-order polynomial (Eq. 4.7).

$$[RhB] = 6.68824 * 10^{-5}S^3 - 1.21657 * 10^{-3}S^2V + 8.34206 * 10^{-3}SV^2 - 1.83408 * 10^{-2}V^3 + 7.86433 * 10^{-2}S^2 - 1.09313SV + 3.61747V^2 + 35.87055S - 237.95975V + 5220.49164 \quad (4.7)$$

The simultaneous effect of color ratio and saturation attributes in smartphone-based colorimetric detection of RhB concentration is also formulated (Eq. 4.8) as the determination coefficient of the above reported polynomials is not satisfactory.

$$[RhB] = -23868.57153C_R^3 - 103.933333C_R^2S - 0.14245C_RS^2 - 5.50906 * 10^{-5}S^3 + 47201.37903C_R^2 + 136.86024C_RS + 9.34778 * 10^{-2}S^2 - 31110.39771C_R - 45.02945S + 6834.24519 \quad (4.8)$$

Considering hue, saturation and value simultaneously as the independent variables in multiple nonlinear regression analysis for RhB concentration quantification, the obtained second-order polynomial based on HSV color model is written by Eq. 4.9.

$$[RhB] = 9.90879 * 10^{-2}H^2 - 4.30941 * 10^{-3}HS + 2.35484 * 10^{-2}HV + 4.80988 * 10^{-4}S^2 + 1.99976 * 10^{-3}SV - 1.45641 * 10^{-2}V^2 - 63.21887H + 1.18079S - 5.24776V + 10003.96754 \quad (4.9)$$

Finally the combined effect of color ratio, saturation and intensity (V) component in smartphone-based colorimetric detection of RhB concentration is formulated through multiple nonlinear regression analysis and the corresponding second-order polynomial is written by Eq. 4.10.

$$[RhB] = 912.61289C_R^2 + 3.19034C_RS - 4.03337C_RV + 2.25299 * 10^{-3}S^2 + 6.92385 * 10^{-3}SV - 5.00951 * 10^{-2}V^2 - 923.00307C_R - 2.5284S + 9.21276V - 2.16265 \quad (4.10)$$

The linearity of the developed polynomials with the RhB concentration range of (0.2-4.0) PPM can be estimated through the determination coefficients associated with those polynomials. The calibration techniques applied for smartphone-based colorimetric measurement of RhB concentration with their corresponding determination coefficients are tabulated in Table 4.3.

**Table 4.3: Calibration techniques applied for the calibration of RhB concentration quantifier**

Calibration Methods	Calibration Attributes	Order of Polynomial	Determination Coefficient ( $R^2$ )
Single Nonlinear regression analysis	Color Ratio ( $C_R$ )	5	0.98209
	Hue (H)	5	0.11417
	Saturation (S)	5	0.99623
	Value (V)	5	0.83032
Multiple nonlinear regression analysis	H & S	3	0.99305
	H & V	3	0.78253
	S & V	3	0.99792
	$C_R$ & S	3	<b>0.99995</b>
	H, S & V	2	0.99574
	$C_R$ , S & V	2	0.99903

#### 4.2.3 Performance Analysis of RhB Concentration Quantifier

For performance evaluation, various calibration techniques are reported in the above section. In this section the developed polynomials associated with those calibration techniques are incorporated sequentially within the detection algorithm of customized smartphone app to find out the most reliable calibration technique for smartphone-based colorimetric measurement of RhB concentration. To do so, seven different RhB solutions are prepared as the test samples according to the process discussed earlier for colorimetric analysis through customized app. The measured RhB concentration of the test samples by smartphone-based colorimeter is compared with their corresponding actual RhB concentration to justify the accuracy of detection.

Over the detection range (0.2-4.0) PPM, color ratio based calibration technique (Eq. 4.1) incorporates maximum 48.2% detection error with an average error of 16.18%. Conventionally color ratio is used as the variable parameter for determining the concentration of a colored compound in a solution through colorimeter. But in case of RhB, the conventional method of determining concentration by smartphone colorimeter based on color ratio shows poor agreement with the actual RhB concentration of the test samples which is not considered for accurate measurement. Throughout the detection range, hue is independent of RhB concentration as a result the determination coefficient of hue based polynomial (Eq. 4.2) is very small and the demonstrated results based on hue do not carry any information about RhB concentration (shown in Table 4.4). Similarly, the performance of RhB concentration quantifier is evaluated by integrating the polynomials (Eq. 4.3) obtained from single nonlinear regression analysis based on saturation and the corresponding measurements provides considerable error of an average 3.15% which is lower than the error associated with color ratio based analysis. However, value based calibration technique cannot provide any information about RhB concentration. Among the calibration technique based on single nonlinear regression analysis, saturation provides better performance and hue provides worst performance.

The performance of multiple nonlinear regression based calibration techniques are also evaluated here by considering the combined effects of colorimetric attributes. At first, hue-saturation based third-order polynomial function (Eq. 4.5) is integrated within the detection algorithm of the developed smartphone app to measure RhB concentration of same test samples. Only hue cannot provide any information about RhB concentration but when both hue-saturation is considered the instrument detects RhB concentration with 16.44% average detection error. On the other hand, till now hue-value based multiple nonlinear regression analysis cannot provide any information of RhB concentration as equation 4.6 cannot fit (determination coefficient,  $R^2= 0.78253$ ) with the experimental data in the (0.2-4.0) PPM RhB concentration range. An average of 9.34% error is incorporated with smartphone-based colorimetric measurement of RhB concentration in case of saturation-value based analysis. This error is less than the error associated with multiple nonlinear regression analyses based on hue-saturation but higher than the error produced by single nonlinear regression analysis based on saturation. Additionally, the multiple nonlinear regression model based on saturation-value performs well to measure RhB concentration higher than 0.5 PPM but the RhB samples with concentration lower than 0.5 PPM are not perfectly detectable using this polynomial (Eq. 4.7).

Now the polynomial (Eq. 4.8) based on color ratio and saturation is considered for RhB concentration measurement because the above mentioned calibration techniques are not able to detect RhB concentration accurately throughout the detection range. This multiple nonlinear regression model is mathematically best fitted ( $R^2= 0.99995$ ) over the whole RhB concentration range of (0.2-4.0) PPM and contains negligible detection error of only 0.95%. Therefore, smartphone-based colorimetric detection using both color ratio and saturation provides actual information about RhB concentration with high accuracy. The performance of RhB concentration quantifier considering the combined effects of hue, saturation and value is found to be better than that of when hue and value are used independently as discussed earlier. In this case the developed second-order polynomial (Eq. 4.9) is mathematically fitted well ( $R^2= 0.99574$ ) over the detection range and incorporates an average of 5.31% detection error. This error is less than the error produced by RGB color components based (color ratio) calibration technique since RGB color model is more sensitive to light illumination than HSV color model and thus detected result can be changed with change in illumination. Finally, the performance of RhB concentration quantifier is analyzed by multiple nonlinear regression based calibration technique considering color ratio, saturation and value that contains an average of 6.67% detection error. The obtained detection error in the present case is higher than the detection error associated with color ratio and saturation based multiple nonlinear regression analyses as the value attributes has no impact on RhB concentration compared to saturation and color ratio.

From all of the above discussion it can be concluded that, color ratio and saturation based calibration technique performs well in colorimetric measurement of RhB concentration. The limit of detection of RhB concentration quantifier is 0.2 PPM because lower than 0.2 PPM cannot detect perfectly as it produces more faded magenta color like white. The test results of smartphone-based colorimetric measurement of RhB concentration for performance analysis among different calibration techniques are summarized in Table 4.4.

**Table 4.4: Test results of smartphone-based colorimetric RhB concentration quantifier for performance analysis among different calibration techniques**

Sample no.	Actual [RhB] (PPM)	Measured [RhB] by considering $C_R$		Measured [RhB] by considering H	Measured [RhB] by considering S		Measured [RhB] by considering V	Measured [RhB] by considering H & S		Measured [RhB] by considering H & V	Measured [RhB] by considering S & V		Measured [RhB] by considering $C_R$ & S		Measured [RhB] by considering H, S & V		Measured [RhB] by considering $C_R$ , S & V	
		[RhB] (PPM)	% Error	[RhB] (PPM)	[RhB] (PPM)	% Error	[RhB] (PPM)	[RhB] (PPM)	% Error	[RhB] (PPM)	[RhB] (PPM)	% Error	[RhB] (PPM)	% Error	[RhB] (PPM)	% Error	[RhB] (PPM)	% Error
Sample 1	0.2	0.1849	7.55	-8555.88	0.1875	6.25	-81.020	0.2893	44.65	0.6856	0.1394	30.3	0.1969	1.55	0.2113	5.65	0.2391	19.55
Sample 2	0.3	0.4446	48.2	-8495.25	0.3133	4.433	-83.500	0.3831	27.7	0.6812	0.3633	21.1	0.3031	1.00	0.2908	3.067	0.2574	14.2
Sample 3	0.5	0.6190	23.8	-8749.21	0.4941	1.18	-95.847	0.5787	15.74	0.9045	0.5230	4.6	0.4853	2.94	0.4215	15.7	0.4736	5.28
Sample 4	0.7	0.5844	16.51	-8505.96	0.7026	0.371	-115.703	0.8236	17.657	1.3794	0.6824	2.514	0.7033	0.471	0.7504	7.2	0.6714	4.086
Sample 5	1.0	0.8745	12.55	-8486.73	0.9716	2.84	-122.44	1.0634	6.34	1.8989	1.0204	2.04	0.9969	0.31	1.0070	0.7	1.0194	1.94
Sample 6	2.5	2.6108	4.432	-8661.71	2.4216	3.136	-129.051	2.5731	2.924	2.1999	2.5640	2.56	2.4906	0.376	2.4711	1.156	2.4669	1.324
Sample 7	4.0	4.0096	0.24	-8524.29	3.8464	3.84	-139.769	3.9965	0.088	4.0683	3.9094	2.265	3.9999	0.003	3.8525	3.688	3.9859	0.323
Average error (%)		16.18		–	3.15		–	16.44		–	9.34		0.95		5.31		6.67	

All of the above nonlinear regression analysis is performed to find out the most reliable calibration technique for smartphone-based colorimetric measurement of RhB concentration. Comparing the detection error associated with each regression analysis it is seen that the multiple nonlinear regression analyses show less error in the colorimetric measurement of RhB concentration than the single nonlinear regression analysis. Among the developed nonlinear regression models, the top six nonlinear regression models having high determination coefficient are selected and plotted in Fig. 4.4 for the comparison. It is found that the color ratio based single nonlinear regression shows the highest detection error for colorimetric measurement of RhB concentration. However, when this color ratio is incorporated with saturation for multiple nonlinear regression analysis, the performance of the smartphone-based colorimeter as the RhB concentration quantifier increases drastically with negligible detection error compared to the other nonlinear regression models.

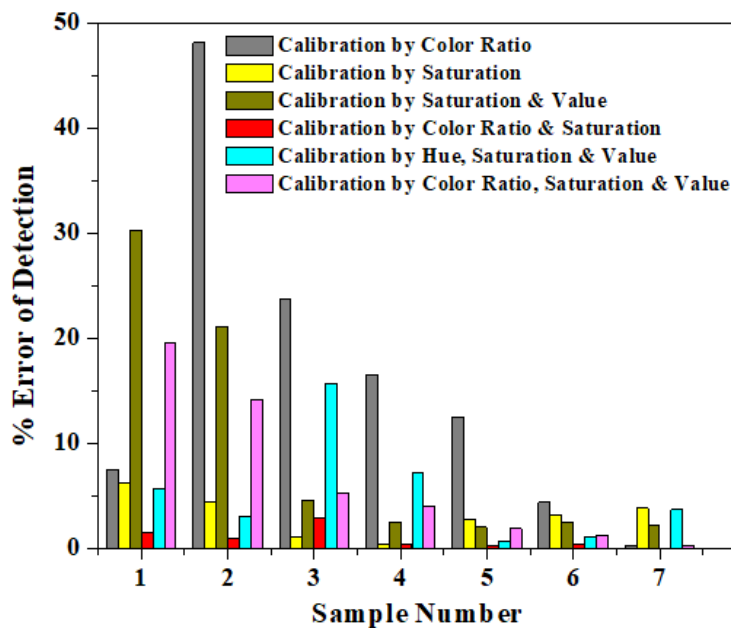


Fig. 4.4: Percentage of detection error associated with smartphone-based colorimetric measurement of RhB concentration for different calibration techniques.

From Fig. 4.4, it can be concluded that calibration by considering both color ratio and saturation is the best approach to calibrate the smartphone-based colorimeter as the RhB concentration quantifier for the detection range from 0.2 to 4.0 PPM with very negligible error (0.95%). So the third-order polynomial associated with color ratio and saturation from multiple nonlinear regression analyses is the optimum calibration equation which is finally incorporated with the detection algorithm of customized app for exact measurement of RhB concentration (Fig. 4.5). The error bars represents the standard deviations for three consecutive measurements of each sample to highlight the performance of the exact repeatability of the smartphone-based colorimeter to determine RhB concentration.

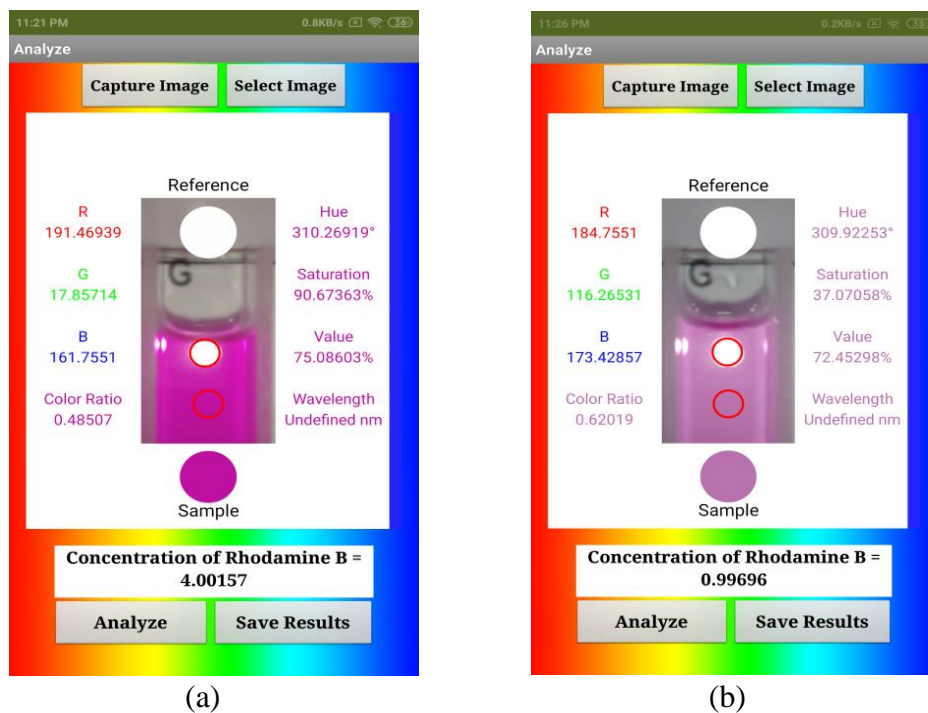


Fig. 4.5: Screenshot images of RhB concentration quantification using customized smartphone app: (a) 4.00157 PPM (actual concentration 4.0 PPM) and (b) 0.99696 PPM (actual concentration 1.0 PPM).

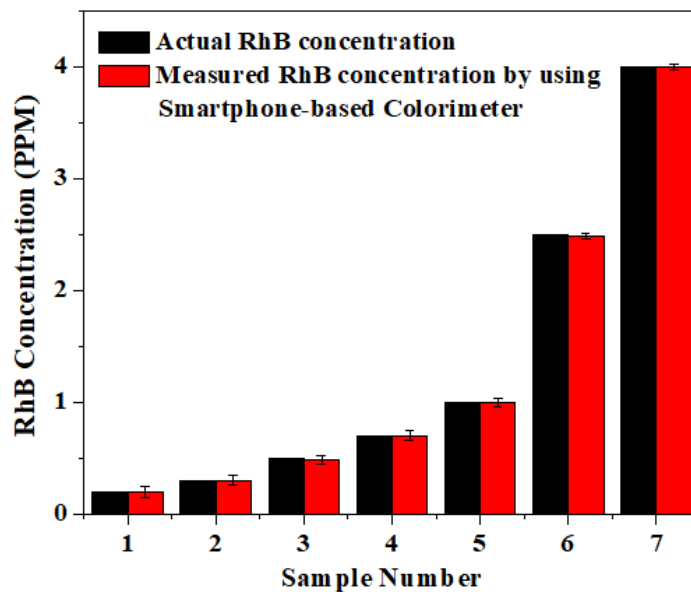


Fig. 4.6: RhB concentration of seven test samples measured on smartphone-based colorimeter compared with corresponding actual concentration.

### 4.3 Digital pH Meter

In this section, the designed smartphone-based colorimeter is demonstrated to measure pH value of liquid samples. In the case of pH detection, the wavelength of color of test samples is only significantly changed with the variation of the pH value rather than the change in intensity. To verify the performance of the designed smartphone-based colorimeter, the pH of different water samples is measured in the presence of a chemosensor named as a universal indicator because the primary goal of this section is to monitor the pH value of drinking water. According to WHO, the acceptable pH value of drinking water is ranging from 6.5 to 8.5 [71], considering this, pH samples are prepared ranges from 4.0 to 9.0 covering the acceptable range of WHO. The designed smartphone-based colorimeter is not only able to measure pH value of drinking water but it can be applied to measure the pH value of any liquid.

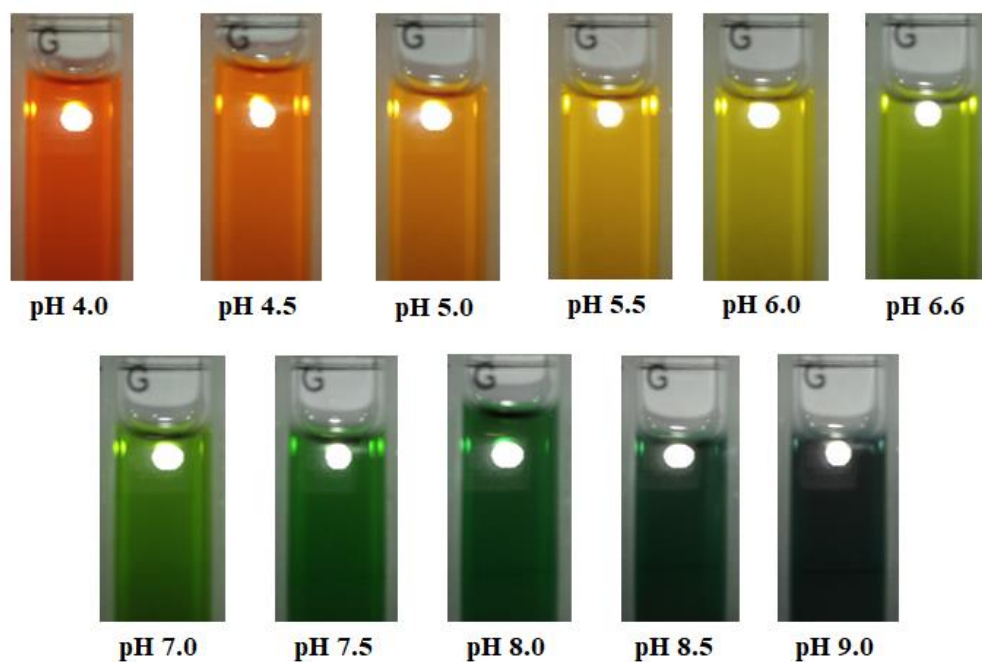
#### 4.3.1 Sample Preparation

For this experiment, a total of 11 standard buffer solutions ranging from pH 4.0 to 9.0 are prepared using the standard acetate (pH = 4.0) and phosphate (pH = 7.0) buffer solutions. These two standard buffer solutions are selected as the stock solutions and then strong based (NaOH) is used to shift the pH value of the buffer solutions in the desired range of detection.

At first, 2.0 gm NaOH is dissolved in 0.5 litre of distilled water to get 0.1 M NaOH. Since NaOH is a strong base, addition of significant amount of prepared 0.1 M NaOH will increase the pH value of buffer solutions. Prepared 0.1 M NaOH is gradually added to 10 ml stock buffer solution of pH 4.0 in a beaker and checked the resultant pH value by standard pH meter (Ezodo, PH5011). Gradually adding NaOH, buffer solutions of pH (4.5- 6.6) are obtained by shifting the pH value of the stock buffer solution of pH 4.0. Similarly, using stock buffer solution of pH 7.0, buffer solutions of pH (7.5- 9.0) are obtained. A total of 11 colorless standard buffer solutions ranging from pH 4.0 to 9.0 are prepared using appropriate amount of NaOH at an average temperature of 25 °C (room temperature) and the pH value of each confirmed by using the standard pH meter. Finally, to prepare pH sample of different pH value for colorimetric measurement, 200 µl of universal indicator is added to 10 ml of each buffer solutions by using micropipette. Universal indicator is used as the chemosensor dye which is mainly a composition of chemosensors such as thymol blue ( $C_{27}H_{30}O_5S$ ), methyl orange ( $C_{14}H_{14}N_3NaO_3S$ ), methyl red ( $C_{15}H_{15}N_3O_2$ ), bromothymol blue ( $C_{27}H_{28}Br_2O_5S$ ), and phenolphthalein ( $C_{20}H_{14}O_4$ ) and it can detect the acidic or basic nature of various substances and liquids at wider scale (pH 3-11). The required amount of distilled water and universal indicator to prepare all pH samples covering the range of (4.0-9.0) is summarized in Table 4.5. Pictorial views of the prepared pH samples for colorimetric measurement are shown in Fig. 4.7.

**Table 4.5: Composition of pH samples of different pH value with universal indicator chemosensor**

Sl. No.	pH value of prepared buffer solutions measured by standard pH meter	Nature of buffer solutions	Required standard Buffer solution (ml)	Required Universal Indicator ( $\mu$ l)	Resultant sample solution for demonstration (ml)
01	4.0	Acidic	10	200	10.20
02	4.5	Acidic	10	200	10.20
03	5.0	Acidic	10	200	10.20
04	5.5	Acidic	10	200	10.20
05	6.0	Less acidic	10	200	10.20
06	6.6	Less acidic	10	200	10.20
07	7.0	Neutral	10	200	10.20
08	7.5	Less basic	10	200	10.20
09	8.0	Less basic	10	200	10.20
10	8.5	Basic	10	200	10.20
11	9.0	Basic	10	200	10.20

**Fig. 4.7: Photograph of pH samples (pH value 4.0-9.0) for smartphone-based colorimetric measurement of pH.**



### 4.3.2 Calibration of Digital pH Meter

Before implementing smartphone-based colorimeter as digital pH meter, it is properly calibrated by following the similar procedure as discussed in the previous section 4.2.2 for RhB concentration quantifier, using standard pH samples. The calibration is performed with the help of developed smartphone app as illustrated in Fig. 4.8 and the calibrated data (RGB & HSV color components, color ratio, wavelength) of eleven pH samples is summarized in Table 4.6 for formulating appropriate calibration equations.

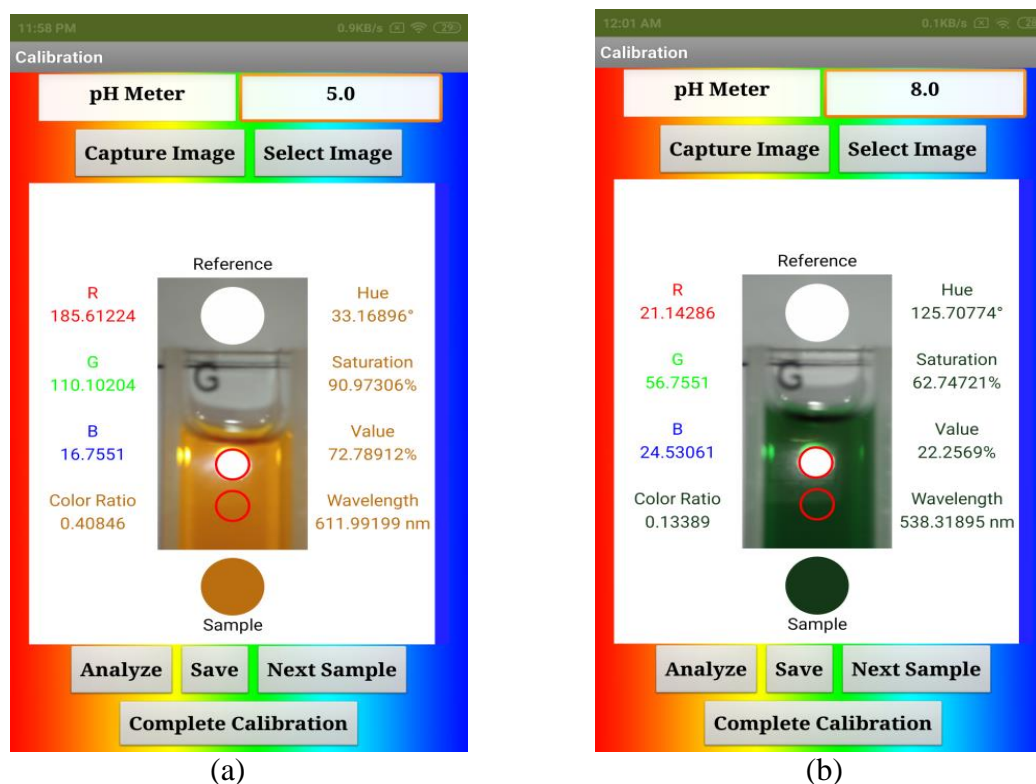


Fig. 4.8: Calibration screen of the developed smartphone app illustrating the colorimetric analysis of two samples with different pH value: (a) pH 5.0, and (b) pH 8.0.

The summarized RGB color components in Table 4.6 measured by smartphone-based colorimeter depicts that at low pH value i.e. at acidic region (pH 4.0-6.0) the value of red color component is high compared to green and blue color components. But with increase in pH value i.e. at neutral region (pH 6.6-7.5) the value of red color component decreases and at the same time the value of green color component increases significantly. On the other hand, in basic region (pH 8.0-9.0), the value of both red and green color components decreases and as a result pH value higher than 8.0 contains low RGB color components that form dark blue color light. However the variation of blue color component is almost constant as compared to red and green color components within the whole detection range of pH value 4.0 to 9.0. Again the reference ROI shows a constant RGB color components of RGB (255, 255, 255) throughout the pH range. As a result, at acidic region, the value of color ratio increases initially.

**Table 4.6: Experimental data table to formulate calibration equations for pH measurement**

pH Value	RGB (Sample)			RGB (Reference)			Color Ratio ( $C_R$ )	HSV (Sample)			Wavelength (nm)
	R	G	B	R	G	B		H°	S%	V%	
4.0	188.82	61.88	13.12	255	255	255	0.3449	16.65	93.05	74.05	625.08
4.5	191.51	85.18	13.49	255	255	255	0.3793	24.16	92.96	75.10	619.13
5.0	185.61	110.10	16.76	255	255	255	0.4085	33.17	90.97	72.79	611.99
5.5	182.47	137.84	18.10	255	255	255	0.4424	43.71	90.08	71.56	603.64
6.0	156.82	141.39	17.67	255	255	255	0.4129	53.35	88.73	61.50	595.99
6.6	106.04	125.69	13.10	255	255	255	0.3201	70.47	89.58	49.29	582.43
7.0	50.86	96.10	14.24	255	255	255	0.2107	93.16	85.18	37.69	564.44
7.5	22.37	69.22	19.08	255	255	255	0.1447	116.07	72.44	27.15	546.29
8.0	21.14	56.76	24.53	255	255	255	0.1339	125.71	62.75	22.26	538.32
8.5	17.22	37.90	23.22	255	255	255	0.1024	137.41	54.55	14.86	526.80
9.0	22.76	26.76	25.76	255	255	255	0.0984	165	14.95	10.49	499.64

After certain pH value of 5.5, the value of color ratio starts to decrease from 0.4424 to 0.0984 with increase in pH value from 5.5 to 9.0. Alternative color is formed according to pH value and consequently the hue attributes of color is changed significantly from 16.65° to 165° as pH increases from 4.0 to 9.0. However, with increase in pH value, both saturation and value parameter follows a decreasing nature (93.05 to 14.95) % and (74.05 to 10.49) % respectively. The reason behind that, with increase in pH value the color of pH samples shifted from orange to blue and the corresponding hue parameter of blue is higher than orange color along with decrease in intensity.

Thus, in case of pH, wavelength shift is most significant compared to the shift of color ratio or color intensity. In addition to this, hue, saturation and value attributes of colorimetric imaging are changed by following a definite pattern but color ratio is changed randomly. Here the attributes of colorimetric detection (color ratio, hue, saturation and value) are individually considered as the independent variable of single nonlinear regression analysis to calibrate this smart sensing instrument. Multiple order polynomials (Eq. 4.11- 4.14) and corresponding fit curves obtained from single nonlinear regression analysis are shown in Fig. 4.9 to illustrate the individual impacts of the above mentioned attributes on pH measurement in the range of (4.0-9.0) using the designed digital pH meter.

$$pH = 31.40995 - 497.94862C_R + 3978.53303C_R^2 - 15041.58723C_R^3 + 26412.91344C_R^4 - 17314.27283C_R^5 \quad (4.11)$$

$$pH = 3.72413 - 0.02275H + 0.00337H^2 - 0.00006H^3 + 4.08391 * 10^{-7}H^4 - 9.82606 * 10^{-10}H^5 \quad (4.12)$$

$$pH = 44.51685 - 4.62096S + 0.20246S^2 - 0.00403S^3 + 3.74857 * 10^{-5}S^4 - 1.32831 * 10^{-7}S^5 \quad (4.13)$$

$$pH = 11.93588 - 0.4606V + 0.02345V^2 - 6.70958 * 10^{-4}V^3 + 9.29460 * 10^{-6}V^4 - 4.88877 * 10^{-8}V^5 \quad (4.14)$$

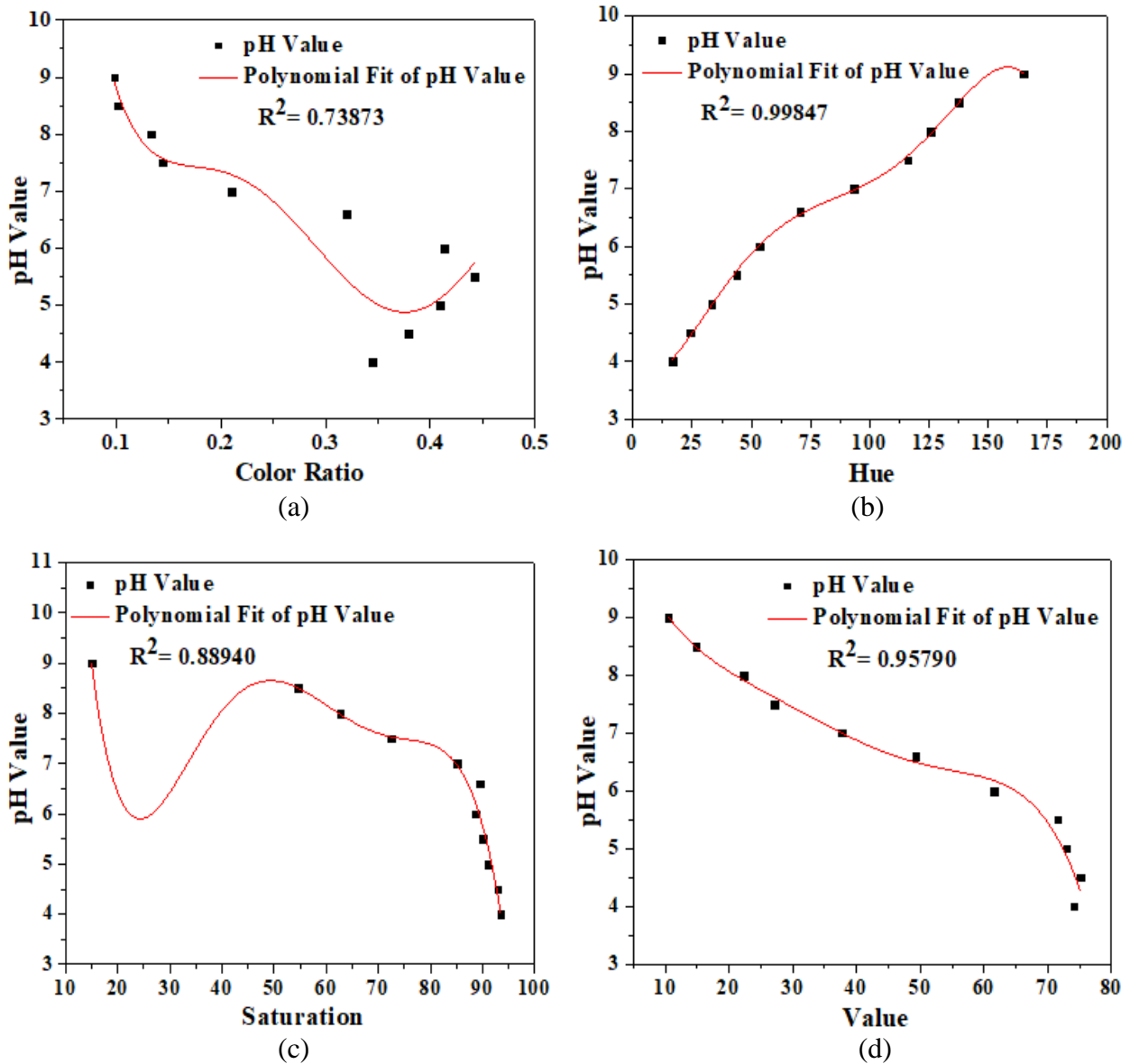


Fig. 4.9: Polynomial fit curve to calibrate the smartphone-based colorimeter as digital pH meter by only considering: (a) color ratio, (b) hue, (c) saturation, and (d) value as independent variable.

Fig. 4.9 illustrates that hue has significant influence but the other attributes of smartphone-based colorimetric detection (color ratio, saturation and value) also have influence on pH value and thus colorimetric detection based on single attributes is not accurate and reliable. Therefore, it is the high time to incorporate the combined impacts of these attributes in the calibration process of digital pH meter through multiple nonlinear regression analysis. Now considering both hue and saturation as the independent variables in multiple nonlinear regression analysis, the obtained third-order polynomial is written by Eq. 4.15.

$$pH = -2.83899 * 10^{-6}H^3 - 1.65203 * 10^{-5}H^2S - 8.92261 * 10^{-6}HS^2 + 1.47824 * 10^{-5}S^3 + 1.52349 * 10^{-3}H^2 + 3.01087 * 10^{-3}HS - 3.19636 * 10^{-3}S^2 - 0.13511H + 0.2023S - 0.1638309956 \quad (4.15)$$

The combined effects of both hue and value attributes are mathematically represented by Eq. 4.16.

$$pH = 1.32541 * 10^{-4}H^3 + 9.32665 * 10^{-4}H^2V + 2.21251 * 10^{-3}HV^2 + 1.70467 * 10^{-3}V^3 - 8.05187 * 10^{-2}H^2 - 0.37567HV - 0.43508V^2 + 16.06086H + 36.95012V - 1042.30785 \quad (4.16)$$

The simultaneous effect of saturation and value attributes in smartphone-based colorimetric detection of pH is formulated through the third-order polynomial expressed by Eq. 4.17.

$$pH = 2.89695 * 10^{-5}S^3 - 3.03759 * 10^{-4}S^2V - 3.31605 * 10^{-4}SV^2 + 2.93986 * 10^{-4}V^3 - 1.21266 * 10^{-2}S^2 + 9.48707 * 10^{-2}SV - 2.17715 * 10^{-2}V^2 - 5.23171 * 10^{-2}S - 3.14313V + 33.80769 \quad (4.17)$$

The above multiple nonlinear regression analysis used two parameters of HSV color model. Now, all of the color components (hue, saturation and value) of HSV color model are considered as the independent variables of multiple nonlinear regression analysis and the corresponding second-order polynomial is mathematically represented by Eq. 4.18.

$$pH = -7.18568 * 10^{-4}H^2 - 1.13635 * 10^{-3}HS + 2.73295 * 10^{-4}HV - 8.32096 * 10^{-4}S^2 + 3.46048 * 10^{-4}SV + 1.00195 * 10^{-3}V^2 + 0.18410H + 0.17752S - 0.19714V - 4.8477 * 10^{-2} \quad (4.18)$$

Finally the combined effect of color ratio, color intensity (V) and wavelength component in smartphone-based colorimetric detection of pH is formulated through multiple nonlinear regression analysis and the corresponding second-order polynomial is written by Eq. 4.19.

$$pH = -34.06076C_R^2 + 5.05958 * 10^{-1}C_RV + 0.21015C_RH - 4.1585 * 10^{-3}V^2 - 4.09722 * 10^{-3}VH - 9.45708 * 10^{-4}H^2 - 12.44175C_R + 0.5161V + 0.3127H - 17.0902 \quad (4.19)$$

Among the polynomials developed for the calibration of digital pH meter, multiple nonlinear regression based calibration techniques are fitted strongly than single nonlinear regression based calibration techniques verified from the value of determination coefficient. The determination coefficients and associated parameters corresponding to above mentioned different calibration techniques for smartphone-based colorimetric pH measurement are tabulated in Table 4.7.

**Table 4.7: Calibration techniques applied for the calibration of digital pH meter**

Calibration Methods	Calibration Attributes	Order of Polynomial	Determination Co-efficient ( $R^2$ )
Single Nonlinear regression analysis	Color Ratio ( $C_R$ )	5	0.73873
	Hue (H)	5	0.99847
	Saturation (S)	5	0.88940
	Value (V)	5	0.95790
Multiple nonlinear regression analysis	H & S	3	0.99989
	H & V	3	0.99977
	S & V	3	0.99977
	H, S & V	2	0.999996
	$C_R$ , H & V	2	<b>0.9999995</b>

### 4.3.3 Performance Analysis of Digital pH Meter

Various calibration techniques are followed in the above section for performance evaluation and find out the most reliable calibration technique for smartphone-based colorimetric measurement of pH value. For performance analysis seven different test samples of unknown pH value from different sources are collected and prepared for colorimetric analysis to determine pH value of those samples using the smartphone-based colorimeter. At first, the pH values of those test samples are measured by incorporating color ratio based polynomial (Eq. 4.11) on customized smartphone app and the corresponding maximum and average error of detection are found as 26.67% and 10.24% respectively. Therefore, measurement of pH value of unknown analyte by smartphone colorimeter based on color ratio as independent variable for single nonlinear regression analysis cannot detect actual pH value and thus incorporates huge error. The developed polynomial (Eq. 4.12) based on hue is well fitted over the detection range of pH 4.0 to 9.0 having determination coefficient 0.99847 and contains maximum 1.00% detection error with an average error of only 0.66%. This low detection error in smartphone-based pH measurement clarify that hue is strongly correlated with pH value and can be implemented for reliable pH measurement purpose. Similarly the average detection error associated with single nonlinear regression analysis based on saturation and value attributes (Eq. 4.13 and Eq. 4.14) are 5.43% and 3.21% respectively which are higher than the average error associated with hue based pH measurement. Comparing the performance of single nonlinear regression analysis, it is found that the calibration of smartphone-based digital pH meter using hue attributes provides high accuracy. But the effect of other colorimetric attributes (color ratio, saturation and value) also considerable for reliable pH measurement. Considering this, the performance of smartphone-based colorimeter as a digital pH meter is also evaluated by implementing the polynomials obtained from multiple nonlinear regression analysis based on the combined effects of color ratio, hue, saturation and value.

Considering the combined effects of hue-saturation and hue-value, the performance of smartphone-based colorimeter is analyzed through measuring the pH value of the same test samples using Eq. 4.15 and Eq. 4.16 and the corresponding average detection errors are found 0.9087% and 1.22% respectively. These errors are smaller compared to the detection error associated with single nonlinear regression analysis based on saturation and value separately. Therefore, the performance of smartphone-based digital pH meter increases significantly by incorporating multiple nonlinear regression analysis. On the other hand, the average detection error of saturation-value (Eq. 4.17) based colorimetric pH detection is found to be 3.40% which is higher than the detection error produced by multiple nonlinear regression analysis based on hue-saturation and hue-value. In the case of colorimetric detection of pH, different pH samples show different color i.e. hue plays most significant role rather than saturation and value. Therefore, if saturation-value based detection algorithm is incorporated, then considerable error will introduce in smartphone-based pH measurement. pH detection accuracy of smartphone-based colorimeter is also evaluated through HSV color model based calibration technique (Eq. 4.18) where all of the HSV color components are considered as independent variables for multiple nonlinear regression analysis that provides maximum 0.446% detection error along with an average detection error of only 0.2027%. This average detection error is less than the average error of above mentioned nonlinear regression analysis for pH measurement using one or two attributes of colorimetric detection. Finally, the pH detection accuracy is evaluated by implementing multiple nonlinear regression analysis where color ratio, hue and value are considered as the independent variables. The developed polynomial (Eq. 4.19) considering color ratio, hue and value is best fitted throughout the pH range ( $R^2 = \sim 1.0$ ) and as a result this calibration technique is able to detect pH value with negligible error of 0.0876% only.

Comparing the detection errors of above mentioned all calibration techniques for smartphone-based colorimetric measurements of pH, it is found that the pH detection algorithm based on color ratio, color intensity and wavelength provides the best accuracy compared to all other detection techniques. It is also clear that if more attributes of colorimetric detection are incorporate to formulate detection algorithm in smartphone-based colorimetric measurement, it can measure the exact pH value compatible with standard pH meter. The test results of smartphone-based colorimetric pH measurement for performance analysis among different calibration techniques are summarized in Table 4.8.

**Table 4.8: Test results of smartphone-based colorimetric pH measurement for performance analysis among different calibration techniques**

Sample no. (Sample name)	Actual pH measured by standard pH meter	Measured pH by considering $C_R$		Measured pH by considering H		Measured pH by considering S		Measured pH by considering V		Measured pH by considering H & S		Measured pH by considering H & V		Measured pH by considering S & V		Measured pH by considering H, S & V		Measured pH by considering H, V & $C_R$	
		pH	% Error	pH	% Error	pH	% Error	pH	% Error	pH	% Error	pH	% Error	pH	% Error	pH	% Error	pH	% Error
<b>Sample 1</b> (Standard buffer solution)	<b>4.0</b>	5.0669	<b>26.67</b>	4.0371	0.928	4.2906	7.265	4.5926	<b>14.82</b>	4.0069	0.173	3.9999	<b>0.003</b>	4.2679	<b>6.698</b>	3.9875	0.313	4.0001	0.0025
<b>Sample 2</b> (Kinley drinking water)	<b>5.4</b>	5.4223	<b>0.413</b>	5.4202	0.374	5.6425	4.491	5.3488	0.948	5.4019	0.035	5.3489	0.946	5.2539	2.706	5.3768	0.430	5.3875	0.231
<b>Sample 3</b> (Oxy drinking water)	<b>6.5</b>	5.3218	18.13	6.4618	0.588	6.0060	7.600	6.6080	1.662	6.4860	0.215	6.3631	2.106	6.6867	2.872	6.5038	0.058	6.4985	0.023
<b>Sample 4</b> (Mum drinking water)	<b>6.6</b>	5.4460	17.48	6.5561	0.665	5.9210	<b>10.29</b>	6.4956	1.582	6.5984	0.024	6.4757	1.883	6.4659	2.032	6.6024	<b>0.036</b>	6.6011	0.017
<b>Sample 5</b> (Standard buffer solution)	<b>7.0</b>	7.2858	4.083	6.9773	<b>0.324</b>	6.9583	<b>0.596</b>	7.0019	<b>0.027</b>	7.0015	0.021	6.9682	0.454	7.0018	<b>0.026</b>	6.9960	0.057	6.9981	0.027
<b>Sample 6</b> (Fresh drinking water)	<b>7.3</b>	7.3669	0.916	7.373	<b>1.00</b>	7.5473	3.388	7.4142	1.564	7.2987	<b>0.018</b>	7.3526	0.721	7.0784	3.036	7.3038	0.079	7.3000	<b>0.00</b>
<b>Sample 7</b> (Supply water of KUET)	<b>7.9</b>	8.2168	4.010	7.9595	0.753	7.5535	4.386	8.0455	1.842	7.6729	<b>2.875</b>	8.0895	<b>2.399</b>	7.3924	6.425	7.8648	<b>0.446</b>	7.9247	<b>0.313</b>
<b>Average error (%)</b>		<b>10.24</b>		<b>0.6617</b>		<b>5.43</b>		<b>3.21</b>		<b>0.9087</b>		<b>1.22</b>		<b>3.40</b>		<b>0.2027</b>		<b>0.0876</b>	

From all of the developed nonlinear regression models for smartphone-based colorimetric detection of pH, the mostly fitted six nonlinear regression models are selected which provide small amount of average detection error with high determination coefficient. The percentage detection errors correspond to these six nonlinear regression models are plotted in Fig. 4.10 which depicts that saturation-value based multiple nonlinear regression incorporates highest detection error to pH measurement. However when color ratio, hue and value components are considered as the independent variables for multiple nonlinear regression analysis then the performance of digital pH meter increases drastically and incorporates very negligible detection error over the desired pH range.

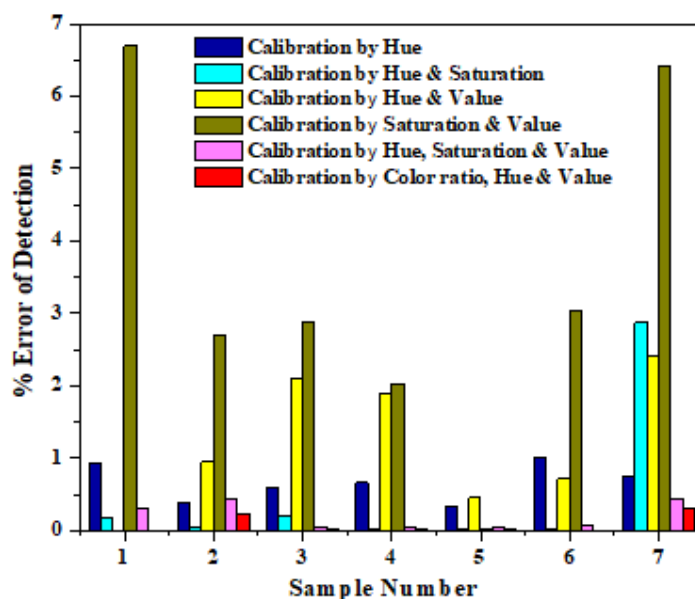


Fig. 4.10: Percentage error of detection associated with smartphone-based colorimetric measurement of pH value using different calibration techniques.

From Fig. 4.10, finally it can be concluded that, calibration by considering color ratio, hue and value as the independent variables of multiple nonlinear regression analysis, is the best technique to calibrate the smartphone-based colorimeter as digital pH meter with  $\sim 100\%$  accuracy. So the developed polynomial (Eq. 4.19) considering the combined effects of color ratio, color intensity and wavelength is selected as the final calibration equation and integrated with the algorithm of customized smartphone app for error free measurement of pH (Fig. 4.11). Finally, the measured pH value of seven different test samples is compared with the pH value measured by conventional glass electrode based standard pH meter, shown in Fig 4.12. The negligible variations between the measurements certify that the developed smartphone-based colorimeter is highly suitable for low cost, field portable and real time pH monitoring. The error bars represents negligible standard deviations for three consecutive measurements of each pH sample measured on smartphone-based colorimeter.



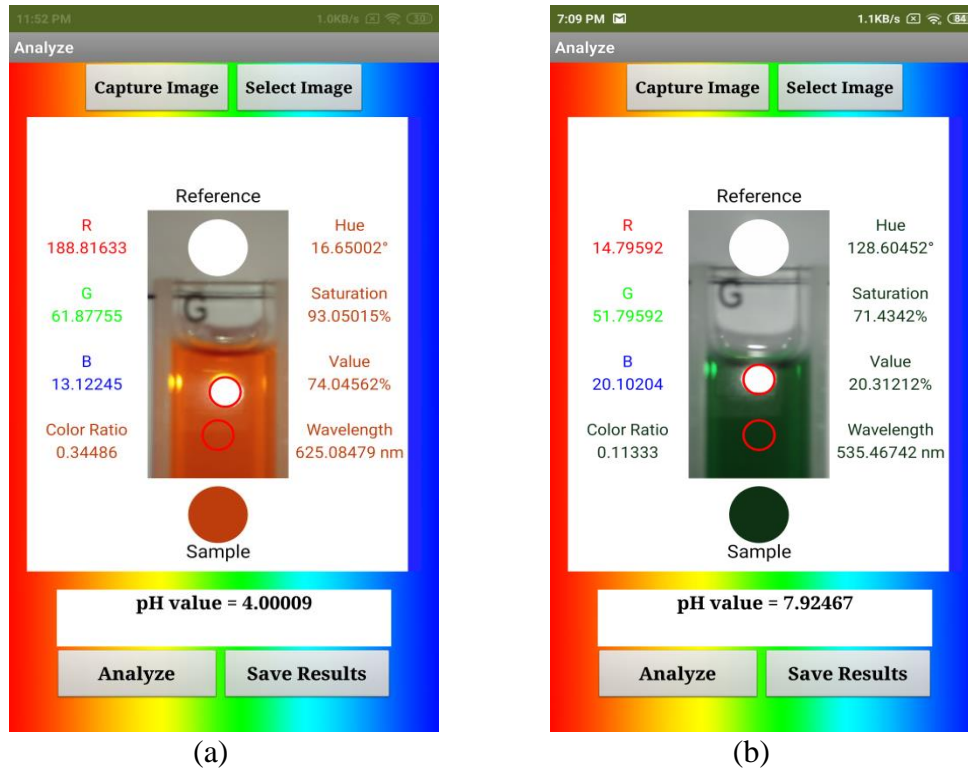


Fig. 4.11: Screenshots of pH measurement using customized smartphone app: (a) standard buffer solution of actual pH 4.0 (measured pH = 4.00009) and (b) supply water of KUET of actual pH 7.9 (measured pH = 7.92467).

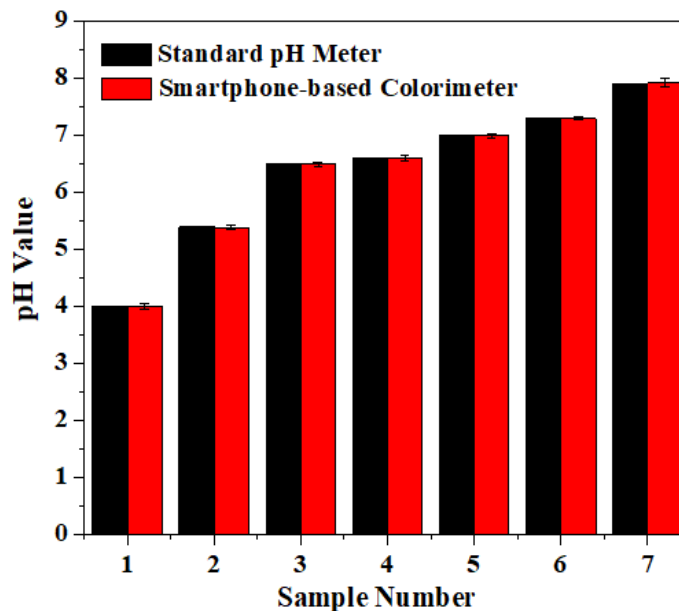


Fig. 4.12: pH value of seven test samples measured on smartphone-based colorimeter and standard pH meter.

#### 4.4 Chlorine Concentration Quantifier

Finally, the designed smartphone-based colorimeter is implemented as chlorine concentration quantifier to evaluate its performance for the cases in colorimetric detection where both intensity and wavelength of color in the test specimen are changed significantly with respect to the desired analytical parameter which has to be determined. In these cases, both intensity and wavelength of color vary without following any specified rules and the pattern of this variation is dependent on the types of analytes. These are the most common cases for colorimetric detection. The conventional smartphone colorimeters are totally unable to handle these cases where both wavelength and intensity of color of the test specimen are varied simultaneously. For the colorimetric detection of chlorine concentration in water, both intensity and wavelength of the reflected light from the sample solution changes simultaneously according to the concentration of chlorine of that sample. But the previously reported smartphone-based colorimeters detected chlorine concentration based on color ratio or color intensity which cannot measure chlorine concentration accurately for whole range of detection [36]. Conventional smartphone-based colorimetric detection techniques do not consider the change of wavelength in conjunction with the change of intensity. In this research, for the first time, we have developed a universal smartphone-based colorimeter that effectively works in all situations; it may be intensity change, tone change or wavelength change of color.

##### 4.4.1 Sample Preparation

In this research KI-starch solution is used as the indicator for cost effective smartphone-based colorimetric measurement of chlorine concentration. The KI-starch solution is prepared according to a well-known modified iodometric method reported in [36]. At first, 30 gm of KI powder is dissolved in 200 ml of distilled water in a beaker. At the same time, 2 gm of starch powder  $[(C_6H_{10}O_5)_n]$  is dissolved in 50 ml of distilled water in a separate beaker. After that, the desired KI-starch solution is obtained by mixing only 30 ml of starch solution to the above 200 ml of KI solution.

To prepare chlorine solution, calcium hypochlorite ( $Ca(ClO)_2$ ) is used as it is typically used in the chlorination process for drinking water and swimming pools for water treatment which is the main active ingredient of bleaching powder or chlorine powder. According to WHO, the acceptable limit of chlorine concentration in drinking water is up to 5 PPM [71]. Considering this, different concentration chlorine solutions ranging from (0.1-8.0) PPM are prepared covering the acceptable range of WHO since the primary goal of this research is to monitor drinking water quality by measuring various parameters of drinking water such as chlorine concentration. At first 25 mg of calcium hypochlorite is dissolved in 250 ml of distilled water to prepare 100 PPM stock solution. This 250 ml stock solution with concentration 100 PPM is further diluted in different amount of distilled water sequentially to get the desired chlorine solutions of concentration (0.1-8.0) PPM. For example, to obtain 1.0 PPM chlorine solution, 100  $\mu$ l of previously prepared stock solution is added with 10 ml of distilled water by using high precision micropipette. After that, the desired chlorine sample for colorimetric measurement is obtained by mixing only 10 ml of above prepared 1.0 PPM chlorine solution to the previously prepared 150  $\mu$ l of KI-starch solution which acts as the chlorine indicator for colorimetric detection.

Total 24 differently concentrated chlorine samples are prepared similarly and the required amount of stock solution, distilled water and KI-starch indicator to prepare all these chlorine samples covering the range of (0.1-8.0) PPM are summarized in Table 4.9. From these chlorine samples as shown in Fig. 4.13, it can be clearly observed that there is a color change in two different tones as the concentration of the chlorine in distilled water gets increased from 0.1 PPM to 8.0 PPM. Chlorine samples within the range of (0.1-1.0) PPM show a bluish color, at chlorine concentration ~1.5 PPM chlorine sample become almost colorless and chlorine concentration within the range of (2.0-8.0) PPM show a greenish color.

**Table 4.9: Preparation of chlorine samples of different concentrations with KI-starch indicator as chemosensor**

Sl. No.	Desired Chlorine Concentration (PPM)	Required Stock Solution of 100 PPM ( $\mu$ l)	Required Distilled Water (ml)	Required KI-Starch Indicator ( $\mu$ l)	Resultant Chlorine Samples (ml)
01	0.1	10	10	150	10.15
02	0.2	20	10	150	10.15
03	0.3	30	10	150	10.15
04	0.4	40	10	150	10.15
05	0.5	50	10	150	10.15
06	0.6	60	10	150	10.15
07	0.7	70	10	150	10.15
08	0.8	80	10	150	10.15
09	0.9	90	10	150	10.15
10	1.0	100	10	150	10.15
11	1.5	150	10	150	10.15
12	2.0	200	10	150	10.15
13	2.5	250	10	150	10.15
14	3.0	300	10	150	10.15
15	3.5	350	10	150	10.15
16	4.0	400	10	150	10.15
17	4.5	450	10	150	10.15
18	5.0	500	10	150	10.15
19	5.5	550	10	150	10.15
20	6.0	600	10	150	10.15
21	6.5	650	10	150	10.15
22	7.0	700	10	150	10.15
23	7.5	750	10	150	10.15
24	8.0	800	10	150	10.15

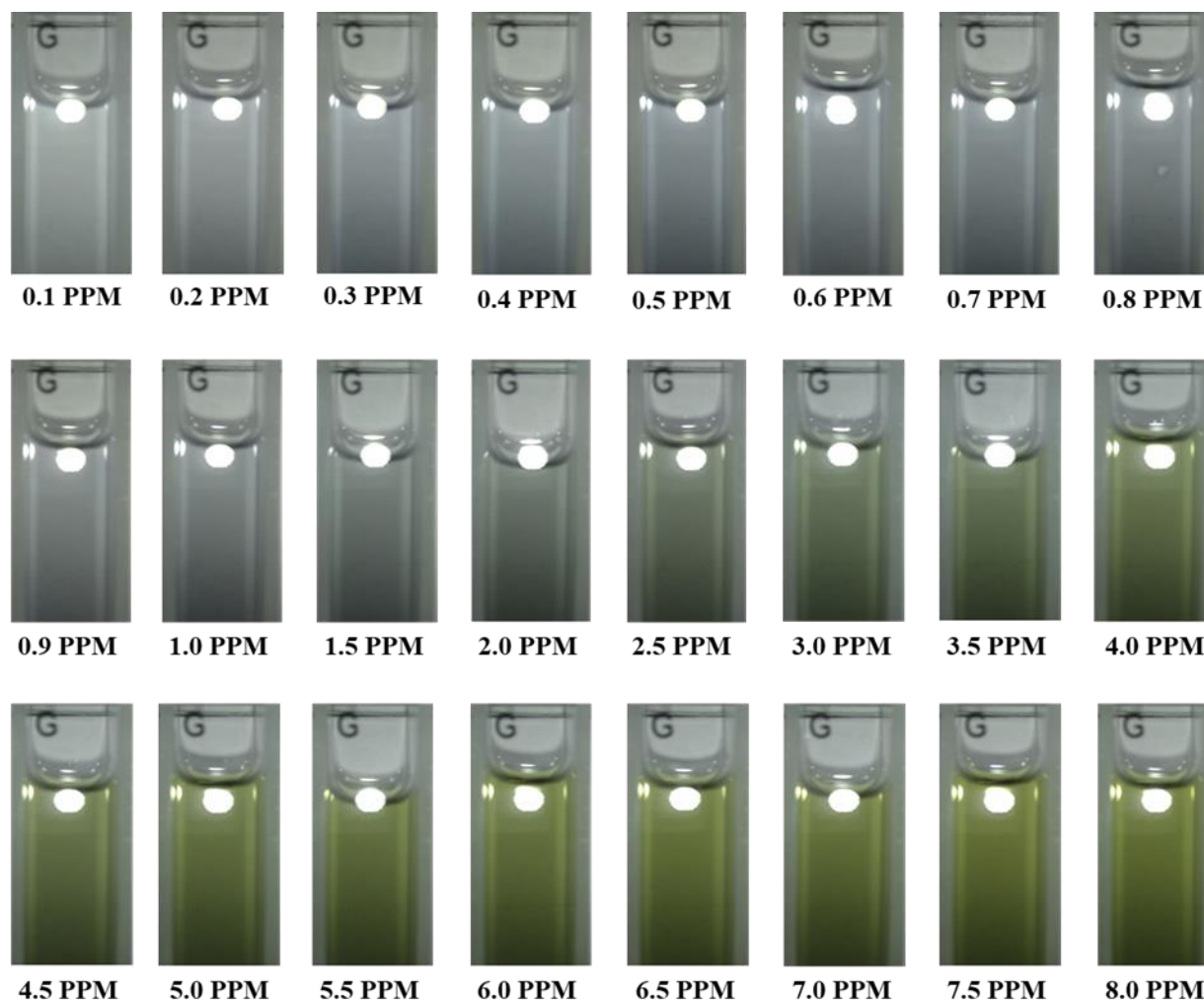


Fig. 4.13: Photograph of chlorine samples (0.1-8.0) PPM for proper calibration of smartphone-based colorimetric measurement of chlorine concentration.

#### 4.4.2 Calibration of Chlorine Concentration Quantifier

Before implementing smartphone-based colorimeter as chlorine concentration quantifier, it is calibrated by following the similar procedure as discussed in the previous section 4.2.2 for RhB concentration quantifier. The calibration process applied for chlorine concentration quantifier is illustrated in Fig. 4.14 for two different chlorine solution of known concentration. After implementing this process for twenty four chlorine samples which are prepared for proper calibration of the developed smartphone-based colorimeter as chlorine concentration quantifier, a complete data table consisting of the essential attributes for formulating appropriate calibration equations is tabulated in Table 4.10.

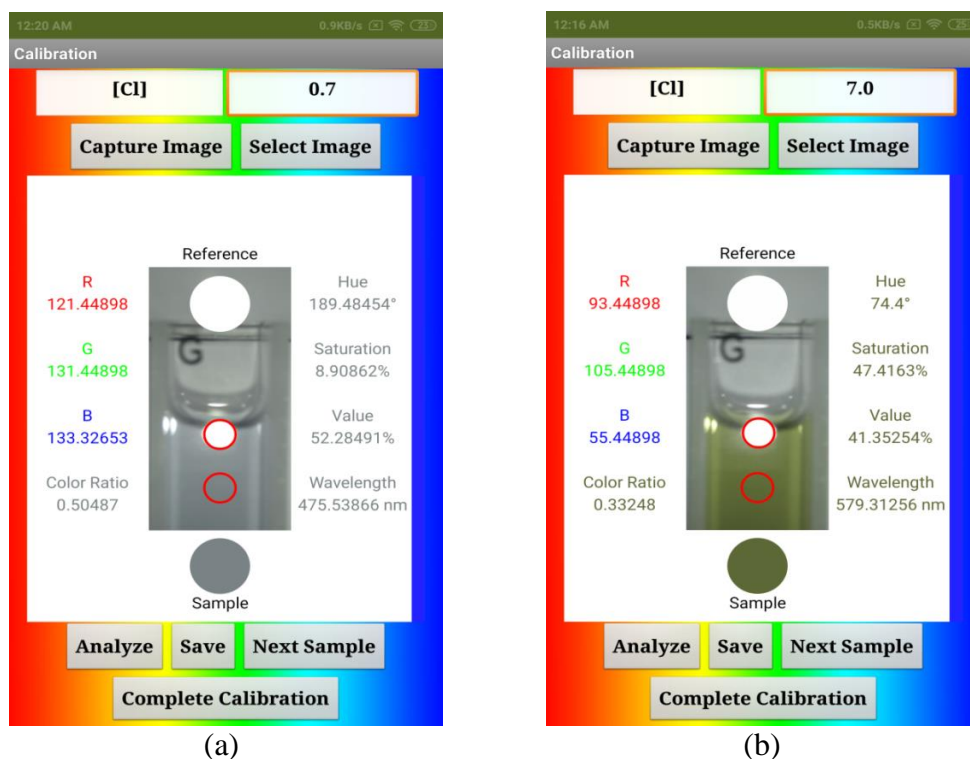


Fig. 4.14: Calibration screen of the developed app illustrating the colorimetric analysis of two samples with different chlorine concentration: (a) 0.7 PPM and (b) 7.0 PPM.

From Table 4.10, it can be said that, throughout the concentration range (0.1-8.0) PPM, hue varies from  $193.52^\circ$  to  $72.30^\circ$  in a random nature covering blue to greenish-yellow region of color space. Within the band of (0.1-0.7) PPM, we get a tone of blue color having wavelength range of (504.56-475.54) nm. Higher than 0.7 PPM, the change of wavelength with increase in chlorine concentration is significant. As a result, within the range of (0.8-3.5) PPM, chlorine solutions form green and greenish-yellow color covering the wavelength range of (484.88-566.89) nm. However, chlorine concentration higher than 3.5 PPM has no influence on sample color that means in the concentration range of (4.0-8.0) PPM, chlorine samples have almost constant wavelength of  $(577 \pm 3)$  nm with varying saturation parameter. Within the concentration band of (0.5-0.8) PPM, saturation parameter shows constant nature because in this band the variation of RGB color components is negligible. However, beyond this range there is a trend of increasing saturation component from 6.85% to 54.27% as the concentration of chlorine get increased from 0.9 to 8.0 PPM. On the other hand, value parameter follows a decreasing nature up to 1.5 PPM chlorine concentration where it reached at 46.16%. But beyond 1.5 PPM, value parameter behaves as constant that means variation of chlorine concentration more than 1.5 PPM has no impact on light intensity specified by value parameter. So it can be concluded that hue, saturation and value all are randomly changing parameter for this colorimetric measurement of chlorine. Each of them become active at a specific band of chlorine concentration and become inactive beyond this band.

**Table 4.10: Experimental data table to formulate calibration equations for chlorine concentration quantification**

[Cl] (PPM)	RGB (Sample)			RGB (Reference)			Color Ratio (C <sub>R</sub> )	HSV (Sample)			Wavelength (nm)
	R	G	B	R	G	B		H°	S%	V%	
0.1	155.37	164.37	161.37	255	255	255	0.6289	160	5.48	64.46	504.56
0.2	143.88	149.94	149.92	255	255	255	0.5801	179.80	6.04	59.37	485.07
0.3	135.94	144.47	146.73	255	255	255	0.5584	192.59	7.36	57.54	472.48
0.4	133.49	143.49	145.10	255	255	255	0.5517	193.52	8.0	56.90	471.56
0.5	123.51	133.51	135.51	255	255	255	0.5131	190	8.86	53.14	475.03
0.6	124.76	134.71	135.73	255	255	255	0.5166	185.58	8.09	53.23	479.39
0.7	121.45	131.45	133.33	255	255	255	0.5049	189.48	8.91	52.28	475.54
0.8	119.80	129.80	130.80	255	255	255	0.4972	180	8.41	51.29	484.88
0.9	122.31	131.31	129.45	255	255	255	0.5007	167.62	6.85	51.49	497.06
1.0	115.24	124.12	121.33	255	255	255	0.4715	161.10	7.15	48.68	503.48
1.5	108.18	117.71	112.45	255	255	255	0.4423	146.85	8.10	46.16	517.50
2.0	101.63	111.63	103.63	255	255	255	0.4143	132	8.96	43.78	532.13
2.5	99.43	110.43	94.43	255	255	255	0.3978	101.25	14.49	43.31	558.03
3.0	96.90	110.49	87.69	255	255	255	0.3857	97.77	20.63	43.33	562.37
3.5	95.59	109.16	82.08	255	255	255	0.3750	90.07	24.81	42.81	566.89
4.0	96.84	108.57	74.33	255	255	255	0.3657	80.56	31.54	42.58	574.43
4.5	95.47	107.47	67.71	255	255	255	0.3538	78.11	36.99	42.14	576.37
5.0	93.92	106.63	62.78	255	255	255	0.3442	77.39	41.13	41.82	576.94
5.5	94.16	106.29	60.29	255	255	255	0.3408	75.81	43.28	41.68	578.19
6.0	94.47	106.92	57.67	255	255	255	0.3386	75.17	46.06	41.93	578.70
6.5	95.84	108.76	56	255	255	255	0.3406	74.69	48.51	42.65	579.08
7.0	93.45	105.45	55.45	255	255	255	0.3325	74.40	50.51	41.35	579.31
7.5	95.67	106.88	52.22	255	255	255	0.3330	72.30	52.41	41.91	580.08
8.0	94.29	106.59	50.10	255	255	255	0.3281	73.07	54.27	41.80	580.37

In the conventional methods [18], [36] color ratio is the only attributes of colorimetric detection which is considered for the calibration of chlorine concentration quantifier. In this research, not only color ratio but also hue, saturation and value attributes of colorimetric imaging are considered as the independent variable for the calibration of this colorimetric sensing instrument. Multiple order polynomials (Eq. 4.20- 4.23) and corresponding calibration fit curves (Fig. 4.15) are developed using single nonlinear regression analysis to represent the individual effects of the above mentioned attributes on the performance of chlorine concentration determination in the range of (0.1-8.0) PPM. The determination coefficients corresponding to these calibration techniques based on single nonlinear regression analysis are tabulated in Table 4.11.

$$[Cl] = 1442.837 - 14748.72083C_R + 60238.88748C_R^2 - 122472.13804C_R^3 + 123725.39494C_R^4 - 49640.77137C_R^5 \quad (4.20)$$

$$[Cl] = 483.72403 - 18.78728H + 0.28706H^2 - 0.00214H^3 + 7.80024 * 10^{-6}H^4 - 1.11119 * 10^{-8}H^5 \quad (4.21)$$

$$[Cl] = -1.77963 + 0.37576S - 0.004S^2 - 2.98202 * 10^{-4}S^3 + 9.66121 * 10^{-6}S^4 - 7.43299 * 10^{-8}S^5 \quad (4.22)$$

$$[Cl] = 14379.7598 - 1336.88547V + 49.55042V^2 - 0.91502V^3 + 0.00842V^4 - 3.0861 * 10^{-5}V^5 \quad (4.23)$$

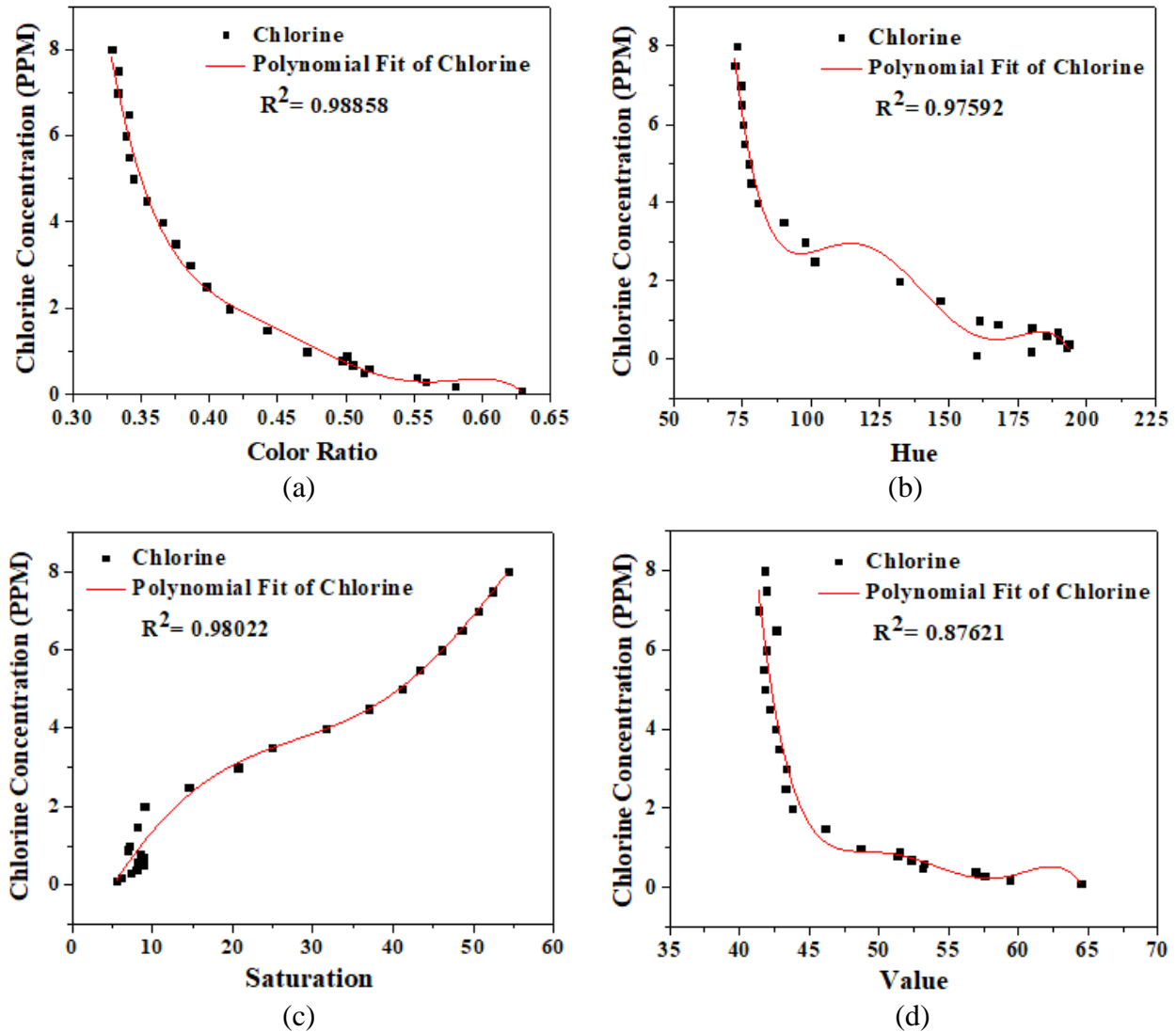


Fig. 4.15: Polynomial fit curve to calibrate the smartphone-based colorimeter as chlorine concentration quantifier by only considering: (a) color ratio, (b) hue, (c) saturation, and (d) value.

Since the attributes of detection (color ratio, hue, saturation and value) are the randomly changing parameters corresponding to the chlorine concentration, combined impacts of these attributes have to be incorporated in the calibration process covering the whole range of detection. In order to verify the impact of multiple attributes simultaneously, multiple nonlinear regression analysis is introduced to formulate calibration equation with two or more independent

variables. Considering both hue and saturation as the independent variables in multiple nonlinear regression analysis, the obtained fifth-order polynomial is written by Eq. 4.24.

$$[Cl] = 1.322 * 10^{-8}H^5 + 1.775 * 10^{-7}H^4S + 1.541 * 10^{-6}H^3S^2 + 6.74 * 10^{-6}H^2S^3 + 6.06 * 10^{-6}HS^4 + 1.783 * 10^{-6}S^5 - 1.195 * 10^{-5}H^4 - 1.36 * 10^{-4}H^3S - 8.206 * 10^{-4}H^2S^2 - 1.751 * 10^{-3}HS^3 - 7.821 * 10^{-4}S^4 + 4.317 * 10^{-3}H^3 + 3.783 * 10^{-2}H^2S + 0.132HS^2 + 0.118S^3 - 0.775H^2 - 4.463HS - 6.829S^2 + 68.579H + 190.68S - 2385.568 \quad (4.24)$$

The combined impact of wavelength and intensity of color in smartphone-based colorimetric detection of chlorine concentration is investigated here by formulating a calibration equation expressed by Eq. 4.25.

$$[Cl] = 3.144 * 10^{-6}H^4 - 4.739 * 10^{-5}H^3V + 2.456 * 10^{-4}H^2V^2 - 4.149 * 10^{-4}HV^3 - 3.995 * 10^{-4}V^4 + 4.852 * 10^{-4}H^3 - 2.951 * 10^{-3}H^2V - 1.702 * 10^{-2}HV^2 + 0.164V^3 - 5.03 * 10^{-2}H^2 + 1.60HV - 12.386V^2 - 25.639H + 363.265V - 3791.187 \quad (4.25)$$

Now saturation and value attributes are considered and the obtained calibration equation is given by Eq. 4.26.

$$[Cl] = 9.158 * 10^{-7}S^4 + 9.039 * 10^{-6}S^3V + 2.808 * 10^{-4}S^2V^2 + 5.941 * 10^{-4}SV^3 + 1.148 * 10^{-4}V^4 - 4.648 * 10^{-4}S^3 - 2.552 * 10^{-2}S^2V - 9.241 * 10^{-2}SV^2 - 2.806 * 10^{-2}V^3 + 0.581S^2 + 4.712SV + 2.495V^2 - 78.974S - 96.161V + 1362.246 \quad (4.26)$$

To evaluate the performance of chlorine concentration quantifier using HSV color components, multiple nonlinear regression analysis is performed here by considering hue, saturation and value simultaneously as the independent variables and a calibration polynomial is obtained (Eq. 4.27).

$$[Cl] = -6.101 * 10^{-5}H^3 - 4.221 * 10^{-4}H^2S + 6.394 * 10^{-4}H^2V - 6.561 * 10^{-4}HS^2 + 3.799 * 10^{-3}HSV + 7.11 * 10^{-4}HV^2 - 1.184 * 10^{-4}S^3 + 4.316 * 10^{-3}S^2V - 5.154 * 10^{-3}SV^2 - 1.205 * 10^{-2}V^3 + 4.72 * 10^{-3}H^2 - 4.124 * 10^{-2}HS - 0.354HV - 0.111S^2 - 0.225SV + 1.874V^2 + 8.773H + 11.094S - 67.344V + 642.803 \quad (4.27)$$

In this section, both RGB and HSV color attributes (color ratio, hue and saturation) are considered to formulate calibration equation (Eq. 4.28) through multiple nonlinear regression analysis.

$$[Cl] = -15616.391C_R^3 + 22.987C_R^2H - 226.517C_R^2S + 4.832 * 10^{-2}C_RH^2 + 0.80C_RHS - 2.926 * 10^{-2}C_RS^2 - 6.085 * 10^{-5}H^3 - 7.153 * 10^{-4}H^2S + 5.036 * 10^{-5}HS^2 + 1.335 * 10^{-4}S^3 + 22380.928C_R^2 - 50.203C_RH + 94.64C_RS + 1.719 * 10^{-2}H^2 - 0.172HS - 9.686 * 10^{-3}S^2 - 7460.074C_R + 10.657H - 8.664S + 669.918 \quad (4.28)$$

The determination coefficients and associated parameters corresponding to above mentioned different calibration techniques for smartphone-based colorimetric chlorine concentration measurement are tabulated in Table 4.11.



**Table 4.11: Calibration techniques applied for the calibration of chlorine concentration quantifier**

Calibration Techniques	Calibration Attributes	Order of Polynomial	Determination Coefficient ( $R^2$ )
Single Nonlinear regression analysis	Color Ratio ( $C_R$ )	5	0.98858
	Hue (H)	5	0.97592
	Saturation (S)	5	0.98022
	Value (V)	5	0.87621
Multiple nonlinear regression analysis	H & S	5	0.99986
	H & V	4	0.98305
	S & V	4	0.99968
	H, S & V	3	0.99982
	$C_R$ , H & S	3	<b>0.99998</b>

#### 4.4.3 Performance Analysis of Chlorine Concentration Quantifier

For performance evaluation, the developed polynomials based on different calibration techniques are incorporated sequentially with the customized smartphone app for smartphone-based colorimetric detection of chlorine concentration. Differently concentrated seven test samples of chlorine are prepared for colorimetric detection by using chlorine concentration quantifier. Its performance based on color ratio (conventional method) is analyzed by determining the chlorine concentration of seven test samples that contains an average error of 11.18%. Therefore, measurement of chlorine concentration by using color ratio as independent variable for single nonlinear regression analysis cannot measure the actual concentration of chlorine. Throughout the detection range (0.1-8.0) PPM, the change of color information with change in chlorine concentration cannot be addressed by only considering color ratio which is calculated from RGB color components. Chlorine concentration measured by implementing polynomials Eq. 4.21 and 4.23 clarify that the individual hue and value attributes based single nonlinear regression is totally unfitted for colorimetric detection of chlorine because they incorporate abnormal detection error of 1615.38% and 6400.76% respectively. Over the detection range, there is no noticeable change in value parameter and as a result value parameter cannot influence chlorine concentration significantly as verified by the average error of detection. The analyzed results considering saturation (Eq. 4.22) associated with an average of 31.37% detection error which is very much lower than the average error provided by single nonlinear regression based on hue and value but higher than the calibration technique based on color ratio. It can be said that smartphone-based colorimetric detection of chlorine concentration using saturation is unfitted for the measurement of low chlorine concentration and moderately fitted for high chlorine concentration range above 3.0 PPM. All of the calibration techniques based on single nonlinear regression analysis cannot measure chlorine concentration reliably because the color change information of chlorine sample during colorimetric measurement cannot be described by only a single attribute and promote to find new reliable technique for determining chlorine concentration.

To meet this, the polynomial obtained from multiple nonlinear regression analysis considering the combined effects of hue and saturation (Eq. 4.24) is implemented to detect chlorine concentration of the previously prepared seven test sample. In the present case, the maximum detection error is of 19.22% with an average detection error of 3.92% which is lower than the error produced by single nonlinear regression analysis discussed earlier. Therefore it can be said that when multiple attributes of colorimetric measurement are considered, smartphone-based colorimeter will able to detect chlorine concentration with considerable error. Similarly, the performance of chlorine concentration quantifier is evaluated through multiple nonlinear regression analysis based on hue-saturation and saturation-value which contain an average of 8.73% and 3.86% detection errors respectively. These errors are less than the average error associated with the calibration technique based on single nonlinear regression using hue, saturation or value separately. Average 1.60% error is incorporated within the detected results of smartphone-based colorimeter when the polynomial (Eq. 4.27) based on combined impacts of hue, saturation and value are considered for colorimetric chlorine measurement. This error is very less than the error produced by RGB color components based (color ratio) analysis and so this method of colorimetric detection of chlorine concentration is too better than the conventional methods with an increased range of detection.

Multiple nonlinear regression based polynomial (Eq. 4.28) considering color ratio, hue and saturation is perfectly fitted with the whole detection range of chlorine (0.1-8.0) PPM ( $R^2=0.99998$ ) and can able to detect chlorine concentration throughout the detection range with least detection error (average 1.16%) which is smaller compared to the above mentioned all nonlinear regression models. It is also noticeable that, over the detection range color ratio, color tone and wavelength all attributes of colorimetric measurement are changed randomly and as result when color ratio, hue and saturation all are considered simultaneously to formulate the desired polynomial then the detection errors are reduced significantly. In addition to this, it can be concluded that if more attributes are incorporated then the results provided by chlorine concentration quantifier will approached toward the actual chlorine concentration. The test results of smartphone-based colorimetric measurement of chlorine concentration for performance analysis among different calibration techniques are summarized in Table 4.12.

**Table 4.12: Test results of smartphone-based colorimetric measurement of chlorine concentration for performance analysis among different calibration techniques**

Sample no.	Actual [Cl] (PPM)	Measured [Cl] by considering $C_R$		Measured [Cl] by considering H		Measured [Cl] by considering S		Measured [Cl] by considering V		Measured [Cl] by considering H & S		Measured [Cl] by considering H & V		Measured [Cl] by considering S & V		Measured [Cl] by considering H, S & V		Measured [Cl] by considering $C_R$ , H & S	
		[Cl] PPM	% Error	[Cl] PPM	% Error	[Cl] PPM	% Error	[Cl] PPM	% Error	[Cl] PPM	% Error	[Cl] PPM	% Error	[Cl] PPM	% Error	[Cl] PPM	% Error	[Cl] PPM	% Error
Sample 1	<b>0.1</b>	0.0761	<b>23.9</b>	7.8534	<b>7753.4</b>	0.1187	18.7	38.9170	<b>38817</b>	0.0980	2.00	0.0994	<b>0.60</b>	0.0993	0.70	0.0992	0.80	0.0993	0.70
Sample 2	<b>0.5</b>	0.5747	14.94	12.6812	2436.2	1.0837	<b>116.7</b>	18.6177	3623.5	0.5961	<b>19.22</b>	0.6172	<b>23.44</b>	0.5610	<b>12.2</b>	0.5213	<b>4.26</b>	0.5156	<b>3.12</b>
Sample 3	<b>1.0</b>	1.1782	17.82	7.9751	697.5	0.6174	38.26	13.5664	1256.6	1.0511	5.11	1.0783	7.83	1.0790	7.90	1.0345	3.45	1.0300	3.00
Sample 4	<b>1.5</b>	1.6359	9.06	6.8834	358.9	0.8821	41.19	11.3840	658.93	1.4850	1.00	1.5144	0.96	1.4412	3.92	1.4902	0.653	1.4935	0.433
Sample 5	<b>3.0</b>	2.8231	5.897	4.3568	45.23	3.1239	4.13	11.1343	271.14	3.0030	0.10	2.5639	14.54	3.0516	1.72	3.0263	0.877	3.0215	0.717
Sample 6	<b>6.0</b>	6.2624	4.373	6.9400	15.67	5.9767	0.388	12.8561	114.27	5.9987	0.022	6.1770	2.95	5.9830	<b>0.283</b>	5.9412	0.98	5.9961	0.065
Sample 7	<b>8.0</b>	7.8201	<b>2.249</b>	7.9394	<b>0.7575</b>	7.9816	<b>0.23</b>	13.1087	<b>63.86</b>	7.9994	<b>0.008</b>	7.1383	10.77	8.0242	0.303	7.9876	<b>0.155</b>	7.9956	<b>0.055</b>
Average error (%)			<b>11.18</b>		<b>1615.38</b>		<b>31.37</b>		<b>6400.76</b>		<b>3.92</b>		<b>8.73</b>		<b>3.86</b>		<b>1.60</b>		<b>1.16</b>

From all of the developed nonlinear regression models for smartphone-based colorimetric detection of chlorine concentration, mostly fitted five nonlinear regression models are selected which provide small amount of detection error with high determination coefficient. The average detection errors correspond to these five nonlinear regression models are plotted in Fig 4.16 which depicts that color ratio based single nonlinear regression incorporates highest detection error (average error of 11.18%) to smartphone-based colorimetric measurement of chlorine concentration. However when color ratio, hue and saturation are considered as the independent variables for multiple nonlinear regression analysis then the performance of smartphone-based colorimetric detection of chlorine concentration increases drastically and incorporates the negligible detection error (average error of 1.16%) over the desired detection range chlorine concentration (0.1-8.0) PPM.

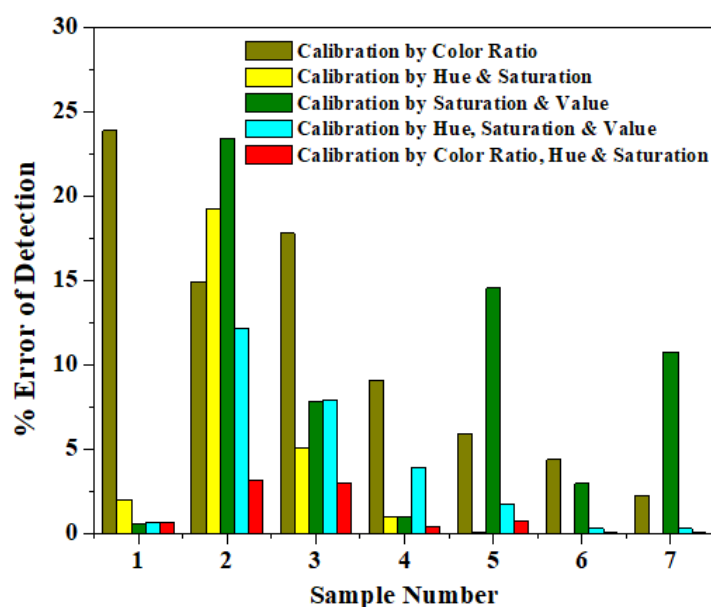


Fig. 4.16: Percentage error of detection associated with smartphone-based colorimetric measurement of chlorine concentration using different calibration techniques.

Therefore, it can be concluded that, calibration by considering color ratio, hue and saturation as the independent variables of multiple nonlinear regression analysis, is the best approach to calibrate the smartphone-based colorimeter as chlorine concentration quantifier for the detection range (0.1-8.0) PPM with very negligible error. So the obtained third-order polynomial associated with color ratio, hue and saturation is selected as the final calibration equation and integrates with the algorithm of customized smartphone app for accurate measurement of chlorine concentration (Fig. 4.17). The measured chlorine concentration of seven different test samples is compared with the actual chlorine concentration and the negligible variations between the measurements certify that the developed smartphone-based colorimeter is highly suitable for low cost, field portable and real time chlorine monitoring. The error bars represents the standard deviations for three consecutive measurements of each sample to highlight the performance of exact repeatability of the smartphone-based colorimeter to determine [Cl].

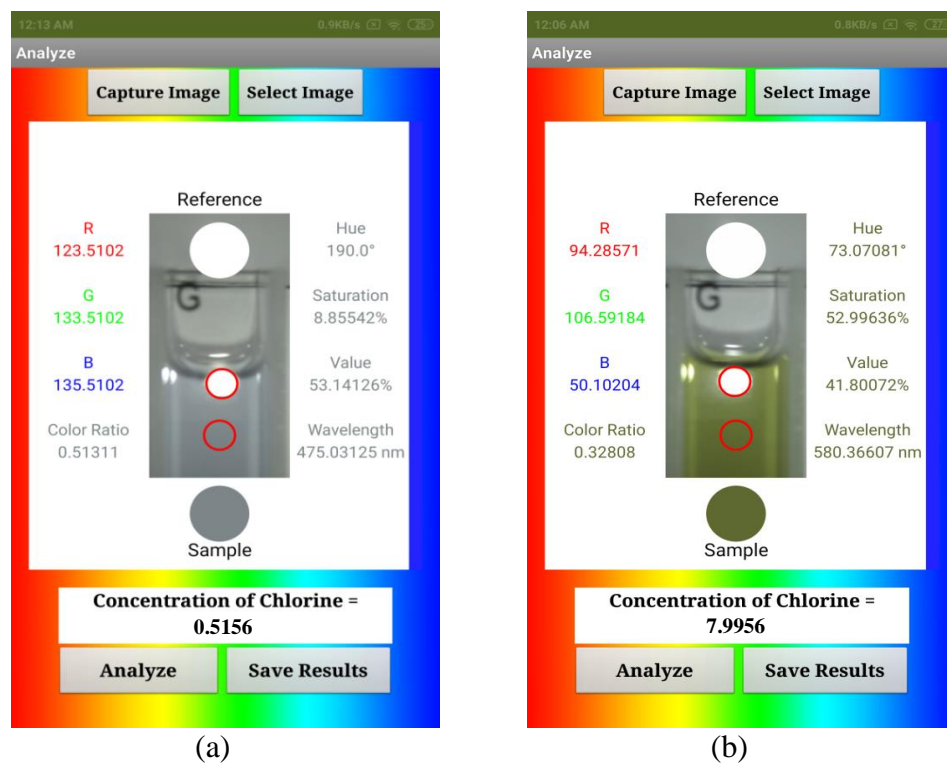


Fig. 4.17: Screenshot images of chlorine concentration quantification using customized smartphone app: (a) 0.5156 PPM (actual concentration 0.5 PPM) and (b) 7.9956 PPM (actual concentration 8.0 PPM).

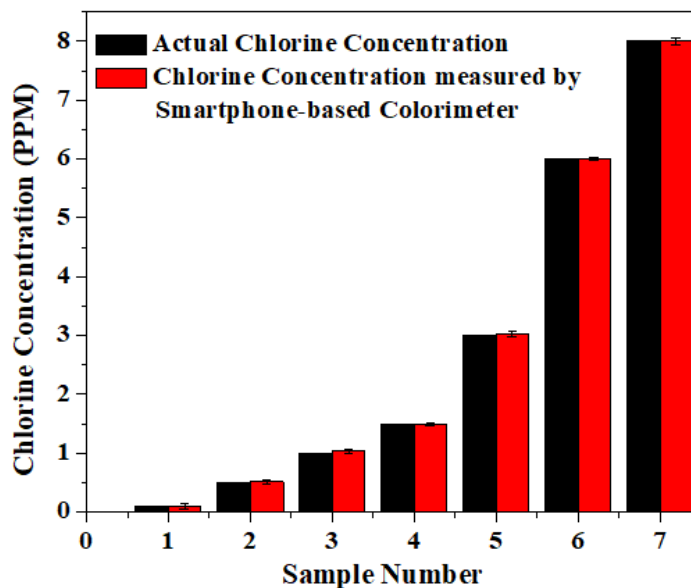


Fig. 4.18: Chlorine concentration of seven test samples measured on smartphone-based colorimeter compared with corresponding actual concentration.

## 4.5 Conclusion

The previously reported conventional smartphone-based colorimeters are only applicable for the colorimetric detection when only the color intensity or wavelength is changed with the variation of analyte which has to be measured. But these conventional colorimeters are not totally capable to handle the situation when both intensity and wavelength of color are changed for any colorimetric detection. This problem is solved in this research by designing and fabricating a smartphone-based colorimeter that can be implemented for any colorimetric detection where color intensity, wavelength and color density are changed solely or simultaneously. As proof of principle, three different practical colorimetric tests named as Rhodamine B concentration quantifier, digital pH meter and chlorine concentration quantifier are performed to evaluate the performance of the designed and fabricated smartphone-based colorimeter. For the case of RhB concentration quantifier, only saturation i.e color density varies significantly with the concentration of RhB and the designed colorimeter can perfectly quantify the RhB concentration. For the colorimetric detection of pH value, wavelength varies most significantly with pH values and the designed colorimeter can also perfectly handle this situation to quantify pH value without any considerable error. Finally the colorimetric test to determine chlorine concentration is implemented where color intensity, wavelength and color density all of these color attributes change significantly with the variation of chlorine concentration and the performance of the designed smartphone-based colorimeter for this case is found outstanding. Therefore it can be concluded that the designed smartphone-based colorimeter is suitable for versatile applications of colorimetric measurements not only for these three colorimetric tests but also to determine any analyte through colorimetric approach.

# Chapter V

## *Conclusion*

---

### **Chapter Outlines:**

**5.1 Conclusion**

**5.2 Future Work**

---

## 5.1 Conclusion

In summary, a totally self-contained and self-referencing smartphone-based colorimeter is designed and fabricated successfully by utilizing the in-built flash LED, CMOS camera sensor, high resolution display and high computational power of smartphone by excluding the additional expensive optics, external light sources and external power supply used in the conventional smartphone-based colorimeters. 3D printing technology is incorporated to fabricate the optical enclosure that makes the designed smartphone-based colorimeter robust for transport and suitable for on-site colorimetric detection. Excluding additional expensive optics and using 3D printed optical enclosure, the manufacturing cost of the designed smartphone-based colorimeter becomes very low, less than 3.0 USD. For the proper functioning of the fabricated smartphone-based colorimeter, a customized smartphone app is developed to capture and analyze digital image for digitization the color change information of any colored analyte. Moreover, the customized smartphone app offers additional advantages in terms of analyzing real time or previously recorded test samples and save the results of colorimetric detection for representation on smartphone screen and further sharing through existing mobile network. For the first time, a novel interpolation and extrapolation algorithm is developed to estimate the wavelength information of the reflected light from the test sample under investigation. Significant errors in colorimetric detection of the conventional smartphone-based colorimeters using color ratio or color intensity are removed by incorporating a unique calibration technique that can adapt with any type of colorimetric detection where color ratio, color intensity and wavelength information are changed solely or simultaneously.

The performance of the fabricated smart sensing instrument is evaluated through the demonstration of three different colorimetric measurements by simply taking and analyzing the photograph of the RhB, pH and chlorine samples treated with the specific chemosensors. For RhB concentration quantification, the designed smartphone-based colorimeter reliably measures the concentration of RhB in the detection range of (0.2-4.0) PPM with an accuracy of 99.05%. With the same optical set-up and with same application software, the designed low-cost smartphone-based colorimeter is capable enough to detect pH value in the range of (4.0-9.0) with high accuracy of 99.91% and measures the chlorine concentration with 98.84% accuracy within the detection range of (0.1-8.0) PPM. This high accuracy strongly clarify that the results obtained from the designed smartphone-based colorimeter are exactly similar with their corresponding actual values and the performance of this instrument is outstanding compared to the previously reported conventional smartphone-based colorimeter and also compatible with conventional bench-top colorimeter. The designed colorimetric platform also provides the facility to incorporate new colorimetric test rather than the existing tests with the help of device calibration which ensures wide applications of the designed smartphone-based colorimeter. From all of the above discussions it can be concluded that the designed smartphone-based colorimeter is very low cost, field portable, highly accurate, robust and can promote diverse fields of bio-analytical investigations in a single smartphone platform. Therefore, the designed smartphone-based colorimeter can be the best solution for colorimetric analysis of any liquid samples as a completely suitable tool for point of care diagnosis, food quality assessment, environmental monitoring and agricultural aspect analysis without the requirement of trained personnel.



## 5.2 Future Work

In this research, a totally self-contained smartphone-based colorimeter is designed and calibrated by incorporating the simultaneous effects of multiple attributes such as color ratio, intensity and wavelength information within the detection algorithm of customized smartphone app. In the process of calibration, multiple nonlinear regression analysis has to be performed to develop  $n$ -th order polynomial for device calibration. But a high processing computer is required to perform this regression analysis to formulate calibration equation on 'Origin' or other platform. In future, simple machine learning algorithm will be incorporated with the customized smartphone app as the replacement of regression technique.

In the present case, the smartphone-based colorimeter is demonstrated only for liquid samples but in future the versatility of the designed colorimeter will be verified by quantifying different analytes in a solid sample. Moreover, IoT connectivity of smartphone will be utilized for real time monitoring and mapping of different analytes for various practical applications into a smartgrid sensor network.

## References

- [1] “Active Smartphone Users per Region 2016-2021”, *Newzoo*. Available: <https://newzoo.com/insights/articles/newzoos-2018-global-mobile-market-report-insights-into-the-worlds-3-billion-smartphone-users/> Accessed Sep. 12, 2019].
- [2] “World Population”, *worldometers*. Available: <https://www.worldometers.info/world-population/> Accessed Sep. 15, 2019.
- [3] [7] N. D. Lane, E. Miluzzo, H. Lu, D. Peebles, T. Choudhury, and A. T. Campbell, “A survey of mobile phone sensing,” *IEEE Communications Magazine*, pp. 140-150, Sep. 2010.
- [4] V. Kilic, G. Alankus, N. Horzum, A. Y. Mutlu, A. Bayram, and M. E. Solmaz, “Single-Image-Referenced Colorimetric Water Quality Detection Using a Smartphone,” *ACS Omega*, 3, pp. 5531–5536, May 2018.
- [5] M. A. Hossain, J. Canning, S. Ast, K. Cook, P. J. Rutledge, and A. Jamalipour, “Combined “dual” absorption and fluorescence smartphone spectrometers,” *Optics Letters*, 40, pp. 1737-1740, Apr. 2015.
- [6] J.R. Hutchison, R. L. Erikson, A. M. Sheen, R. M. Ozanicha, and R. T. Kelly, “Reagent-free and portable detection of *Bacillus anthracis* spores using a microfluidic incubator and smartphone microscope,” *Analyst*, 140, pp. 6269-6276, Aug. 2015.
- [7] M. A. Hossain, J. Canning, S. Ast, P. Rutledge, T. L. Yen, and A. Jamalipour, “Lab-in-a-phone: Smartphone-based portable fluorometer for pH measurements of environmental water,” *IEEE Sensors Journal*, 15(9), pp.5095-5102, Sep. 2015.
- [8] L. J. Wanga, N. Naudeb, Y. C. Changa, A. Crivarob, M. Kamounb, P. Wangb, and L. Li, “An Ultra-low Cost Smartphone Octochannel Spectrometer for Mobile Health Diagnostics,” *Journal of Biophotonics*, 11, pp. e201700382, Mar. 2018.
- [9] S. Kim, D. Cho, J. Kim, M. Kim, S. Youn, J. E. Jang, M. Je, D. H. Lee, B. Lee, D. L. Farkas, and J. Y. Hwang, “Smartphone-based multispectral imaging: system development and potential for mobile skin diagnosis,” *Biomedical Optics Express*, 7, pp. 5294-5307, Dec. 2016.
- [10] X. Xu, A. Akay, H. Wei, S. Wang, B. P. -Murphy, B. -E. Erlandsson, X. Li, W. Lee, J. Hu, L. Wang, and F. Xu, “Advances in smartphone-based point-of-care diagnostics,” *Proceedings of the IEEE*, 103(2), pp. 236-247, Mar. 2015.
- [11] Y. Intaravanne, S. Sumriddetchkajorn, and J. Nukeaw, “Cell phone-based two-dimensional spectral analysis for banana ripeness estimation,” *Sensors and Actuators B: Chemical-Elsevier*, 168 pp. 390-394, Apr. 2012

- [12] J. Guo, J. X. H. Wong, C. Cui, X. Li, and H. Z. Yu, "A smartphone-readable barcode assay for the detection and quantitation of pesticide residues," *Analyst*, 140, pp. 5518-5525, Jun. 2015.
- [13] T. Guo, R. Patnaik, K. Kuhlmann, A. J. Raib, and S. K. Sia, "Smartphone dongle for simultaneous measurement of hemoglobin concentration and detection of HIV antibodies," *Lab on a Chip*, 15, pp. 3514-3520, Jul. 2015.
- [14] W. Martinez, S. T. Phillips, E. Carrilho, S. W. Thomas, H. Sindi, and G. M. Whitesides, "Simple telemedicine for developing regions: Camera phone and paper based microfluidic devices for realtime, off-site diagnosis," *Analytical Chemistry*, 80(10), pp. 3699-3707, Apr. 2008.
- [15] A. Garcia, M. M. Erenar, E. D. Marinetto, C. A. Abad, I. D. Orbe-Paya, A. J. Palma, L. F. C. Vallvey, "Mobile phone platform as portable chemical analyzer," *Sensors and Actuators B: Chemical- Elsevier*, 156(1), pp. 350-359, Apr. 2011.
- [16] D. Santra, S. Mandal, A. Santra, and U. K. Ghorai, "Cost effective and wireless portable device for estimation of hexavalent Chromium, Fluoride and Iron in drinking water," *Analytical Chemistry*, 90(21), pp. 12815-12823, Oct. 2018.
- [17] M. Mancuso, E. Cesarmanb and D. Erickson, "Detection of Kaposi's sarcoma associated herpesvirus nucleic acids using a smartphone accessory," *Lab on a Chip*, 00, pp. 3809-3816, Jul. 2014.
- [18] S. Sumriddetchkajorn, K. Chaitavon, and Y. Intaravanne, "Mobile-platform based colorimeter for monitoring chlorine concentration in water," *Sensors and Actuators B: Chemical- Elsevier*, 191, pp. 561-566, Oct. 2013.
- [19] J. I. Hong and B. Y. Chang, "Development of the smartphone-based colorimetry for multi-analyte sensing arrays," *Lab on a Chip*, 14, pp. 1725-1732, Feb. 2014.
- [20] S. Dutta, G. P. Saikia, D. J. Sarma, K. Gupta, P. Das, and P. Nath, "Protein, enzyme and carbohydrate quantification using smartphone through colorimetric digitization technique," *Journal of Biophotonics*, 10, pp. 623-633, Jun. 2016.
- [21] X. Li, F. Yang, J. X. H. Wong, and H. Z. Yu, "Integrated Smartphone-App-Chip System for On-Site Parts-PerBillion-Level Colorimetric Quantitation of Aflatoxins," *Analytical Chemistry*, 89, pp. 8908-8916, Jul. 2017.
- [22] A. Motalebizadeh, H. Bagheri, S. Asiaei, N. Fekratc, and A. Afkhami, "New portable smartphone-based PDMS microfluidic kit for the simultaneous colorimetric detection of arsenic and mercury," *RSC Advances*, 8, pp. 27091-27100, Jul. 2018.
- [23] Y. Jung, J. Kim, O. Awofeso, H. Kim, F. Regnier, and E. Bae, "Smartphone-based colorimetric analysis for detection of saliva alcohol concentration," *Applied Optics*, vol. 54, pp. 9183-9189, Nov. 2015.

- [24] M. E. Solmaz, A. Y. Mutlu, G. Alankus, V. Kilic, A. Bayram, and N. Horzum, "Quantifying colorimetric tests using a smartphone app based on machine learning classifiers," *Sensors and Actuators B: Chemical-Elsevier*, 255 (2), pp. 1967-1973, Aug. 2017.
- [25] T. S. Park, and J. Y. Yoon, "Smartphone Detection of Escherichia coli From Field Water Samples on Paper Microfluidics," *IEEE Sensors Journal*, 15(3), pp. 1902-1907, Mar. 2015.
- [26] J. H. Lee, B. Fan, T. D. Samdin, D. A. Monteiro, M. S. Desai, O. Scheideler, H. E. Jin, S. Kim, and S. W. Lee, "Phage-Based Structural Color Sensors and Their Pattern Recognition Sensing System," *ACS Nano*, 11, pp. 3632-3641, Mar. 2017.
- [27] J. L. Delaney, C. F. Hogan, J. Tian, and W. Shen, "Electrogenerated Chemiluminescence Detection in Paper-Based Microfluidic Sensors," *Analytical Chemistry*, 83, pp. 1300-1306, Jan. 2011.
- [28] I. Hussain, K.U. Ahamad, and P. Nath, "Low-cost, robust and field portable smartphone platform photometric sensor for fluoride level detection in drinking water," *Analytical Chemistry*, vol. 89, pp. 1767-775, Dec. 2016.
- [29] R. Monosik, V. B. d. Santos, and L. Angnes, "A simple paper-strip colorimetric method utilizing dehydrogenase enzymes for analysis of food components," *Analytical Methods*, 7, pp. 8177-8184, Aug. 2015.
- [30] M. Dangkulwanich, K. Kongnithigarn, and N. Aurnoppakhun, "Colorimetric Measurements of Amylase Activity: Improved Accuracy and Efficiency with a Smartphone," *Journal of Chemical Education*, 95, pp. 141-145, Dec. 2017.
- [31] X. Wang, M. Mahoney, and M. E. Meyerhoff, "Inkjet-Printed Paper-Based Colorimetric Polyion Sensor Using a Smartphone as a Detector," *Analytical Chemistry*, 89, pp. 12334-12341, Oct. 2017.
- [32] B. Coleman, C. Coarsey, M. A. Kabir, W. Asghar, "Point-of-care Colorimetric Analysis through Smartphone Video," *Sensors and Actuators B: Chemical- Elsevier*, 282, pp. 225-231, Mar. 2019.
- [33] N. S. K. Gunda, S. Naicker, S. Shinde, S. Kimbahune, S. Shrivastavac, and S. Mitra, "Mobile Water Kit (MWK): a smartphone compatible low-cost water monitoring system for rapid detection of total coliform and E. coli," *Analytical Methods*, 6, pp. 6236-6246, Jun. 2014.
- [34] O. Mudanyali, S. Dimitrov, U. Sikora, S. Padmanabhan, I. Navruza and A. Ozcan, "Integrated rapid-diagnostic-test reader platform on a cellphone," *Lab on a Chip*, vol. 12, pp. 2678-2686, Apr. 2012.
- [35] Q. Wei, R. Nagi, K. Sadeghi, S. Feng, E. Yan, S. J.Ki, R. Caire, D. Tseng, and A. Ozcan, "Detection and Spatial Mapping of Mercury Contamination in Water Samples Using a Smart-Phone," *ACS Nano*, vol. 8, pp. 1121-1129, Jan. 2014.

- [36] S. Sumriddetchkajorn, K. Chaitavon, and Y. Intaravanne, "Mobile device-based self-referencing colorimeter for monitoring chlorine concentration in water," *Sensors and Actuators B: Chemical-Elsevier*, 182, pp. 592–597, Mar. 2013.
- [37] M.Y. Jia, Q. Wu, H.Li, Y. Zhang, Y. F. Guan, and L. Feng, "The calibration of cellphone camera-based colorimetric sensor array and its application in the determination of glucose in urine," *Biosensors and Bioelectronic*, Jul. 2015.
- [38] S. D. Kim, Y. Koo, and Y. Yun, "A Smartphone-Based Automatic Measurement Method for Colorimetric pH Detection Using a Color Adaptation Algorithm," *Sensors*, 17, pp. 1604-1616, Jul. 2017.
- [39] X. Li, F. Yang, J. X. H. Wong, and H. Z. Yu, "Integrated Smartphone-App-Chip System for On-Site Parts-PerBillion-Level Colorimetric Quantitation of Aflatoxins," *Analytical Chemistry*, 89, pp. 8908-8916, Jul. 2017.
- [40] Y. Intaravanne, S. Sumriddetchkajorn, and J. Nukeaw, "Cell phone-based two-dimensional spectral analysis for banana ripeness estimation," *Sensors and Actuators B: Chemical-Elsevier*, 168 pp. 390-394, Apr. 2012.
- [41] T. H. Wu, C. C. Chang, J. Vaillant, A. Bruyant, and C. W. Lin, "DNA biosensor combining single-wavelength colorimetry and a digital lock-in amplifier within a smartphone," *Lab on a Chip*, 16, pp. 4527-4533, Oct. 2016.
- [42] A. Zhdanov, J. Keefe, L. F. Waite, K. R. Konnaiyan, and A. Pyayt, "Mobile phone based ELISA (MELISA)," *Biosensors and Bioelectronic- Elsevier*, 103, pp. 138-142, Dec. 2017.
- [43] A. F. Coskun, J. Wong, D. Khodadadi, R. Nagi, A. Teya, and A. Ozcan, "A personalized food allergen testing platform on a cellphone," *Lab on a Chip*, 13, pp. 636–640, Nov. 2012.
- [44] A. Y. Mutlu, V. Kılıç, G. K. Özdemir, A. Bayram, N. Horzum, and M. E. Solmaz, "Smartphone Based Colorimetric Detection via Machine Learning," *Analyst*, 142, pp. 2434-2441, May 2017.
- [45] N. L. Ruiz, V. F. Curto, M. M. Erenas, F. B. Lopez, D. Diamond, A. J. Palma, and L. F. C. Vallvey, "Smartphone-Based Simultaneous pH and Nitrite Colorimetric Determination for Paper Microfluidic Devices," *Analytical Chemistry*, 86, pp. 9554-9562, Aug. 2014.
- [46] U. M. Jalal, G. J. Jin, and J. S. Shim, "Paper–Plastic Hybrid Microfluidic Device for Smartphone-Based Colorimetric Analysis of Urine," *Analytical Chemistry*, 89, pp. 13160-13166, Nov. 2017.
- [47] T. S. Park, C. Baynes, S. I. Choc, and J. Y. Yoon, "Paper microfluidics for red wine tasting," *RSC Advances*, 4, pp. 24356-24362, May 2014.
- [48] P. Brangel, A. Sobarzo, C. Parolo, B. S. Miller, P. D. Howes, S. Gelkop, J. J. Lutwama, J. M. Dye, R. A. McKendry, L. Lobel, and M. M. Stevens, "A Serological Point-of-Care Test for

the Detection of IgG Antibodies against Ebola Virus in Human Survivors,” *ACS Nano*, 12, pp. 63-73, Dec 2017.

[49] Y. Jung, J. Kim, O. Awofeso, H. Kim, F. Regnier, and E. Bae, “Colorimetric analysis of saliva–alcohol test strips by smartphone-based instruments using machine-learning algorithms,” *Applied Optics*, 56, pp. 84-92, Jan. 2017.

[50] V. Kilic, G. Alankus, N. Horzum, A. Y. Mutlu, A. Bayram, and M. E. Solmaz, “Single-Image-Referenced Colorimetric Water Quality Detection Using a Smartphone,” *ACS Omega*, 3, pp. 5531-5536, May 2018.

[51] Wenchi Zhang, Xiangheng Niu, Xin Li, Yanfang He, Hongwei Song, Yinxian Peng, Jianming Pan, Fengxian Qiu, Hongli Zhao, Minbo Lan, “A smartphone-integrated ready-to-use paper-based sensor with mesoporous carbon-dispersed Pd nanoparticles as a highly active peroxidase mimic for H<sub>2</sub>O<sub>2</sub> detection,” *Sensors and Actuators B: Chemical*, 265, pp. 412-420, Mar. 2018.

[52] S. Gautam, B. S Batule, H.Y. Kim, K. S. Park, and H. G. Park, “Smartphone-based portable wireless optical system for the detection of target analytes,” *Biotechnology Journal*, 12, pp. 1600581, Dec. 2016.

[53] H. Wanga, Y. Sun, H.Li, W. Yue, Q. Kang, and D. Shen, “A smartphone-based ratiometric resonance light scattering device for field analysis of Pb<sup>2+</sup> in river water samples and immunoassay of alpha fetoprotein using PbS nanoparticles as signal tag,” *Sensors and Actuators B: Chemical, Elsevier*, 271, pp. 358-366, May 2018.

[54] X. L. Guo, Y. Chen, H. L. Jiang, X. B. Qiu, and D. L. Yu, “Smartphone-Based Microfluidic Colorimetric Sensor for Gaseous Formaldehyde Determination with High Sensitivity and Selectivity,” *Sensors*, vol. 18, pp. 3141-3151, Sep. 2018.

[55] G. Zilberstein, R. Zilberstein, U. Maor, E. Baskin, S. Zhang, and P.G. Righetti, “Remote sensing of formaldehyde fumes in indoor environments,” *Analytical Metrods*, 33, Apr. 2016.

[56] W. Xiao, C. Huang, F. Xu, J. Yan, H. Bian, Q. Fu, K. Xie, L. Wang, and Y. Tang, “A Simple and Compact Smartphone-Based Device for the Quantitative Readout of Colloidal Gold Lateral Flow Immunoassay Strips,” *Sensors and Actuators B: Chemical- Elsevier*, 266, pp. 63-70, Mar. 2018,

[57] I. Hussain, K. Ahamadb, and P. Nath, “Water turbidity sensing using a smartphone,” *RSC Advances*, 6, pp. 22374–22382, Feb. 2016.

[58] S. Lee, V. Oncescu, M. Mancuso, S. Mehtac, and D. Erickson, “A smartphone platform for the quantification of vitamin D levels,” *Lab on a Chip*, 14, pp. 1437-1442, Feb. 2014.

[59] V. Oncescu, M. Mancusob, and D. Erickson, “Cholesterol testing on a smartphone,” *Lab on a Chip*, 14, pp. 759-763, Nov. 2013.

- [60] T. H. Wu, C. C. Chang, J. Vaillant, A. Bruyant, and C. W. Lin, "DNA biosensor combining single-wavelength colorimetry and a digital lock-in amplifier within a smartphone," *Lab on a Chip*, 16, pp. 4527-4533, Oct. 2016.
- [61] W. Chen, F. Cao, W. Zheng, Y. Tian, Y. Xianyu, P. Xu, W. Zhang, Z. Wang, K. Deng, and X. Jiang, "Detection of the nanomolar level of total Cr[(III) and (VI)] by functionalized gold nanoparticles and a smartphone with the assistance of theoretical calculation models," *Nanoscale*, 7, pp. 2042-2049, Dec. 2014.
- [62] J. Fang, X. Qiu, Z. Wan, Q. Zou, K. Su, N. Hu, and P. Wang, "A sensing smartphone and its portable accessory for on-site rapid biochemical detection of marine toxins," *Analytical Methods*, 8, pp. 6895-6902, Aug. 2016.
- [63] W. Choi, J. Shin, K.A Hyun, J. W. Song, and H. I. Jung, "Highly sensitive and accurate estimation of bloodstain age using smartphone," *Biosensors and Bioelectronic*, 130, pp. 414-419, Apr. 2019.
- [64] T. C. Stubbings, and H. Hutter, "Combining multispectral image information using color," *Analytical Chemistry*, 72(7), pp. 282A-288A, Apr. 2000.
- [65] H. Yu, Y. Tan, and B. T. Cunningham, "Smartphone fluorescence spectroscopy," *Analytical Chemistry*, 86(17), pp. 8805-13, Sep. 2014.
- [66] "Better access to safe drinking water", *UNICEF*.  
Available: <https://www.unicef.org/bangladesh/en/better-access-safe-drinking-water>  
[Accessed Mar. 01, 2019]
- [67] "Measuring chlorine levels in water supplies", *World Health Organization*. Available: [https://www.who.int/water\\_sanitation\\_health/publications/2011/tn11\\_chlorine\\_levels\\_en.pdf](https://www.who.int/water_sanitation_health/publications/2011/tn11_chlorine_levels_en.pdf)  
[Accessed May 01, 2019]
- [68] "Drinking Water Chlorination", *American Chemistry Council*.  
Available: <https://chlorine.americanchemistry.com/Chlorine-Benefits/Safe-Water/Disinfection-Practices.pdf>  
[Accessed Mar. 01, 2019]
- [69] "Chlorine Disinfection of Produce Washwater", *Michigan State University*.  
<https://msu.edu/~brook/publications/aeis/aeis653.htm>  
[Accessed Mar. 01, 2019]
- [70] "Harmful Effects of Chlorine in Water", *FilterWater.com*  
Available: <http://www.filterwater.com/t-articles.harmfuleffectsofchlorine.aspx>  
[Accessed Mar. 01, 2019]
- [71] "Guidelines for Drinking-water Quality, Fourth Edition", *World Health Organization*.  
Available: <https://apublica.org/wp-content/uploads/2014/03/Guidelines-OMS-2011.pdf>  
[Accessed Apr. 10, 2019]
- [72] F. Kimme, P. Brick, S. Chatterjee, and T. Q. Khanh, "Optimized flash light-emitting diode spectra for mobile phone cameras," *Applied Optics*, vol. 52, pp. 8779-8788, Dec. 2013.

[73] “Light Entering a Camera”, Digital Earth Watch.

Available: <https://sites.google.com/a/globalsystemsscience.org/digital-earth-watch/tools/digital-cameras-overview/what-happens-to-the-near-infrared-entering-the-camera>

[Accessed Sep. 10, 2019]

[74] N. A. Ibraheem, M. M. Hasan, R. Z. Khan, and P. K. Mishra, “Understanding Color Models: A Review,” *ARPN Journal of Science and Technology*, vol. 2, pp. 265-275, Apr. 2012.

[75] G. D Hastings, and A. Rubin” Colour spaces - a review of historic and modern colour models,” *South African Optometrist*: vol. 71, pp. 133-143, 2012.

[76] Nishad P. M, and D. R. M. Chezian, “VARIOUS COLOUR SPACES AND COLOUR SPACE CONVERSION ALGORITHMS,” *Journal of Global Research in Computer Science*, vol. 4, pp. 44-48, Jan. 2013.

[77] “Magenta”, *Wikipedia*.

Available: <https://en.wikipedia.org/wiki/Magenta>

[Accessed Aug. 10, 2019]



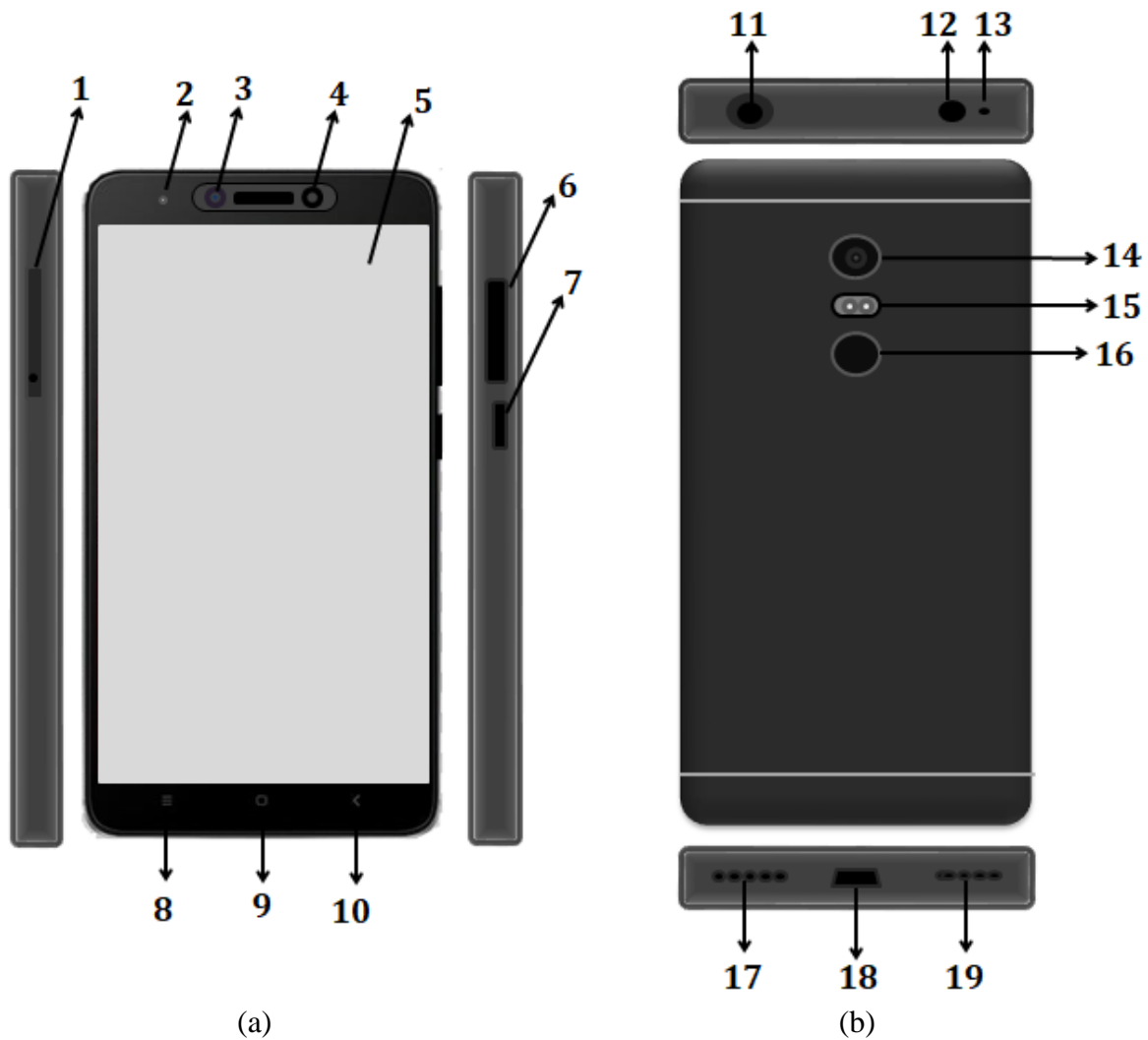
## Appendix

### Smartphone's model, features and specifications

**Table A1: Features and specifications of the Xiaomi Redmi Note 4 smartphone used in designing smartphone-based colorimeter**

Features	Quantity
Model	Xiaomi Redmi Note 4
Network	<b>Technology:</b> GSM / HSPA / LTE <b>2G bands:</b> GSM 900 / 1800 / 1900 <b>3G bands:</b> HSDPA 850 / 900 / 1900 / 2100 <b>4G bands:</b> LTE band 1(2100), 3(1800), 4(1700/2100), 5(850), 7(2600), 8(900), 20(800), 38(2600), 40(2300) <b>Speed:</b> HSPA 42.2/5.76 Mbps, LTE-A (2CA) Cat6 300/50 Mbps
Display	<b>Type:</b> IPS LCD capacitive touchscreen, 16M colors <b>Size:</b> 5.5 inches, 83.4 cm <sup>2</sup> (~72.7% screen-to-body ratio) <b>Resolution:</b> 1080 x 1920 pixels, 16:9 ratio (~401 ppi density)
Platform	<b>OS:</b> Android 6.0 (Marshmallow), upgradable to 7.0 (Nougat); MIUI 10 <b>Chipset:</b> Qualcomm MSM8953 Snapdragon 625 (14 nm) <b>CPU:</b> Octa-core 2.0 GHz Cortex-A53 <b>GPU:</b> Adreno 506
Memory	<b>Card slot:</b> microSD, up to 256 GB <b>Internal:</b> 32GB 3GB RAM, 64GB 3GB RAM, 64GB 4GB RAM
Camera	<b>Main Camera:</b> 13 MP, f/2.0, 1.12µm, PDAF, Dual-LED dual-tone flash, panorama, HDR 1080p@30fps, 720p@120fps (video) <b>Front camera:</b> 5 MP, f/2.0, 1080p@30fps (video)
Communications	<b>WLAN:</b> Wi-Fi 802.11 a/b/g/n, Wi-Fi Direct, hotspot <b>Bluetooth:</b> 4.1, A2DP, LE <b>GPS:</b> Yes, with A-GPS, GLONASS, BDS <b>Infrared port:</b> Yes <b>Radio:</b> FM radio <b>USB:</b> microUSB 2.0, USB On-The-Go
Battery	Non-removable <b>Li-Po 4100</b> mAh battery
Sensors	Fingerprint (rear-mounted), accelerometer, gyro, proximity, compass

## Locations of some components and sensors of Xiaomi Redmi Note 4 smartphone:



- 1 SIM and SD card slot
- 2 LED indicator
- 3 Proximity sensor
- 4 Front camera
- 5 High resolution display
- 6 Volume rocker
- 7 Power button
- 8 Recent apps key
- 9 Home key
- 10 Back key return

- 11 Headphone connector
- 12 IR blaster
- 13 Secondary mic
- 14 Camera
- 15 Flash LED
- 16 Fingerprint sensor
- 17 Mic
- 18 Micro USB port
- 19 Speaker

Fig. A1: Locations of some components and sensors of Xiaomi Redmi Note 4 smartphone (a) front view and (b) back view.